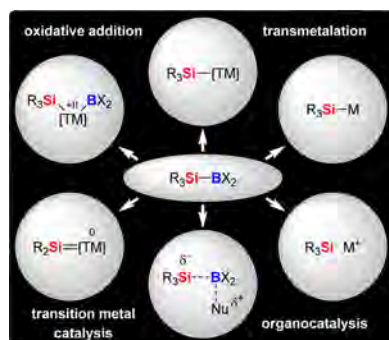


# Activation of the Si–B Interelement Bond: Mechanism, Catalysis, and Synthesis

Martin Oestreich,\* Eduard Hartmann, and Marius Mewald

Institut für Chemie, Technische Universität Berlin, Strasse des 17. Juni 115, 10623 Berlin, Germany



## CONTENTS

1. Introduction
  2. Preparation of Si–B Compounds
  3. Mechanisms of Si–B Bond Activation
  4. Functionalization of Unsaturated Compounds
    - 4.1. 1,2-Addition to Isolated C–C Multiple Bonds
      - 4.1.1. Alkynes
      - 4.1.2. Alkenes
    - 4.2. 1,2-, 1,4-, and 1,*n*-Addition to C–C Multiple-Bond Systems
      - 4.2.1. 1,3- and 1,6-Dienes
      - 4.2.2. 1,7-Diynes and 1,3- and 1,6-Enynes
      - 4.2.3. Allenes
    - 4.3. 1,2-Addition to C–Het Double Bonds
      - 4.3.1. Aldehydes
      - 4.3.2. Imines
      - 4.3.3. Carbon Dioxide
    - 4.4. 1,4-Addition to  $\alpha,\beta$ -Unsaturated Carbonyl and Carboxyl Compounds
    - 4.5. Allylic and Propargylic Substitution
      - 4.5.1. Allylic Precursors
      - 4.5.2. Propargylic Precursors
    - 4.6. Dearomatization of Pyridines and Pyrazine
  5. Functionalization of Strained-Ring Compounds
    - 5.1. Methylene cyclopropanes
    - 5.2. Vinylcyclopropanes and Vinylcyclobutanes
    - 5.3. Biphenylene
  6. (2 + 2 + 1)- and (4 + 1)-Cycloadditions of Multiple-Bond Systems
  7. Functionalization of Carbenoids and Related Compounds
    - 7.1. Carbenoids
    - 7.2. Isonitriles
  8. Summary
- Author Information  
Corresponding Author  
Notes  
Biographies

Acknowledgments  
References

AL  
AL

## 1. INTRODUCTION

Synthetic chemistry is almost unimaginable without three main group elements, namely, boron, silicon, and tin. When attached to a carbon atom of any hybridization, these functional groups serve as exceptionally versatile linchpins in synthesis, selectively transforming into an enormous breadth of C–C and C–Het bonds. Areas such as cross-coupling or classes of reagents such as allylic and propargylic/allenyl metals are largely dominated by these main group elements. The main group element-functionalized intermediate is, however, usually the vehicle to arrive at a target molecule without any of these heteroatoms. Nevertheless, methods for the formation of bonds between carbon and main group elements, i.e., accessing main group element-based compounds, are likewise essential to the overall development of the field.

Interelement compounds, that is, compounds containing an interelement bond,<sup>1</sup> are attractive main group element precursors as these provide the opportunity to transfer both bonding partners to an unsaturated substrate. All six possible combinations of these three elements are known (Figure 1) and

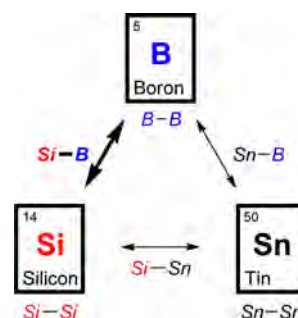


Figure 1. Interelement compounds from boron, silicon, and tin.

are applied to the functionalization of unsaturated compounds.<sup>2–6</sup> Out of these, the Si–B bond displays several attractive features.<sup>4,5</sup> It is sufficiently stable with appropriate substitution at the boron atom (cf. section 2), and the electronegativity difference of boron and silicon allows for chemoselective activation of the Si–B bond (cf. section 3). Also, distinct reactivities of the boryl and silyl groups are likely to enable their sequential introduction into a carbon skeleton with high levels of regiocontrol. The incredibly diverse

Received: August 20, 2012

chemistry of Si–B compounds is currently witnessing tremendous growth, and that is now documented by dozens of stereoselective C–Si/C–B and C–Si bond-forming reactions (cf. sections 4–7).

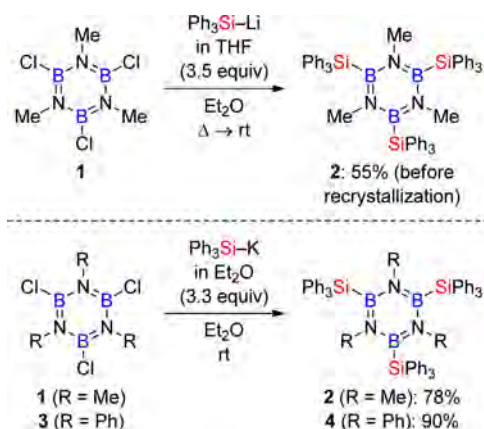
Si–B chemistry initially belonged to inorganic chemistry, and the majority of work on the preparation of Si–B compounds was done by Heinrich Nöth at the Universität München in Germany. It was his group that identified and understood parameters that lend stabilization to the Si–B bond, and the Nöth group elaborated several procedures that later became standard. Aside from a seminal report by John Buynak from the Southern Methodist University in Dallas/Texas, applications of Si–B compounds were extensively investigated by several groups from Kyoto University in Japan. Masaki Shimizu and Tamejiro Hiyama developed transition metal-free stoichiometric reactions, and Michinori Suginome (now together with Tochimichi Ohmura) and the late Yoshihiko Ito introduced transition metal-catalyzed reactions and shaped the field into what is it today. The name of Masato Tanaka must also be mentioned for his early contributions. Our laboratory, previously at the Universität Münster and now at the Technische Universität Berlin, further advanced the field by the development of catalytic Si–B activation by transition metal–alkoxide/hydroxide complexes. We summarize here all known methods to prepare Si–B compounds (silylboronic esters and silylboranes) and present the different modes of Si–B activation. The major portion of this review provides a comprehensive survey of applications, including (tentative) reaction mechanisms, many of which have now been verified by quantum-chemical calculations.

## 2. PREPARATION OF SI–B COMPOUNDS

Decades before Si–B compounds found their way into synthetic organic chemistry, i.e., the functionalization of unsaturated C–C and, to a lesser extent, C–Het bonds, the focus had been on the formation of this interelement linkage as well as on its chemical stability. As long as half a century ago, the laboratories of Seyferth<sup>7</sup> (upper) and Ryschkewitsch<sup>8</sup> (lower) independently reported the preparation of borazines containing three Si–B bonds ( $1 \rightarrow 2$  and  $3 \rightarrow 4$ , Scheme 1). The Si–B bond was formed by displacement of a B–Cl bond using a silicon alkali metal nucleophile.

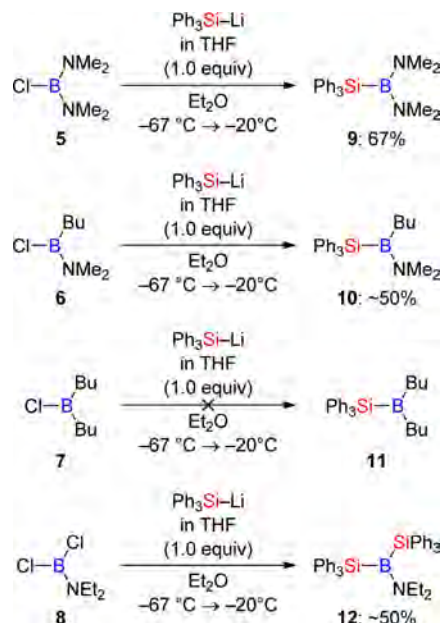
The “trimeric” borazines were of no synthetic use but provided the idea of a stable Si–B bond at a boron atom that is  $\pi$ -stabilized by an adjacent nitrogen atom.<sup>9</sup> It was the laboratory

Scheme 1. Borazines with Si–B Bonds



of Nöth that shortly thereafter began a systematic investigation of the elementary chemistry of “monomeric” Si–B compounds.<sup>10,11</sup> By analogy, these authors showed that  $\text{Ph}_3\text{Si-B(NMe}_2)_2$  is accessible in good chemical yield from an amino-substituted chloroborane and a metalated silane ( $5 \rightarrow 9$ , Scheme 2). The reaction is seminal in the sense that it has

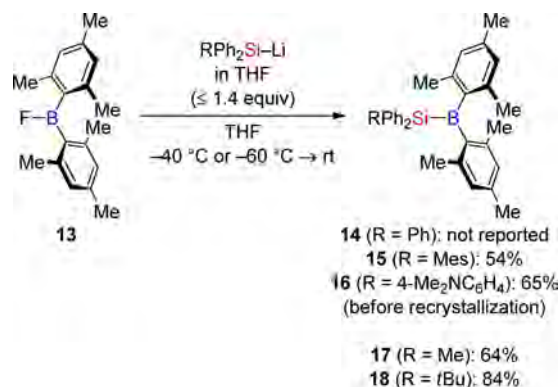
Scheme 2. “Monomeric” Si–B Compounds with Electronically Shielded Boron Atom



become (with other substituents at the silicon and nitrogen atoms) a practical entry into the preparation of several often used Si–B compounds through ligand exchange<sup>10b</sup> at the boron atom. Variation of the substituents at the boron atom further verified that *electronic shielding* of the boron atom by the nitrogen lone pair(s) is essential (Scheme 2).<sup>10</sup> With only alkyl groups at the boron atom as in  $\text{Ph}_3\text{Si-BBu}_2$  (**11**), the borane is not stable.<sup>10</sup> However, Birot, Pillot, and co-workers recently accomplished the preparation of *sterically shielded* silicon-substituted boranes with mesityl groups attached to the boron atom ( $13 \rightarrow 14$ –**18**, Scheme 3).<sup>12</sup>

The nucleophilic substitution of electronically or sterically shielded haloboranes with an appropriate silicon nucleophile (generating lithium or potassium halides) had already emerged

Scheme 3. “Monomeric” Si–B Compounds with Sterically Shielded Boron Atom



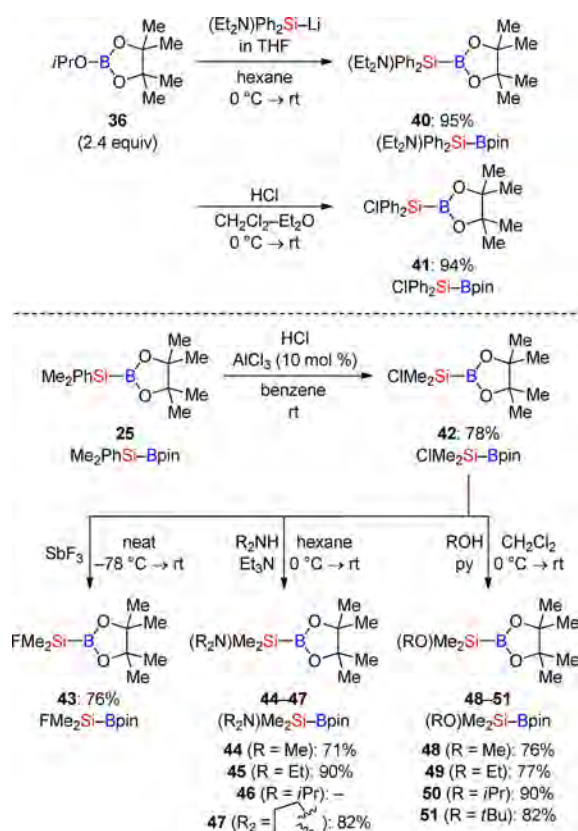




allowed for the installation of different triorganosilyl groups in reasonable yields.

Summarized in a recent full account, Suginome and co-workers elaborated the syntheses of several  $\text{XR}_2\text{Si-Bpin}$  compounds with heteroatom functionalization at the silicon atom.<sup>23</sup> Following the established route to Si-B reagents, the amino-substituted silicon moiety was introduced by nucleophilic substitution at the boron atom employing the metalated Tamao silane<sup>24</sup> ( $36^{21} \rightarrow 40$ , Scheme 7, upper). The amino

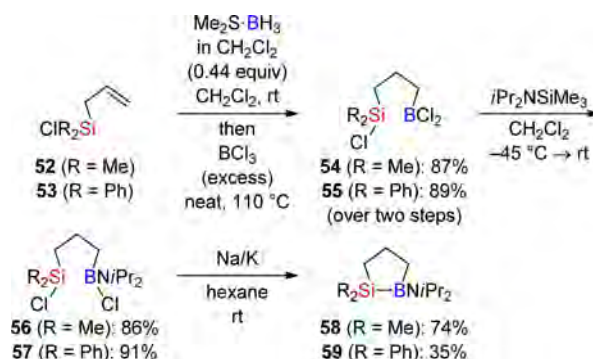
**Scheme 7. Functionalized Silicon-Substituted Bpin Compounds**



group was easily replaced by a chloro substituent upon treatment with hydrochloric acid ( $40 \rightarrow 41$ ), thereby demonstrating that functional group manipulations at the silicon atom are feasible in the presence of the Si-B bond. Consequently, the phenyl group in  $\text{Me}_2\text{PhSi-Bpin}$  was displaced by a chloro substituent to afford  $\text{ClMe}_2\text{Si-Bpin}$  ( $25 \rightarrow 42$ , Scheme 7, lower). The Si-Cl bond in **42** then served as a linchpin to form Si-F (as in **43**), Si-N (as in **44–47**), and Si-O bonds (as in **48–51**)<sup>25</sup> in reasonable yields. The upper and lower sequences complement one another, arriving at  $\text{ClPh}_2\text{Si-Bpin}$  (**41**) and  $\text{XR}_2\text{Si-Bpin}$ , respectively.<sup>23</sup>

Suginome, Murakami, and co-workers also succeeded in the preparation of Si-B reagents with endocyclic Si-B bonds (Scheme 8).<sup>26</sup> The cyclization precursors were available through hydroboration of allylic silanes ( $52 \rightarrow 54$  and  $53 \rightarrow 55$ ), followed by installation of an amino group at the boron atom ( $54 \rightarrow 56$  and  $55 \rightarrow 57$ ). Reductive intramolecular coupling of the chlorosilane and chloroborane groups using sodium–potassium alloy then formed the Si-B bond ( $56 \rightarrow 58$  and  $57 \rightarrow 59$ ). That strategy traces back to the early work of Nöth where such reductive couplings were even accomplished

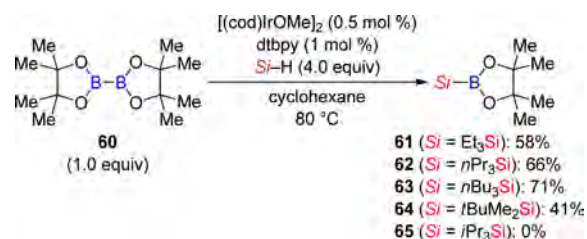
**Scheme 8. Nöth-Type Si-B Compound with an Endocyclic Si-B Bond**



in intermolecular cases with all-alkyl-substituted chlorosilanes.<sup>10b</sup>

Recently, the Hartwig group reported a transition metal-catalyzed Si-B bond formation ( $60 \rightarrow 61–65$ , Scheme 9).<sup>27</sup>

**Scheme 9. Iridium-Catalyzed Si-H Bond Boration**

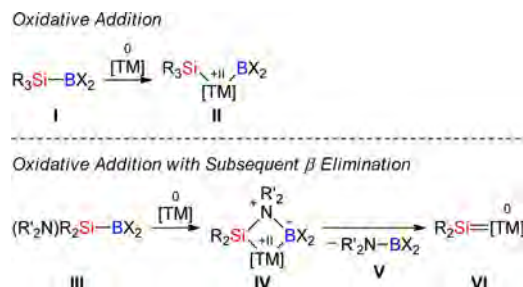


The advantage of the new method is that silanes not substituted with an aryl group participate in the Si-H bond activation. Procedures involving metalated silanes usually require one aryl group at the silicon atom to allow for reductive metalation of the chlorosilane precursor. Berry and co-workers had reported a metal-mediated Si-B bond formation many years ago (not shown).<sup>28</sup> Silylene-insertion reactions<sup>29</sup> as well as disilene functionalization<sup>30</sup> are beyond the scope of this review.

### 3. MECHANISMS OF SI-B BOND ACTIVATION

The mechanisms of Si-B bond activation are diverse, ranging from oxidative addition/reductive elimination transition metal catalyses over stoichiometric and catalytic transmetalation processes to photochemical homolytic cleavage. This section is organized according to the prevalence of these mechanisms in synthetic transformations rather than providing a chronological listing. The discovery by Ito and co-workers<sup>16</sup> and also Tanaka and co-workers<sup>17</sup> that the Si-B bond oxidatively adds to various low-valent transition metals ( $\text{I} \rightarrow \text{II}$  with TM = platinum(0), palladium(0), and nickel(0); Scheme 10, upper) more than a decade ago marked the beginning of the rich synthetic chemistry of Si-B compounds.<sup>4b</sup> These authors found that, subsequent to oxidative addition, migratory insertion of C-C multiple bonds occurs at the stage of intermediate **II** (C-B bond formation) with reductive elimination closing a catalytic cycle (C-Si bond formation). By this, both main group elements are incorporated into the carbon skeleton in a regiocontrolled and stereoselective fashion. A recent report by Suginome and co-workers<sup>31</sup> where a leaving group at the silicon atom of the Si-B reagent allows for  $\beta$ -elimination with the boron fragment at the palladium atom in

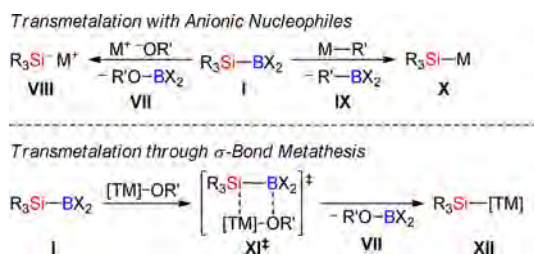
Scheme 10. Si–B Bond Activation by Oxidative Addition



complex IV significantly advanced the oxidative addition approach. A transition metal-stabilized silylene, i.e., a silylene transfer reagent, is thereby catalytically generated in a convenient way (III  $\rightarrow$  IV  $\rightarrow$  VI with TM = palladium(0), Scheme 10, lower).

The obvious method to chemoselectively cleave the Si–B bond is by the addition of a strong nucleophile that would attack at the more Lewis acidic boron atom. That had not been investigated until a decade ago when Kawachi, Minamimoto, and Tamao disclosed the stoichiometric boron–metal exchange at silicon with either alkoxides or carbanions (I  $\rightarrow$  VIII with M = K or I  $\rightarrow$  X with M = Li or MgX; Scheme 11, upper).<sup>32</sup>

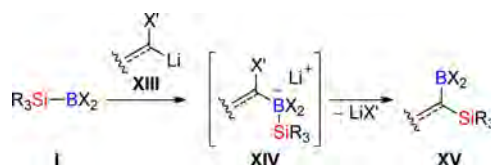
Scheme 11. Si–B Bond Activation by Transmetalation



These methods provide a practical access to nucleophilic silicon with alkaline (earth) metal counteranions but have been rarely applied to synthetic problems. Although both methods are stoichiometric in the main group metal, recent progress in transition metal–alkoxide/hydroxide-catalyzed Si–B bond activation opened the door to catalytically generated transition metal-based silicon nucleophiles (I  $\rightarrow$  XI $^\ddagger$   $\rightarrow$  XII with TM = rhodium(I), copper(I), and nickel(II); Scheme 11, lower).<sup>4a</sup> The catalysis is believed to involve a  $\sigma$ -bond metathesis-type transition state such as XI $^\ddagger$ . Different from the oxidative addition/reductive elimination transition metal catalysis (Scheme 10, upper), it is only the silicon group in the transmetalation methodology (Scheme 11, lower) that is transferred to an acceptor molecule; the boryl group is sacrificed.

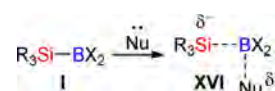
Another well-investigated transformation is the activation of the Si–B reagent by the substrate itself (I  $\rightarrow$  XIV  $\rightarrow$  XV, Scheme 12). Hiyama and co-workers demonstrated for several alkylidene-type<sup>33</sup> as well as allylic<sup>34</sup> carbenoids that nucleophilic attack at the boron atom (cf. I  $\rightarrow$  X, Scheme 11, upper) is followed by intramolecular migration of the silicon atom to the same carbon atom. That carbenoid insertion into Si–B bonds makes use of both main group elements, providing a beautiful access to 1,1-difunctionalized compounds. The activating substrate might also be a neutral nucleophile, and 1,1- (with isonitriles) or 1,2-/1,4-difunctionalization (with electron-deficient heterocycles) becomes possible (not shown).

Scheme 12. Si–B Bond Activation with Carbenoids Followed by Intramolecular Migration of the Silicon Group



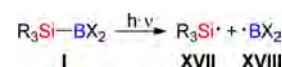
Just recently, neutral Si–B bond activators were introduced that facilitate release of the silicon nucleophile (I  $\rightarrow$  XVI, Scheme 13).<sup>35,36</sup> Catalytic amounts of a Lewis base or the Lewis basic substrate itself thereby enable the metal-free intermolecular silyl transfer.

Scheme 13. Metal-Free Si–B Bond Activation with Nucleophiles Followed by Intermolecular Transfer of the Silicon Group



There is also a single example (in a synthetic context) of homolytic Si–B bond cleavage by UV irradiation (I  $\rightarrow$  XVII + XVIII, Scheme 14).<sup>37</sup>

Scheme 14. Photochemical Si–B Bond Activation



## 4. FUNCTIONALIZATION OF UNSATURATED COMPOUNDS

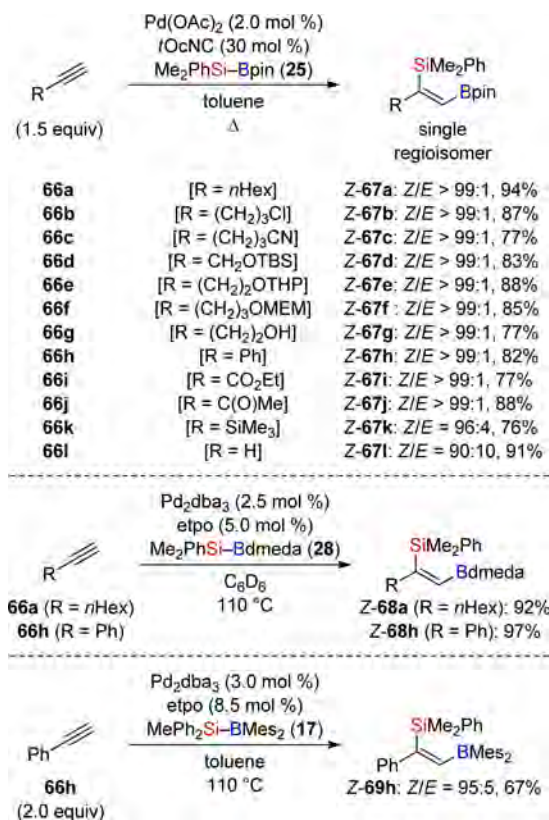
Si–B bond activation applied to the functionalization of C–C multiple bonds is probably most extensively examined. Its diverse facets encompass control of chemo-, regio-, and stereoselectivity, often all at the same time in a single transformation. As illustrated in the following sections, seemingly minor changes in the catalytic system result in totally different reaction outcomes. These subtle effects have not always been predictable but are now reliable methods for the selective formation of C–Si and C–B bonds.

### 4.1. 1,2-Addition to Isolated C–C Multiple Bonds

**4.1.1. Alkynes.** Transition metal-catalyzed functionalization of alkynes with Si–B reagents marked the beginning of the research area. Ito and co-workers<sup>16</sup> and, shortly thereafter, Tanaka and co-workers<sup>17</sup> reported the regioselective silaboration of terminal alkynes. Already in their initial report, the former authors tested the influence of the Si–B reagent as well as the low-valent transition metal.<sup>16a</sup> It was found that palladium–isocyanide complexes were superior to palladium–phosphine complexes (and Wilkinson's catalyst). (Ph<sub>3</sub>P)<sub>4</sub>Pt also afforded promising regioselectivity and yield. The robustness of the Bpin group during purification had already been realized at this early stage, and Me<sub>2</sub>PhSi–Bpin (**25**) then quickly became the standard Si–B reagent. Several terminal alkynes with various functional groups in the alkyl chain reacted with high levels of regio- and diastereocontrol (Scheme 15, upper).<sup>16</sup> Without exception, the boryl group is joined to the terminal carbon atom whereas the silyl group is connected to the internal carbon atom. Moreover, E/Z ratios were excellent



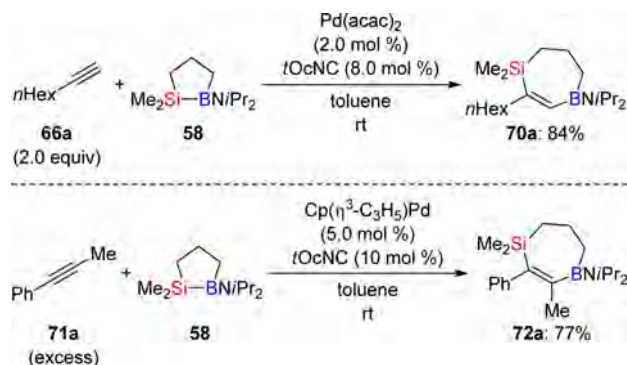
Scheme 15. Z-Selective Silaboration of Terminal Alkynes



for almost all alkynes, and Z configuration was major, corresponding to a formal syn-addition of the Si–B bond across the C–C triple bond. The catalysis also works with  $\text{Me}_2\text{PhSi-Bcat}$  (24) and  $\text{Me}_2\text{PhSi-B}(\text{NEt}_2)_2$  (21) in comparable yields, again with high regioselectivity.<sup>16a</sup> The group of Tanaka introduced the palladium–etpo system in combination with  $\text{Me}_2\text{PhSi-Bdmeda}$  (28) in the regioselective silaboration of terminal alkynes (Scheme 15, center).<sup>17</sup> The palladium–etpo system was later employed by Birot, Pillot, and co-workers in the 1,2-addition of not heteroatom-stabilized  $\text{MePh}_2\text{Si-BMes}_2$  (17) across phenylacetylene (66h  $\rightarrow$  Z-69h, Scheme 15, lower).<sup>12b</sup>

Suginome, Murakami, and co-workers extended this methodology to cyclic 58 with an endocyclic Si–B bond, and reactions with terminal and internal alkynes were regioselective (66a  $\rightarrow$  70a and 71a  $\rightarrow$  72a, Scheme 16).<sup>26</sup> Both palladium(0) catalyses furnished the heterocycles 70a and 72a with the

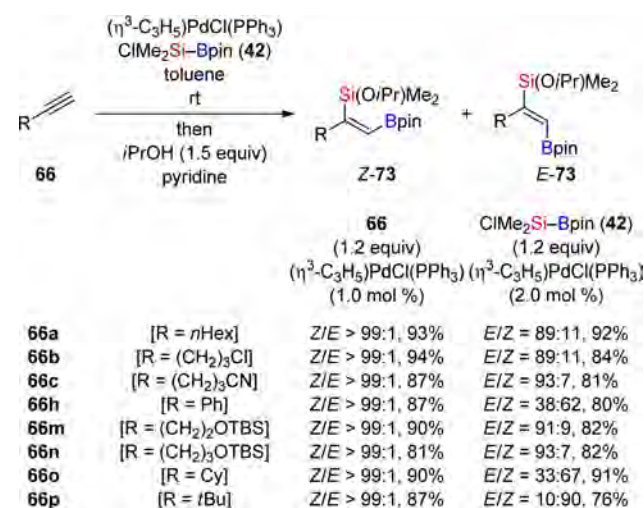
Scheme 16. Silaboration of Alkynes with the Cyclic 58



boron and silicon atoms embedded into a seven-membered ring. The connectivities were in agreement with previous findings, with the boron atom attached to the less-hindered C(sp<sup>2</sup>) atom.

A remarkable effect was recently reported by the Suginome group.<sup>38</sup> It was found that, for almost all R groups, double-bond isomerization from Z to E occurs with excess of chloro-substituted  $\text{ClMe}_2\text{Si-Bpin}$  (42) (66  $\rightarrow$  E-73, Scheme 17, right

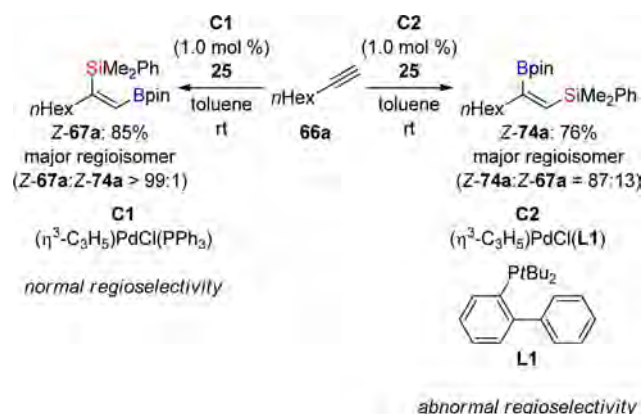
Scheme 17. Stereodivergent Silaboration of Terminal Alkynes



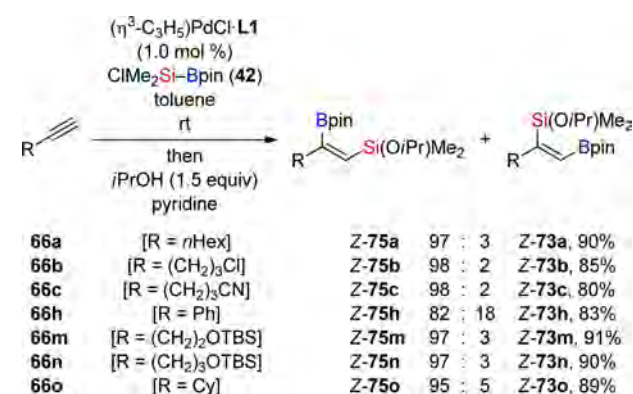
column). However, the isomerization also depends on the presence of isopropanol/pyridine, initially added to transform the chlorosilane into the more stable silyloxy group. Preliminary control experiments verified that 42, the palladium catalyst, and isopropanol are involved; the equilibration of Z to E isomers would not begin until the addition of isopropanol/pyridine. The position of the equilibrium was dependent on the steric demand of the R substituent, and with bulky Cy and  $t\text{Bu}$  groups, quantitative isomerization into E configuration was prevented. Not surprisingly, conventional Z selectivity was obtained with excess alkyne (66  $\rightarrow$  Z-73, Scheme 17, left column). The details of the mechanism have, however, not been delineated yet.<sup>38</sup>

Aside from the control of the alkene geometry, Ohmura, Suginome, and co-workers also succeeded in controlling the regioselectivity (Scheme 18).<sup>39</sup> As documented by the above examples, the boryl group is transferred to the alkyne terminus in the palladium(0)-catalyzed reaction with  $\text{Me}_2\text{PhSi-Bpin}$  (25) when simple phosphine ligands such as  $\text{Ph}_3\text{P}$  are used (66a  $\rightarrow$  Z-67a, normal regioselectivity). Conversely, the employment of the bulky phosphine (biphenyl-2-yl) $t\text{Bu}_2\text{P}$  (L1) reversed the regioselectivity completely to yield abnormal regioselectivity (66a  $\rightarrow$  Z-74a). The ligand effect was investigated in detail in addition reactions of  $\text{ClMe}_2\text{Si-Bpin}$  (42) to various terminal alkynes (Scheme 19).<sup>39</sup> The mechanism was probed in a series of experiments (cf. Scheme 50 in section 4.2.2), and the order of bond-forming events was also investigated by quantum-chemical calculations (cf. Scheme 54 in section 4.2.3). These data suggested that C–B bond formation occurs prior to the formation of the C–Si bond. Hence, the steric bulk of the phosphine accounts for the observed switch of the regioselectivity in a ligand-controlled regioselective alkyne insertion into the Pd–B bond. Moreover,

Scheme 18. Influence of the Phosphine Ligand on Regioselectivity



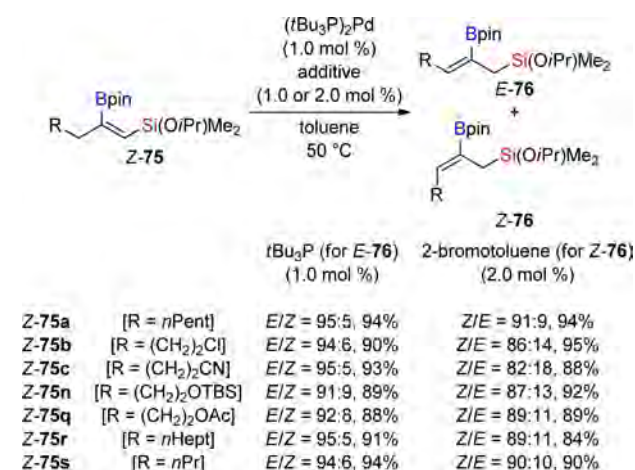
Scheme 19. Inverse Regioselectivity in the Silaboration of Terminal Alkynes



the authors provided experimental evidence that the migratory insertion is reversible (not shown).<sup>39</sup>

A useful extension of this reaction was reported by the same authors.<sup>40</sup> The 1,2-difunctionalized alkenes obtained from the palladium(0) catalysis with *abnormal* regioselectivity were selectively converted into either *E*- or *Z*-configured  $\beta$ -borated allylic silanes in a palladium(0)-catalyzed double-bond migration reaction (Scheme 20). The stereochemistry of the newly formed double bond could be controlled by additives.

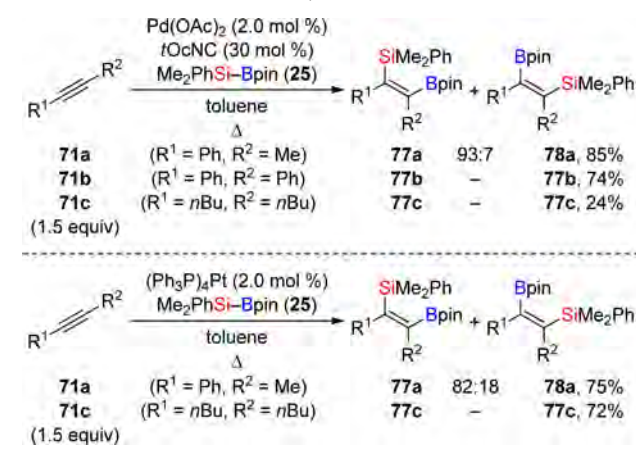
Scheme 20. Stereoselective Double-Bond Migration in 1,2-Difunctionalized Alkenes



Use of an additional equivalent of the phosphine based on (*t*Bu<sub>3</sub>P)<sub>2</sub>Pd favored *E*-alkene geometry (Z-75 → E-76, kinetic products), whereas the addition of catalytic amounts of an aryl bromide resulted in preferential formation of the *Z*-alkenes (Z-75 → Z-76, thermodynamic products). The additional phosphine ligand was believed to retard double-bond migration as well as alkene isomerization; the complex formed in the presence of an aryl bromide additive was found to accelerate both events. Remarkably, application of these protocols to 1,2-difunctionalized alkenes formed with *normal* regioselectivity just resulted in isomerization but not migration, favoring *E* geometry (not shown).

A few examples of internal alkynes were also reported (Scheme 21).<sup>16</sup> That usually brings about regioselectivity issues,

Scheme 21. Palladium(0)- and Platinum(0)-Catalyzed Silaboration of Internal Alkynes



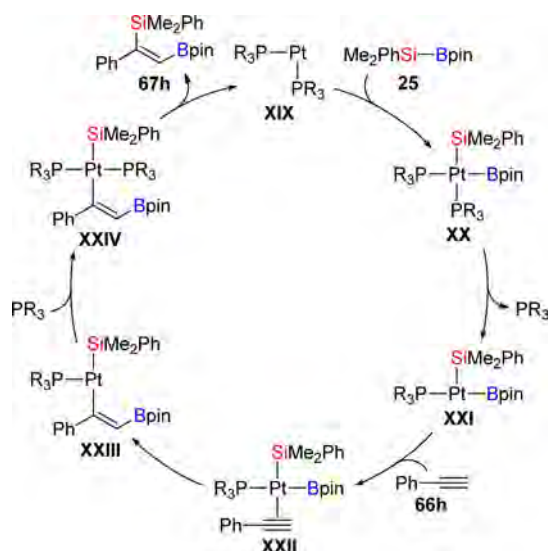
but a decent ratio of regioisomers was obtained in one palladium(0)-catalyzed case (71a → 77a and 78a, upper). Palladium(0)-catalyzed addition of 25 across an alkyl-substituted internal alkyne afforded a low yield of the adduct (71c → 77c, upper). That poor yield was substantially higher in the related platinum(0) catalysis (71c → 77c, lower), and that is one of the few instances where the platinum(0)-catalyzed Si-B bond activation is clearly superior to the palladium(0)-catalyzed procedure.

The mechanism of the platinum(0)-catalyzed silaboration of alkynes was investigated by the laboratory of Ozawa in stoichiometric experiments with silyl(boryl)platinum(II) complexes (Scheme 22).<sup>41</sup> These complexes XX, bearing different phosphine ligands, were prepared by oxidative addition of Me<sub>2</sub>PhSi-Bpin (25) to a platinum(0) precursor (XIX → XX). This step was found to be favored for compact phosphine ligands such as Me<sub>2</sub>PhP or Me<sub>3</sub>P. Kinetic studies revealed that a ligand dissociation is likely to occur *trans* to the silyl group prior to alkyne coordination (XX → XXI). The subsequent alkyne insertion into the Pt-B bond was explained by kinetic reasons and is supported by thermodynamic data reported by Sakaki et al. on the basis of calculated bond energies (XXII → XXIII → XXIV).<sup>42</sup> The reductive elimination step that closes the catalytic cycle (XXIV → XIX + 67h) is, in turn, facilitated by bulky phosphines.

Ito and co-workers also investigated a nickel(0)-based catalytic system in the reaction of Me<sub>2</sub>PhSi-Bpin (25) and alkynes.<sup>43</sup> The outcome of the nickel(0) catalysis is distinct from that of the catalyses with palladium(0) and platinum(0).

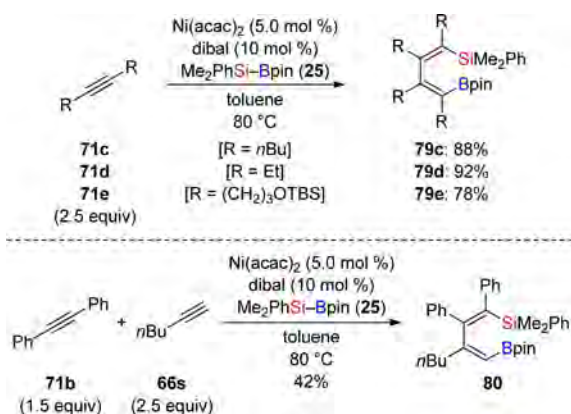


Scheme 22. Proposed Mechanism for the Platinum(0)-Catalyzed Silaboration of Phenylacetylene



With alkyl-substituted internal alkynes, homodimerization occurred in excellent yields ( $71\text{c-e} \rightarrow 79\text{c-e}$ , Scheme 23, 23,

Scheme 23. Nickel(0)-Catalyzed Silaborative Dimerization of Alkynes

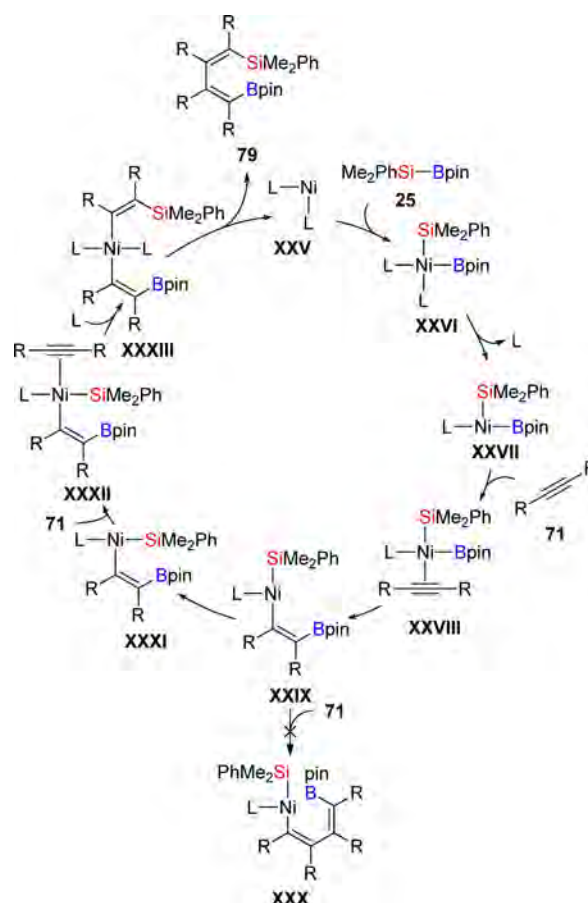


upper). More reactive tolan (71b) was inert in the homocoupling but participated in the cross-coupling with a terminal alkyne (66s), yielding a single regioisomer in moderate yield along with both homodimerization products ( $71\text{b} + 66\text{s} \rightarrow 80$ , Scheme 23, lower).

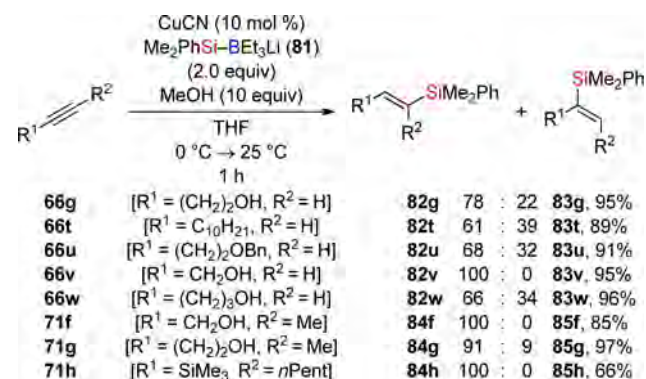
The proposed mechanism<sup>43</sup> for the dimerization commences with the oxidative addition of  $\text{Me}_2\text{PhSi-Bpin}$  (25) to nickel(0) ( $\text{XXV} \rightarrow \text{XXVI}$ , Scheme 24). Ligand dissociation is then followed by alkyne coordination ( $\text{XXVI} \rightarrow \text{XXVII}$ ). Again, the alkyne inserts exclusively into the Ni-B bond ( $\text{XXVIII} \rightarrow \text{XXIX}$ ). Insertion of another molecule of the alkyne into the newly formed C-Ni bond in XXIX was excluded as no trimerization was observed ( $\text{XXIX} \rightarrow \text{XXX}$ ). Alkyne insertion into the Ni-Si bond is expected to be faster, leading to a nickel(II) complex with two vinyl groups ( $\text{XXIX} \rightarrow \text{XXXIII}$ ). Reductive elimination then forms the new C-C bond and releases nickel(0) ( $\text{XXXIII} \rightarrow \text{XXV} + 79$ ).

A seminal contribution to the transition metal-catalyzed silylation of alkynes that does not involve oxidative addition of the Si-B bond to the transition metal was made by Oshima

Scheme 24. Proposed Mechanism for the Nickel(0)-Catalyzed Silaborative Dimerization of Alkynes



and co-workers as early as 1986.<sup>44</sup> In the presence of catalytic amounts of CuCN, borate  $\text{Me}_2\text{PhSi-BEt}_3\text{Li}$  (81) was used to convert terminal as well as internal alkynes to the corresponding vinylic silanes ( $66 \rightarrow 82 + 83$  and  $71 \rightarrow 84 + 85$ , Scheme 25). Protic additives, e.g., MeOH, emerged as

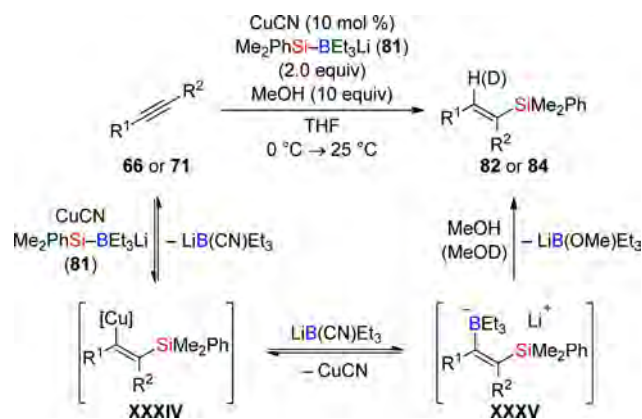
Scheme 25. Copper(I)-Catalyzed 1,2-Addition of  $\text{Me}_2\text{PhSi-BEt}_3\text{Li}$  (81) to Alkynes

crucial for full conversion. The regioselectivity of the transformation is dominated by the substrate structure, and the best results were achieved with unprotected propargylic alcohols 66v and 71f, respectively ( $66\text{v} \rightarrow 82\text{v}$  and  $71\text{f} \rightarrow 84\text{f}$ ). Moreover, a SiMe<sub>3</sub> substituent was beneficial to the selective formation of only one regioisomer ( $71\text{h} \rightarrow 84\text{h}$ ).



Several aspects are emphasized by the authors with regard to a possible reaction mechanism: The addition of  $\text{Me}_2\text{PhSi-BEt}_3\text{Li}$  (**81**) to the alkyne proceeds exclusively in a *cis* fashion (Scheme 26). Control experiments verified its reversible nature

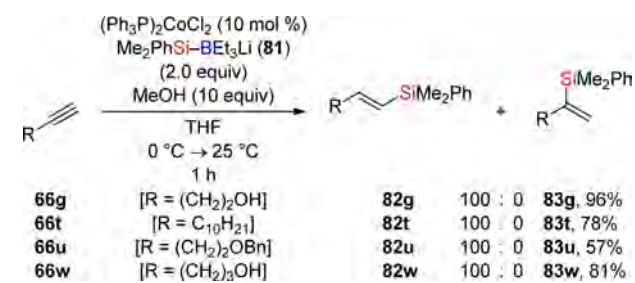
**Scheme 26.** Possible Reaction Path of the Copper(I)-Catalyzed 1,2-Addition of  $\text{Me}_2\text{PhSi-BEt}_3\text{Li}$  (**81**) to Alkynes



so that an equilibrium between the alkyne (**66** or **71**), copper(I) complex **XXXIV**, and vinyl borate **XXXV** exists. Under protic conditions, the equilibrium is shifted to the product (**82** or **84**) by protonation of either of the intermediates **XXXIV** and **XXXV**. It is noteworthy that no reaction is observed in the absence of a copper(I) source.

An interesting observation was made when screening other transition metals:  $(\text{Ph}_3\text{P})_2\text{CoCl}_2$  proved to be a potent catalyst for the conversion of terminal alkynes providing exclusively one regioisomer (Scheme 27). Conversion of representative alkynes

**Scheme 27.** Cobalt(II)-Catalyzed Regioselective 1,2-Addition of  $\text{Me}_2\text{PhSi-BEt}_3\text{Li}$  (**81**) to Alkynes

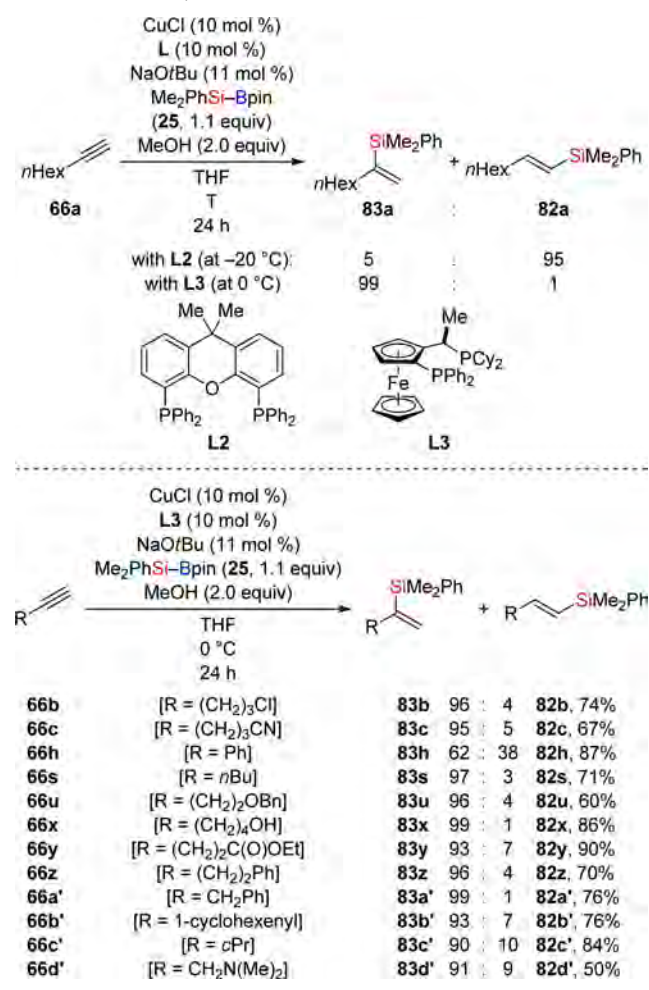


that furnished only moderate ratios in the copper(I)-catalyzed series was now regioselective (**66** → **82**). Other transition metals, e.g., palladium(0), ruthenium(II), or nickel(II), were not effective in this reaction.

Whereas Oshima's protocols<sup>44</sup> display a preference for the linear products (Schemes 25 and 27), Loh and co-workers introduced a modified catalytic system that allows for the selective synthesis of either linear or branched vinyl silanes by variation of the added phosphine ligand (Scheme 28, upper).<sup>45</sup> This time with  $\text{Me}_2\text{PhSi-Bpin}$  (**25**), a combination of  $\text{CuCl}$ ,  $\text{NaOtBu}$ , and **L2** in THF promoted the reaction of terminal alkyne **66a** to give the linear compound **82a** selectively (**66a** → **82a**). Alternatively, branched vinyl silane **83a** was accessible by choosing **L3** as ligand (**66a** → **83a**).

With the optimized system for branched products, the substrate scope of the reaction was explored (Scheme 28,

**Scheme 28.** Copper(I)-Catalyzed Regiodivergent Silylation of Terminal Alkynes

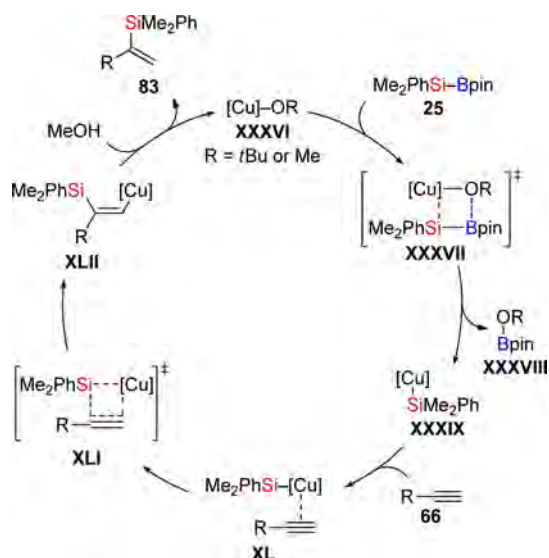


lower). A wide range of functional groups including chloride, nitrile, ester, or amide was compatible with the reaction conditions, and generally good yields as well as synthetically useful regioisomeric ratios were feasible. It is worth mentioning that even an alkene moiety remained unaffected (**66b'** → **83b'**). Only phenylacetylene (**66h**) furnished a significantly decreased regioselectivity, presumably owing to the electron-deficient character of the terminal alkyne carbon (**66h** → **83h** + **82h**, **83h/82h** = 62:38).

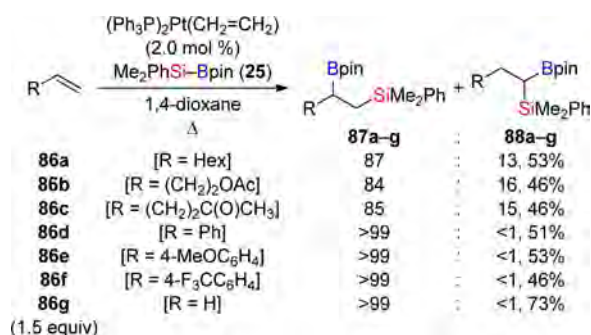
A mechanism for the silylcupration of acetylenes was previously reported,<sup>46</sup> and the key features also apply to the present system (Scheme 29). The in situ-generated  $\text{Cu(I)-SiMe}_2\text{Ph}$  complex **XXXIX** (**XXXVI** → **XXXVII** → **XXXIX**) is likely to coordinate the alkyne (**XXXIX** → **XL**). Insertion of the C–C triple bond into the Cu–Si bond putatively proceeds through a four-membered transition state (**XLI**) arriving at vinyl copper species **XLII** (**XL** → **XLI** → **XLII**). Upon protonation, product **83** is obtained along with the regenerated copper alkoxide **XXXVI** (**XLII** → **XXXVI** + **83**).

**4.1.2. Alkenes.** Silaboration of alkenes also traces back to the seminal work of the Ito group.<sup>47</sup> In contrast to the *normal* regioselectivity seen with C–C triple bonds, the platinum(0)-catalyzed addition of  $\text{Me}_2\text{PhSi-Bpin}$  (**25**) across terminal C–C double bonds results in 1,2-difunctionalized alkanes with the silyl group selectively attached to the terminal carbon atom (**86a–g** → **87a–g**, Scheme 30). The other regioisomer was not

Scheme 29. Proposed Catalytic Cycle for the Copper(I)-Catalyzed Regioselective Silylation of Terminal Alkynes



Scheme 30. Platinum(0)-Catalyzed Regioselective Silaboration of Terminal Alkenes

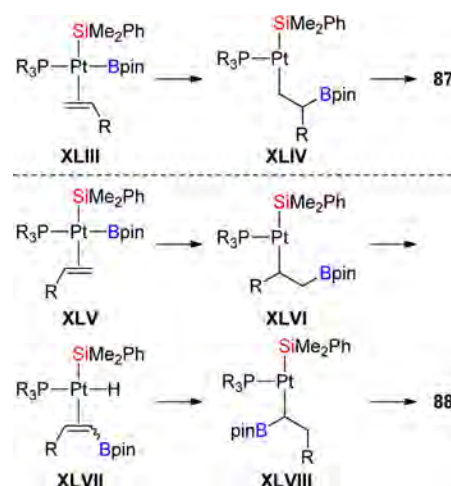


even detected but, instead, 1,1-difunctionalization was a minor side-reaction in a few cases (88a–c, Scheme 30). It is important to note that palladium–isocyanide complexes, which had been the catalysts of choice for the alkyne silaboration (cf. Scheme 15, upper, in section 4.1.1), were completely ineffective in this transformation. The mechanistic rationale is similar to that for the platinum(0) catalysis with alkynes (cf. Scheme 22 in section 4.1.1). Regioselective alkene insertion into the Pt–B bond is followed by reductive elimination to form the C–Si bond (XLIII → XLIV → 87, Scheme 31). The 1,1-disubstituted byproduct is supposed to be the result of a β-hydride elimination of intermediate XLVI (XLVI → XLVII) followed by hydroplatination with reverse regioselectivity (XLVII → XLVIII).<sup>47</sup>

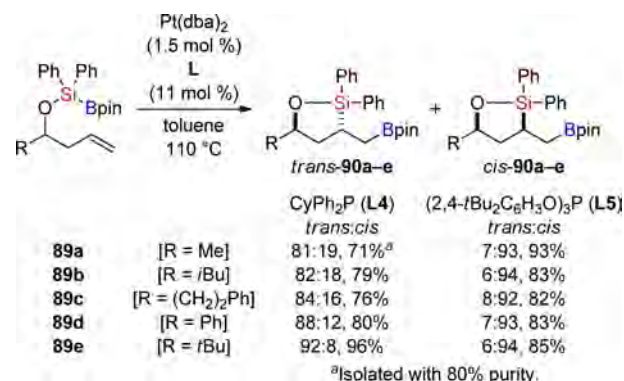
A few years ago, the laboratory of Sugimoto introduced an intramolecular variant of the above-described reaction where the formation of a 1,1-difunctionalized byproduct was not observed (Scheme 32).<sup>48</sup> A major aspect of this work is the ligand-dependent diastereoselectivity. With CyPh2P, silaboration across the tethered alkene is essentially trans-selective (89a–e → *trans*-90a–e, left column) whereas use of the bulky phosphite ligand (2,4-*t*Bu2C6H3O)3P resulted predominantly in the formation of the *cis*-isomers (89a–e → *cis*-90a–e, right column).

Distinctly different reactivity for this kind of substrates was observed when the terminal alkene was 1,1-disubstituted (91a–

Scheme 31. Key Steps of the Platinum(0)-Catalyzed Silaboration of Alkenes and Formation of the Byproduct

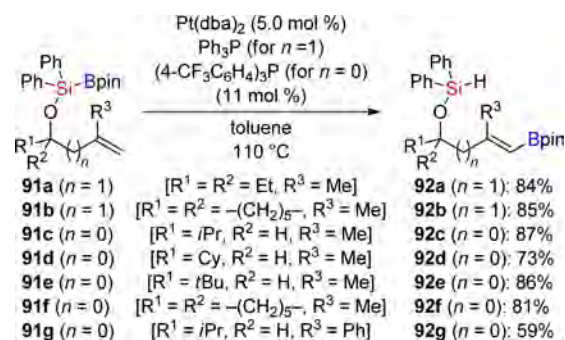


Scheme 32. Diastereoselective Intramolecular Silaboration of Alkenes



g, Scheme 33).<sup>49</sup> Dehydrogenative boration of the alkene terminus rather than silaboration occurred (91a–g → 92a–g).

Scheme 33. Intramolecular Dehydrogenative Boration of Alkenes



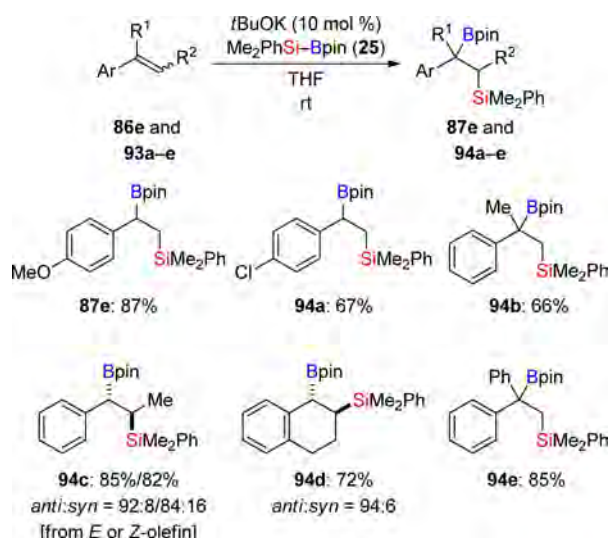
The authors suggested that the additional substituent at the alkene steers the reaction toward β-hydride elimination after C–B bond formation. Reductive elimination of the Si–Pt–H intermediate closes the catalytic cycle (not shown).

Very recently, a transition metal-free silaboration of aryl-substituted alkenes (mainly styrenes) was published by the Ito group of Hokkaido University.<sup>50</sup> The highly regioselective addition of Me2PhSi-Bpin (25) across several terminal and



internal alkenes was catalyzed by *t*BuOK, delivering the boryl group into the benzylic position in all cases (**86e** → **87e** and **93a–e** → **94a–e**, Scheme 34). Moreover, the diastereoselec-

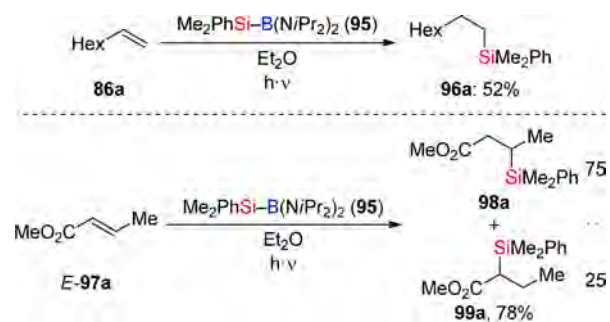
**Scheme 34.** Base-Catalyzed Silaboration of Aryl-Substituted Alkenes



tivity for internal alkenes is remarkable, and anti relative configuration is favored (**94c** and **94d**). It is interesting that either double-bond isomer of **93c** afforded the same major diastereomer. Conversely, aliphatic alkenes or acrylates showed no reaction under these conditions. The activation of the Si–B bond relies on the addition of *tert*-butoxide to the boron atom of  $\text{Me}_2\text{PhSi-Bpin}$  (**25**). The tetrahedral geometry at the boron atom was verified in stoichiometric NMR experiments. Further mechanistic details were, however, not reported by the authors.

Matsumoto and Ito investigated the photochemical homolytic cleavage of silyboranes.<sup>37</sup> When diamino-substituted  $\text{Me}_2\text{PhSi-B}(\text{NiPr}_2)_2$  (**95**) was irradiated in the presence of a terminal alkene, an alkylsilane, resulting from the addition of a silyl radical to the terminal position of the alkene, was isolated in moderate yield (**86a** → **96a**, Scheme 35, upper). The boryl

**Scheme 35.** Radical Silylation of Alkenes by Photochemical Si–B Bond Cleavage



fragment was not incorporated into the product. The hydrogen atom terminating the radical reaction is believed to originate mainly from the isopropyl groups of the aminoborane **95**. However, a solvent screening revealed that the reaction works particularly well in ether solvents, and the involvement of tetrahydrofuran (THF) as a hydrogen atom source was shown in a deuteration experiment. The intermediate boryl radical is

likely to abstract a hydrogen atom to form a hydroborane. Moreover, methyl crotonate also underwent this radical silylation although with moderate regioselectivity (**E-97a** → **98a** + **99a**, Scheme 35, lower), and with substoichiometric amounts of **95** a radical polymerization of the alkene with silyl groups as polymer termini was observed (not shown).<sup>37</sup>

#### 4.2. 1,2-, 1,4-, and 1,*n*-Addition to C–C Multiple-Bond Systems

**4.2.1. 1,3- and 1,6-Dienes.** Catalytic functionalization of 1,3-dienes is connected to several selectivity issues. Aside from differentiation between a 1,2- and a 1,4-addition, control of the regioselectivity as well as the double-bond geometry (in the case of 1,4-addition) must be considered. Diastereoselective or even enantioselective variants are also desirable. Again, the seminal contribution emerged from the Ito laboratory a decade ago.<sup>51</sup> Although palladium–isocyanide complexes, well-suited for alkyne silaboration, were completely ineffective, catalysts based on platinum furnished the 1,4-addition adducts yet as 1:1 mixtures of double-bond isomers. Conversely, a catalytic system derived from  $\text{Ni}(\text{acac})_2$  and dibal catalyzed the 1,4-addition of  $\text{Me}_2\text{PhSi-Bpin}$  (**25**) in high yields with complete control of the alkene geometry in favor of the *Z*-isomer (Scheme 36). Several

**Scheme 36.** 1,4-Silaboration of Acyclic 1,3-Dienes



acyclic 1,3-dienes were subjected to this protocol, affording the corresponding adducts with allylic boryl and silyl groups (Table 1). The only drawback of this method is the poor regioselectivity for the unsymmetrically substituted substrates **100b** and **100c** (entries 2 and 3).

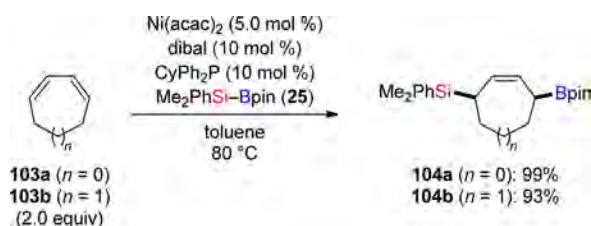
For the silaboration of cyclic 1,3-dienes, the elaborated reaction setup had to be modified as no product was obtained.<sup>51</sup> With the ligand  $\text{CyPh}_2\text{P}$ , the reaction was *cis*-selective and proceeded in excellent yields for cyclohexa-1,3-

**Table 1.** 1,4-Silaboration of Acyclic 1,3-Dienes

entry	substrate	product(s)	101:102 ratio	yield [%]
1			—	90
2			72:28	92
3			67:33	84
4			—	90

diene and cyclohepta-1,3-diene (**103a** and **103b**, Scheme 37). In turn, cyclopentadiene as well as cycloocta-1,3-diene were

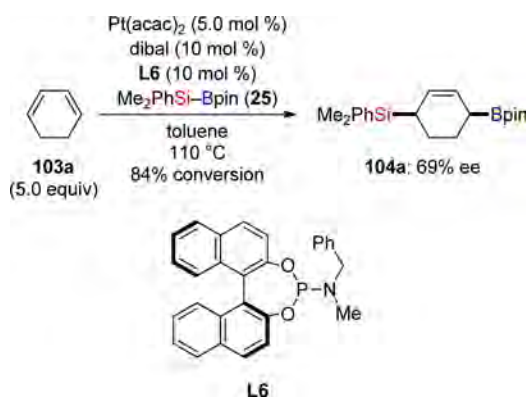
**Scheme 37. Cis-Selective 1,4-Silaboration of Cyclic 1,3-Dienes**



inert. The effect of the added phosphine ligands in platinum(0)-catalyzed silaborations on the kinetics of the oxidative addition and reductive elimination was investigated in detail by Moberg, Jutand, and co-workers with the aid of electrochemical methods.<sup>52</sup>

On the way to an asymmetric version of the previously illustrated silaboration of cyclohexa-1,3-diene (cf. **103a** → **104a**, Scheme 37), Gerdin and Moberg tested dozens of chiral phosphine and phosphoramidite ligands in combination with  $\text{Ni}(\text{acac})_2$  and  $\text{Pt}(\text{acac})_2$ .<sup>53</sup> Moderate enantioselectivity and high conversion were achieved in the platinum(0)-catalyzed variant with phosphoramidite **L6** (Scheme 38).

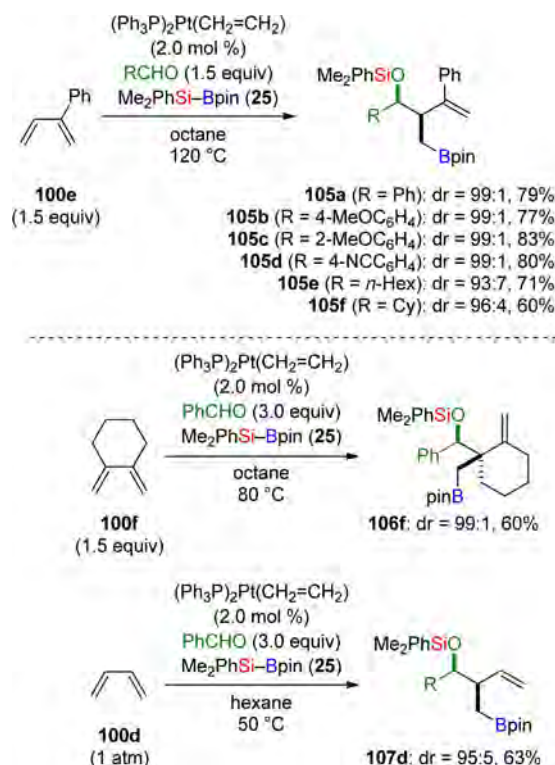
**Scheme 38. Enantioselective Silaboration of Cyclohexa-1,3-diene**



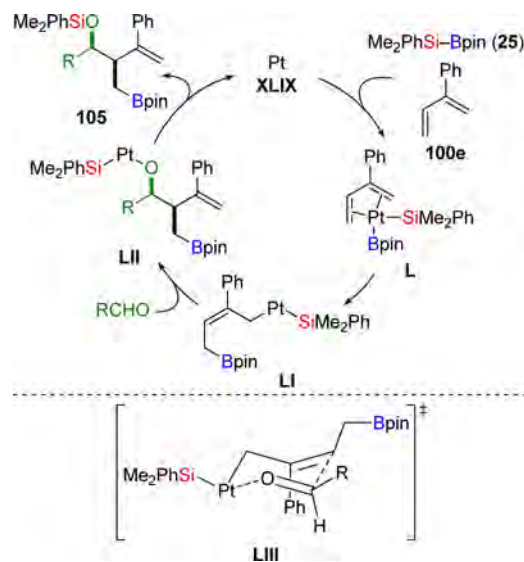
In an attempt to combine the 1,4-silaboration with an allylboration of an aldehyde in a domino reaction, Ito and co-workers found the unexpected outcome of an intercepted 1,4-silaboration.<sup>54</sup> Three new bonds (a C–B, a C–C, and a Si–O bond) were formed, arriving at silicon-protected homoallylic alcohols (**100e** → **105a–f**, Scheme 39, upper). Fortunately, this platinum(0)-catalyzed reaction proceeded with high regio- and diastereoselectivity for several aldehydes in the reaction with 2-phenylbuta-1,3-diene (**100e**) and  $\text{Me}_2\text{PhSi-Bpin}$  (**25**). The same reaction was observed for 1,2-dimethylenecyclohexane (**100f**) and buta-1,3-diene (**100d**) (Scheme 39, lower).

The authors explained the formation of the unexpected product by the addition of the allylic platinum(II) intermediate **LI** to the aldehyde (**LI** → **LII**, Scheme 40, upper) instead of the usual C–Si bond formation through reductive elimination. The platinum(0) complex **XLIX** is reformed by reductive elimination of the alkoxy(silyl)platinum complex **LII** with concomitant Si–O bond formation (**LII** → **105**). The high diastereoselectivity was rationalized by a cyclic transition state

**Scheme 39. Silaborative C–C Bond Formation Between 1,3-Dienes and Aldehydes**



**Scheme 40. Proposed Mechanism of the Silaborative C–C Bond Formation**



for the aldehyde addition step with platinum(II) as Lewis acid (**LIII**, Scheme 40, lower).<sup>54</sup>

Saito, Kobayashi, and Sato succeeded in elaborating a nickel(0)-catalyzed three-component coupling of 1,3-dienes, aldehydes, and  $\text{Me}_2\text{PhSi-Bpin}$  (**25**).<sup>55</sup> A key intermediate in this process is the cyclic allylnickel complex **LIV** with a Ni–O bond, which is generated through oxidative cycloaddition of the 1,3-diene and an aldehyde to a nickel(0) complex (**100** or **109** → **LIV**, Scheme 41). Together with  $\text{Me}_2\text{PhSi-Bpin}$  (**25**), transmetalation or  $\sigma$ -bond metathesis affords then the allylic nickel(II) species **LV** (**LIV** → **LV**) and final reductive



Reaction scheme for the asymmetric allylic alkylation of **100** or **109** with **Me<sub>2</sub>PhSi-Bpin** (**25**) and **R<sup>3</sup>CHO** (2.5 equiv) in DMF at rt, catalyzed by **Ni(cod)<sub>2</sub>** (10 mol %) and ligand (10 mol %). The reaction proceeds via a **L<sub>n</sub>Ni<sup>0</sup>** complex, forming intermediate **LIV** (a nickelacycle with a **Me<sub>2</sub>PhSi-Bpin** group), which then yields product **108** or **110** (after hydrolysis) and regenerates the **L<sub>n</sub>Ni<sup>0</sup>** catalyst.

From optimization studies, ligand **L7** was identified as appropriate, allowing for the reaction of diene **100g** with various aldehydes to furnish the corresponding products **108a–g** as single diastereomers with high enantiomeric purities (**100g** → **108a–g**, Scheme 42, upper). Generally good chemical yields

**100g**

**L7**  
 $(R^1 = \text{CHPh}_2)$

**108a** ( $R^2 = 4\text{-MeC}_6\text{H}_4$ ): 96% ee, 89%  
**108b** ( $R^2 = 4\text{-MeOC}_6\text{H}_4$ ): 92% ee, 92%  
**108c** ( $R^2 = 4\text{-CF}_3\text{C}_6\text{H}_4$ ): 85% ee, 29%  
**108d** ( $R^2 = 1\text{-C}_{10}\text{H}_7$ ): 92% ee, 72%  
**108e** ( $R^2 = i\text{Pr}$ ): 96% ee, 68%  
**108f** ( $R^2 = i\text{Bu}$ ): 97% ee, 56%  
**108g** ( $R^2 = \text{Cy}$ ): 94% ee, 74%

---

**100h** [ $R^1 = \text{SiMe}_2\text{Ph}$ ,  $R^2 = \text{H}$ ]  
**100i** [ $R^1 = (\text{CH}_2)_2\text{Ph}$ ,  $R^2 = \text{H}$ ]  
**109a** [ $R^1 = 4\text{-MOMOC}_6\text{H}_4$ ,  $R^2 = \text{Me}$ ]  
**109b** [ $R^1 = R^2 = \text{Ph}$ ]

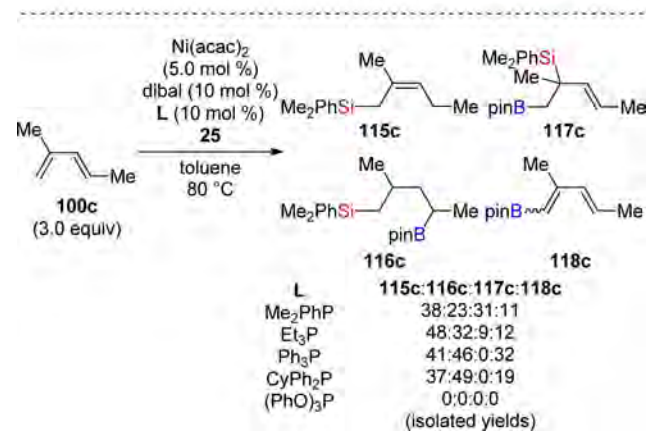
**108h**: 82% ee, 80%  
**108i**: 66% ee, 62%  
**110a**: 92% ee, 22%  
**110b**: 20% ee, 51%

1,3-dienes **109a** and **110a** were less suitable, giving either low yield (**109a**  $\rightarrow$  **110a**, 22% yield, 92% ee) or diminished enantiomeric excess (**109b**  $\rightarrow$  **110b**, 51% yield, 20% ee). Nevertheless, this approach provides an efficient catalytic asymmetric access to enantiomerically enriched allylic silanes.

Reaction scheme showing the asymmetric allylation of pinacol boronate ester **111** with  $\text{Me}_2\text{PhSi}-\text{Bpin}$  (**25**) catalyzed by  $(\text{PPh}_3)_4\text{Pt}$  (3.0 mol %) in toluene at  $80^\circ\text{C}$ . The product is **112**, a single diastereomer (56% yield, not assigned).

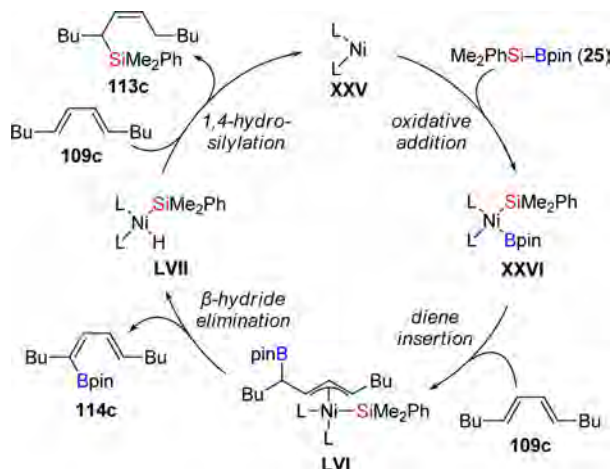
Reaction scheme for the asymmetric hydrogenation of 109c:

109c (2.0 equiv) reacts with  $\text{Ni}(\text{acac})_2$  (5.0 mol %),  $\text{dibal}$  (10 mol %),  $\text{Et}_3\text{P}$  (10 mol %), and  $\text{Me}_2\text{PhSi-Bpin}$  (25) in toluene at 80 °C to yield 113c (Z/E > 97:3, 77%) and 114c (E/E/Z,E = 5:1, 90%).



As neither a hydrosilane nor a hydroborane had been added to the reaction mixture, the authors explained the reaction outcome by a disproportionation mechanism (Scheme 45).<sup>57</sup> After the insertion of the 1,3-diene **109c** into the Pt–B bond

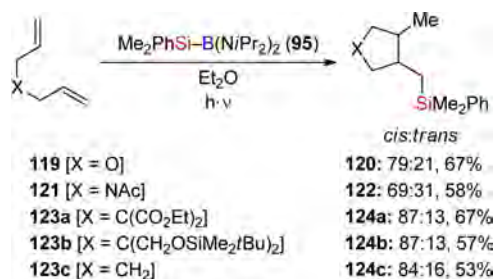
### Scheme 45. Proposed Mechanism for the Silaborative Disproportionation



(XXVI  $\rightarrow$  LVI), the allylnickel intermediate LVI is likely to suffer  $\beta$ -hydride elimination (LVI  $\rightarrow$  LVII) rather than reductive elimination with both terminal carbon atoms of the allylic system LVI substituted. This step delivers the borated product 114c along with the Si–Ni–H complex LVII. The latter is then available for a 1,4-hydrosilylation with another molecule of the diene (LVII + 109c  $\rightarrow$  113c).

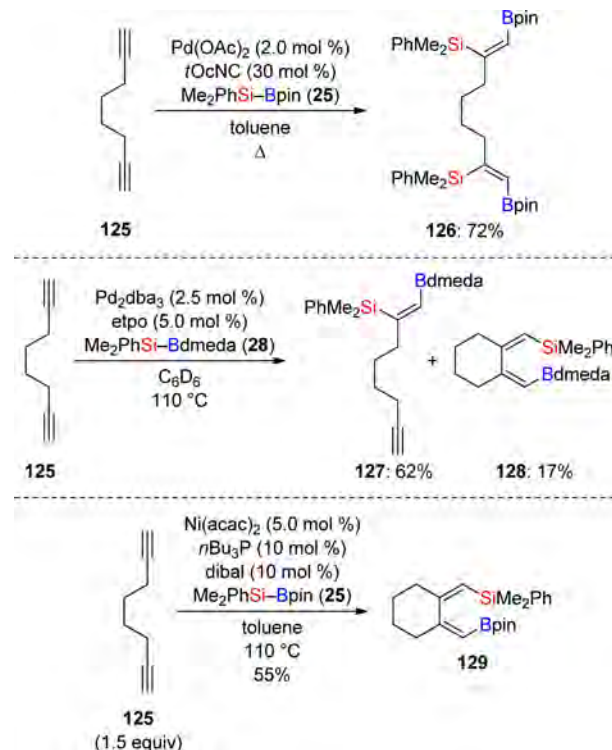
The photochemical cleavage of  $\text{Me}_2\text{PhSi-B}(\text{NiPr}_2)_2$  (**95**) was investigated by Matsumoto and Ito not only for alkenes (cf. Scheme 35 in section 4.1.2) but also in the presence of 1,6-dienes.<sup>37</sup> A radical alkene silylation–5-*exo*-cyclization sequence furnished tetrahydrofurans (**119** → **120**), pyrrolidines (**121** → **122**), and cyclopentanes (**123a–c** → **124a–c**) in acceptable yields but with moderate diastereoselectivities (Scheme 46). As in the photochemical alkene silylation, the diaminoboryl group was not incorporated into the final product but served as a hydrogen source.

**Scheme 46. Silylative Radical 5-*Exo*-Cyclization of 1,6-Dienes**



**4.2.2. 1,7-Diynes and 1,3- and 1,6-Enynes.** The silaboration of octa-1,7-diyne (**125**) was independently investigated by the groups of Ito<sup>16b,43</sup> and Tanaka.<sup>17</sup> The outcome was subtly dependent on the transition metal–ligand combination. The ligand was crucial in the palladium(0)-catalyzed variants. An isocyanide ligand led to clean formation of the double 1,2-addition product (**125** → **126**, Scheme 47, upper)<sup>16b</sup> while the etpo ligand furnished a mixture of mono 1,2-addition product **127** and cyclic byproduct **128** (Scheme 47, center).<sup>17</sup> The cyclization product **129** became the main product when a nickel(0) catalyst was used (Scheme 47, lower), corresponding to the intramolecular version of the

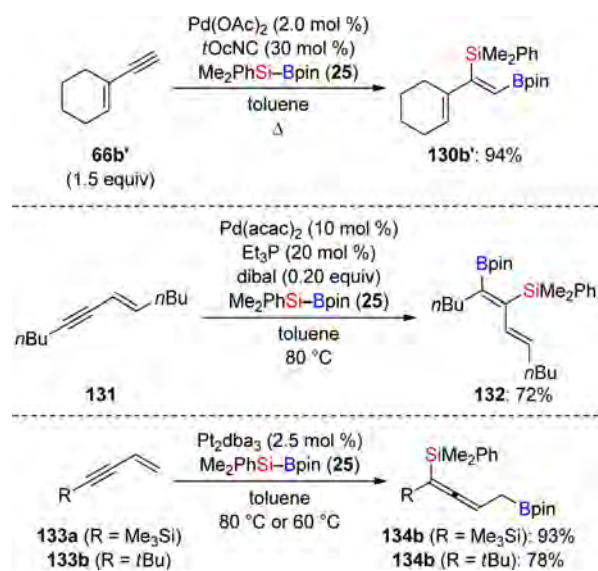
**Scheme 47. Silaboration of Oct-1,7-diyne**



nickel(0)-catalyzed dimerization of alkynes (cf. Schemes 23 and 24 in section 4.1.1).<sup>43</sup>

Similar to the 1,7-diyne structure, the 1,3-enyne motif also possesses different reactivities toward Si–B compounds. Silaboration of 1-ethynylcyclohexene (**66b'**) had already been included in the seminal paper by Ito and co-workers (**66b'** → **130b'**, Scheme 48, upper).<sup>16a</sup> **130b'** is derived from a chemoselective addition of Me<sub>2</sub>PhSi–Bpin (**25**) across the triple bond, leaving the double bond unreacted. Building on this finding, Lützen and Möberg extensively investigated several 1,3-enynes in palladium(0)- and platinum(0)-catalyzed silabo-

**Scheme 48. Silaboration of 1,3-Enynes: 1,2- versus 1,4-Addition**

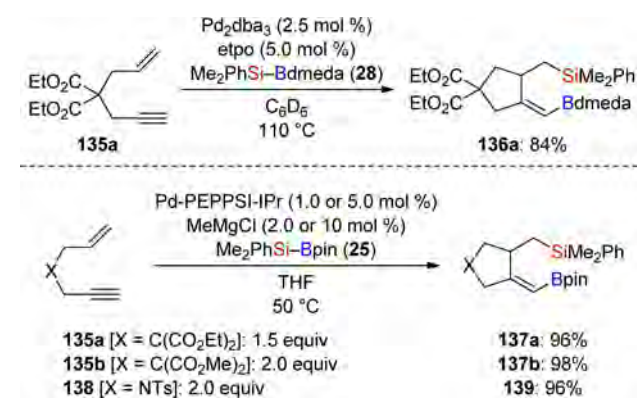




rations.<sup>58</sup> It turned out that the 1,2-addition of  $\text{Me}_2\text{PhSi-Bpin}$  (**25**) across the C–C triple bond is the normal reactivity as for **131** (**131**  $\rightarrow$  **132**, Scheme 48, center), and that the control of the regioselectivity was not facile for some substrates. A bulky R group installed at the alkyne terminus thwarted 1,2-addition, and 1,4-addition yielded allenyl products (**133a**  $\rightarrow$  **134a** and **133b**  $\rightarrow$  **134b**, Scheme 48, lower).

As part of their seminal work, Tanaka and co-workers also reported a high-yielding silaborative cyclization of a 1,6-enyne (**135a**  $\rightarrow$  **136a**, Scheme 49, upper).<sup>17</sup> C–B bond formation in

Scheme 49. Silaborative Cyclizations of 1,6-Enynes

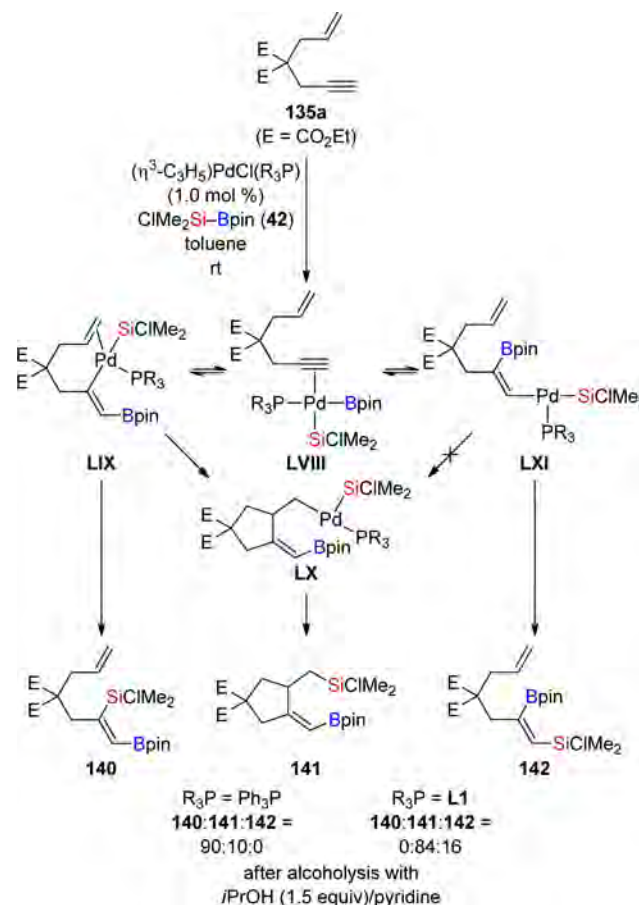


the terminal position is in agreement with the generally accepted mechanistic picture. Moberg and co-workers extended the scope of this reaction by applying a palladium–PEPPSI–carbene complex (PEPPSI = pyridine-enhanced precatalyst preparation stabilization and initiation).<sup>59</sup> Their protocol afforded excellent yields for cyclopentanes **137a** and **137b**, as well as for pyrrolidine **139** (Scheme 49, lower).

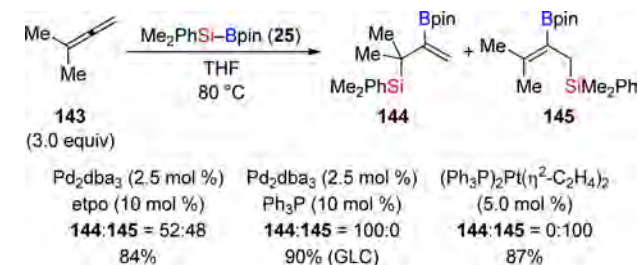
Ohmura, Sugimoto, and co-workers used 1,6-enynes as a probe to gain insight into the mechanism of the regioselective alkyne silaboration.<sup>39</sup> Conceivable reaction pathways are summarized in Scheme 50. The silaborative cyclization products, observed in the aforementioned reactions, result from a regioselective insertion of the C–C triple bond into the Pd–B bond (LVIII  $\rightarrow$  LIX) followed by insertion of the C–C double bond into the C–Pd bond (LIX  $\rightarrow$  LX). The reaction is terminated by reductive elimination, thereby forming the terminal C–Si bond (LX  $\rightarrow$  **141**). However, this reaction is highly ligand-dependent. With  $\text{Ph}_3\text{P}$ , reductive elimination appears to be faster than cyclization, leading to 1,2-addition (LIX  $\rightarrow$  **140**). In contrast, with sterically demanding **L1**, cyclic compound **141** is formed predominantly (LX  $\rightarrow$  **141**) along with a small amount of “inverse addition” product (LXI  $\rightarrow$  **142**).

**4.2.3. Allenes.** The silaboration of allenes is a beautiful illustration of an evolution from gaining control over regioselectivity to controlling the diastereo- and, finally, enantioselectivity of a reaction. It all started with two seminal contributions about 10 years ago, one by the laboratory of Tanaka<sup>60</sup> and one by Ito and co-workers.<sup>61</sup> The former group investigated the influence of different catalytic systems on the silaboration of 1,1-dimethylallene (**143**) with  $\text{Me}_2\text{PhSi-Bpin}$  (**25**) (Scheme 51). Although a palladium–etpo combination showed no regioselectivity (Scheme 51, left), addition of  $\text{Ph}_3\text{P}$  resulted in a completely selective reaction with the boryl group connected to the central carbon atom and the silyl group connected to the more substituted terminus (**143**  $\rightarrow$  **144**,

Scheme 50. Possible Reaction Pathways of 1,6-Enynes



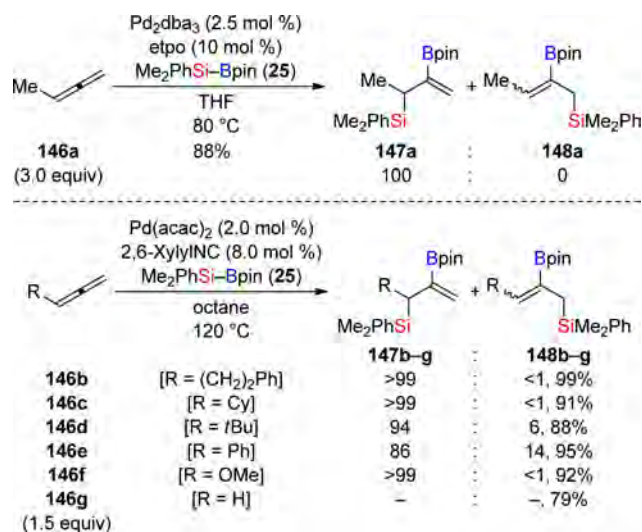
Scheme 51. Influence of the Transition Metal–Ligand on the Silaboration of 1,1-Dimethylallene



Scheme 51, center). The application of a platinum catalyst reversed this selectivity, now positioning the silyl group at the unsubstituted terminus (**143**  $\rightarrow$  **145**, Scheme 51, right).  $\text{Me}_2\text{PhSi-Bdmeda}$  (**28**), which had proven to react in alkyne silaboration (cf. Scheme 15, center, in section 4.1.1), was not applicable to allenes.<sup>60</sup>

Conversely, the regioselectivity was also high with the palladium–etpo catalyst for 1-methylallene (**146a**  $\rightarrow$  **147a**, Scheme 52, upper).<sup>60</sup> Ito and co-workers introduced a modified palladium–isocyanide complex that effectively catalyzed the difunctionalization of monosubstituted allenes in high yields and with excellent regioselectivities (**146b–g**  $\rightarrow$  **147b–g**, Scheme 52, lower).<sup>61</sup> Again, the boryl group was transferred to the central position without exception, and the silyl group was preferentially attached to the substituted allene carbon. The manifold synthetic applications of  $\beta$ -borated allylic silanes were

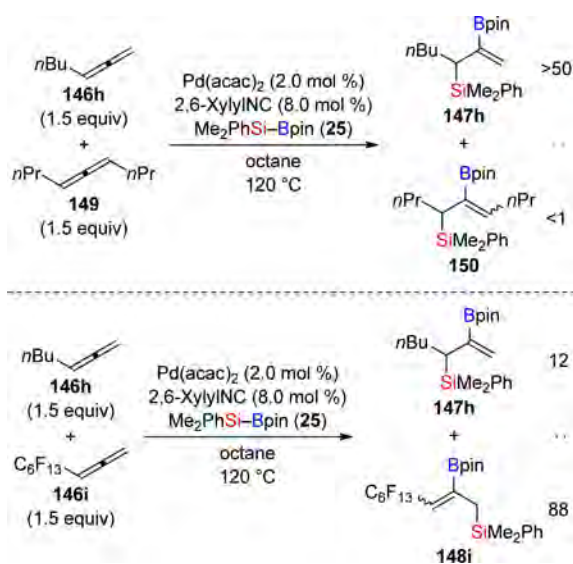
Scheme 52. Regioselective Silaboration of Monosubstituted Allenes



demonstrated by Suginome and Ito in a separate publication (not shown).<sup>62</sup>

To elucidate the mechanism and to clarify the origin for the regioselectivity, Suginome and Ito conducted several control experiments<sup>63</sup> and performed theoretical investigations in collaboration with Ehara, Nakatsuji, and co-workers some years later.<sup>64</sup> First, it was shown that monosubstituted allene **146h** reacted preferentially in the presence of 1,3-disubstituted **149**, although both substrates were found to undergo addition of the Si-B bond across the internal double bond in separate experiments (Scheme 53, upper). Second, electron-poor allene

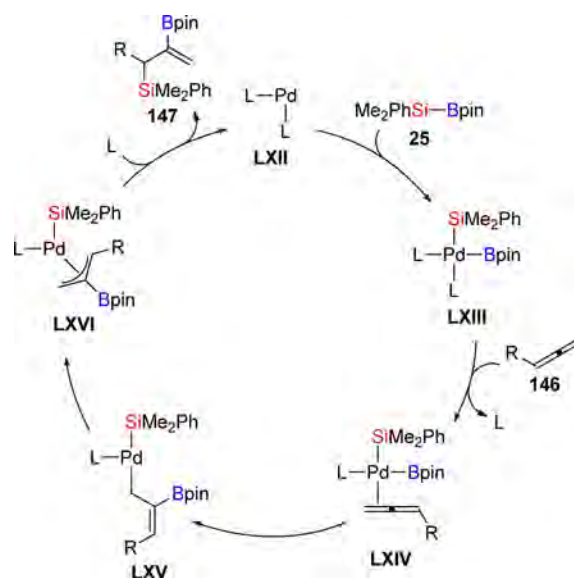
Scheme 53. Competition Experiments Between Differently Substituted Allenes



**146i** reacted faster than electron-rich allene **146h** as demonstrated in another competition experiment (Scheme 53, lower).<sup>63</sup> Moreover, a change of regioselectivity was observed for electron-withdrawing substituents as in **146i**.<sup>61,63</sup>

These results, together with the theoretical investigations,<sup>64</sup> were merged into a detailed mechanistic picture (Scheme 54).<sup>63</sup> After oxidative addition of Me<sub>2</sub>PhSi-Bpin (**25**) to the

Scheme 54. Proposed Mechanism for the Palladium(0)-Catalyzed Silaboration of Allenes



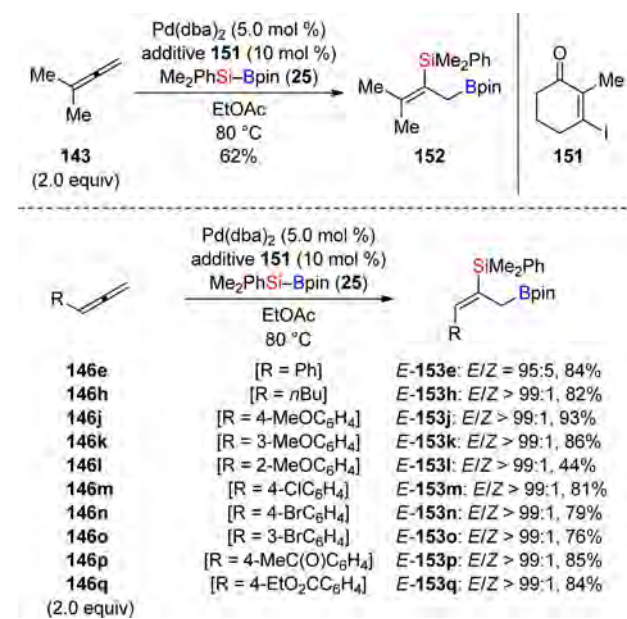
palladium(0) complex (LXII  $\rightarrow$  LXIII), the allene **146** displaces the ligand trans to the silyl group (LXIII  $\rightarrow$  LXIV). The subsequent insertion of the allene into the Pd-B bond was found to be rate-determining and proceeds with the more electron-deficient, i.e., terminal, double bond (LXIV  $\rightarrow$  LXV). Reductive elimination from the thus-formed  $\sigma$ -allylic palladium intermediate LXV cannot proceed due to the trans relationship of the silyl and allyl ligands in LXV. The crucial step in terms of the regioselectivity is the conversion of the  $\sigma$ - into the  $\pi$ -allylic complex LXVI, which enables an instantaneous reductive elimination from the cis complex (LXVI  $\rightarrow$  LXII + **147**). This step is supposed to be faster than interconversion of *cis*- and *trans*- $\pi$ -allylic intermediates (not shown), from which the other regioisomer would be released. Hence, reductive elimination is kinetically controlled, and that explains the predominant formation of the thermodynamically less stable internal addition compound **147**.<sup>64</sup>

Quite contrary to the examples discussed above, the presence of an organic iodide totally changes the regioselectivity of the silaboration reaction (Scheme 55).<sup>65</sup> Cheng and co-workers reported that the presence of catalytic amounts of **151** led to a 1,2-addition product with the silyl group attached to the central allene carbon atom and the boryl group in the terminal position (**143** $\rightarrow$ **152**, Scheme 55, upper). The effect was general for several 1,1- and monosubstituted allenes, and *E/Z*-ratios were excellent for the latter (**146**  $\rightarrow$  *E*-**153**, Scheme 55, lower).

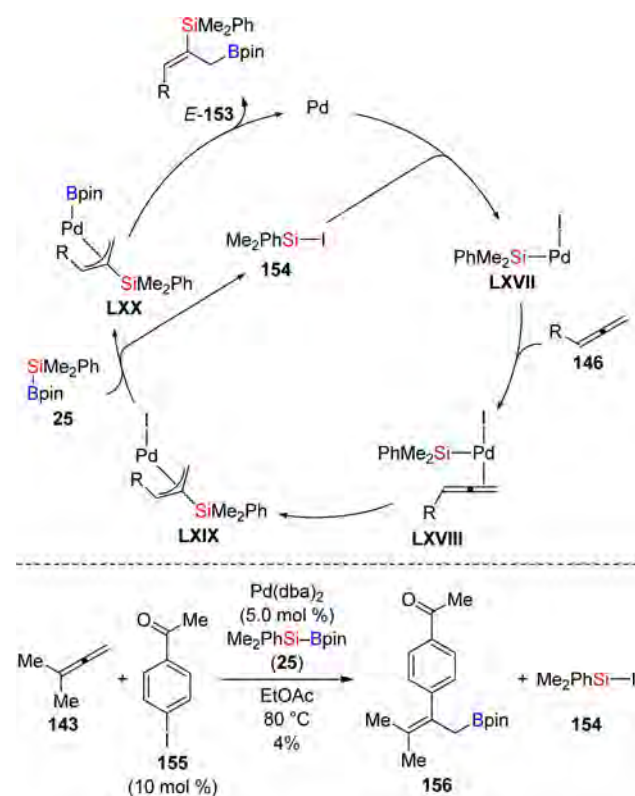
As *normal* selectivity was observed without this additive (cf. Schemes 51 and 52), it was obvious that iodide **151** accounts for this remarkable effect.<sup>65</sup> The authors suggested a mechanism that is fundamentally different from that of the iodide-free setup. The oxidative addition/reductive elimination mechanism (cf. Scheme 54) is replaced by a transmetalation mechanism with regard to Si-B bond activation (Scheme 56, upper). To initiate the catalysis, oxidative addition of the C-I bond in additive **151** to palladium(0) and subsequent transmetalation with Me<sub>2</sub>PhSi-Bpin (**25**) liberates Me<sub>2</sub>PhSi-I (**154**). We note here that the chemoselectivity of the transmetalation of the Pd-I intermediate is opposite to that of Cu-O and Rh-O complexes (cf. Scheme 11, lower in section 3). The resulting arylpalladium(II) complex with a Pd-B bond



Scheme 55. Silaboration of Allenes with Reverse Regioselectivity



Scheme 56. Mechanistic Rationale for the Silaboration with Inversed Regioselectivity

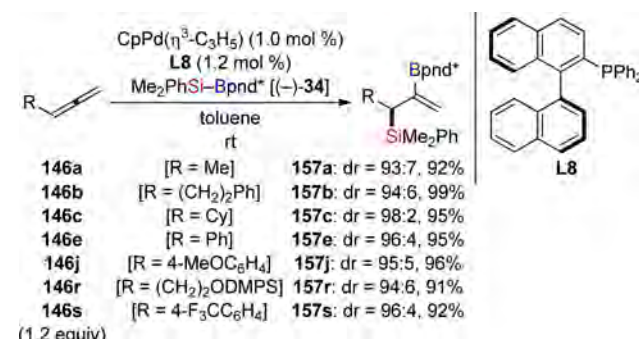


further reacts with the allene to afford a 1,2-addition adduct (not shown). The formation of this adduct was verified using aryl iodide 155, and 4% isolated 156 nicely agrees with 5 mol % catalyst loading (Scheme 56, lower). The Si-I reagent 154 generated in the initial turnover then oxidatively adds to palladium(0) (154 → LXVII). Silapalladation of the less-substituted double bond of the allene produces an allylic intermediate (LXVII → LXVIII → LXIX) that transmetalates

with Me<sub>2</sub>PhSi-Bpin (25) (LXIX → LXX), thereby regenerating Me<sub>2</sub>PhSi-I (154) and forming allyl(boryl)palladium intermediate LXX. The catalytic cycle closes with C-B bond formation in the final reductive elimination (LXX → E-153). Comparable results are obtained by direct use of Me<sub>2</sub>PhSi-I (154) as additive.<sup>65</sup> The diastereoselectivity in favor of *E*-configuration was explained by the steric repulsion of the R substituent and the silyl group in the silapalladation step (LXVIII → LXIX).

An approach to asymmetric silaboration of allenes was reported by Sugimoto, Murakami, and co-workers a decade ago.<sup>19</sup> A matched combination of the pinanediol-derived enantiopure silylboronic ester (–)-34 and the chiral ligand L8 afforded the allylic silanes 157 in excellent yields and with high diastereoselectivities (Scheme 57). The catalyst precursor

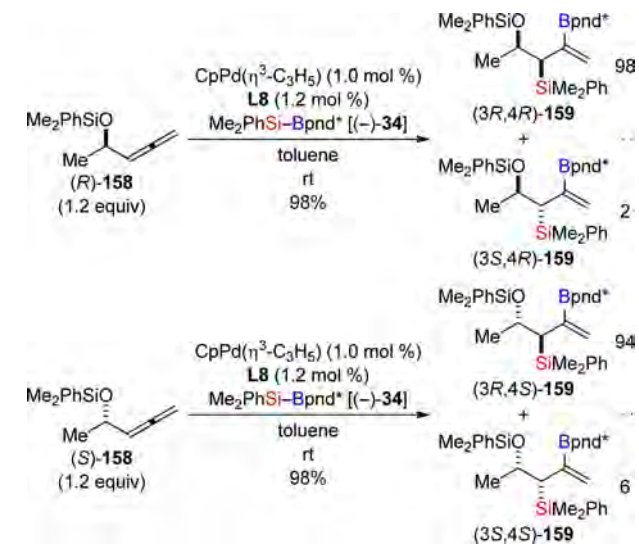
Scheme 57. Reagent- and Catalyst-Controlled Diastereoselective Silaboration of Allenes



CpPd(η<sup>3</sup>-C<sub>3</sub>H<sub>5</sub>) even allowed for running the reactions at room temperature. The fact that both the chiral catalyst and the chiral reagent had an influence on the selectivity was further verified when achiral Me<sub>2</sub>PhSi-Bpin (25) was used together with L8; only moderate enantioselectivity of 68% ee was obtained (not shown).<sup>19</sup>

In an extension of this work, Ohmura and Sugimoto applied this silaboration to α-chiral allenes (Scheme 58).<sup>66</sup> It was nicely shown that the combination of the chiral ligand L8 and the

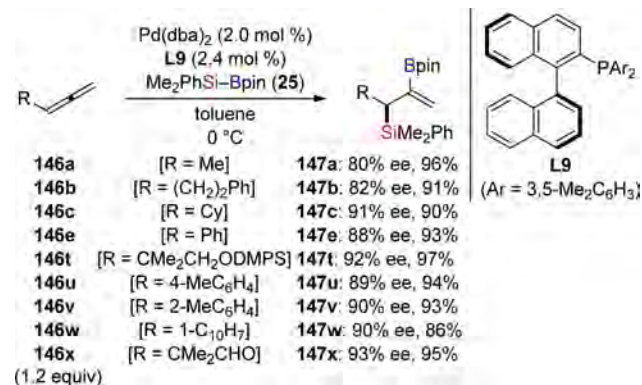
Scheme 58. Diastereoselective Silaboration of α-Chiral Allenes



chiral reagent (–)-**34** overrides the stereochemical information present in the molecule, that is, catalyst and reagent control outcompete substrate control. This method enabled access to all possible stereoisomers of the protected  $\beta$ -silyl alcohol **159**.

A few years later, Suginome and co-workers succeeded in the elaboration of an enantioselective variant of the silaboration of allenes by tuning the axially chiral ligand **L8**.<sup>67</sup> With **L9**, enantioselectivities as high as 93% ee were obtained (**146**  $\rightarrow$  **147**, Scheme S9). Also, a substrate containing both allene and alkyne moieties was chemoselectively silaborated at the allene function (not shown).<sup>67</sup>

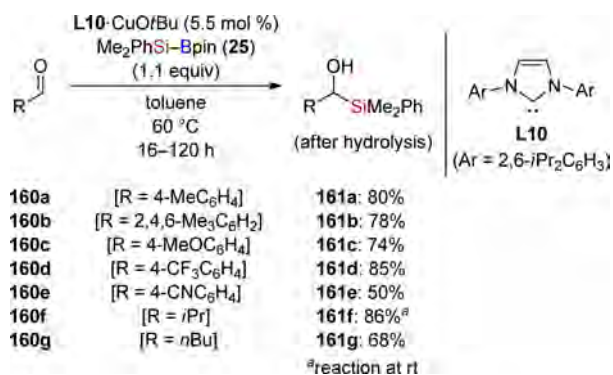
Scheme S9. Enantioselective Silaboration of Allenes



#### 4.3. 1,2-Addition to C–Het Double Bonds

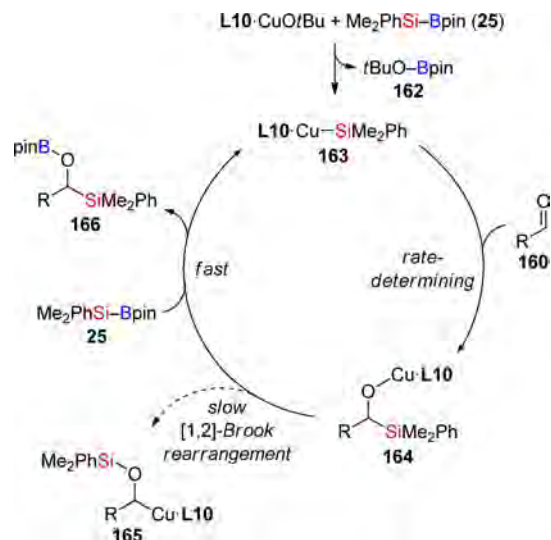
**4.3.1. Aldehydes.** In the recent past, the possibility of the catalytic generation of nucleophilic Cu–Si reagents through transmetalation of copper(I) alkoxide/hydroxide complexes with Me<sub>2</sub>PhSi–Bpin (**25**) attracted considerable interest. Among others, the 1,2-addition of silicon nucleophiles to aldehydes represents a potential field of application. Accordingly, Kleeberg and our group investigated this reaction in detail with stoichiometric and catalytic experiments combined with NMR spectroscopic measurements.<sup>68</sup> Our findings resulted in the elaboration of a convenient protocol for the synthesis of  $\alpha$ -silyl alcohols using preformed **L10**·CuOtBu as catalyst (Scheme 60). Transformation of aromatic and aliphatic aldehydes at 60 °C in toluene afforded the products in generally good yields, usually within 16 h. However, prolonged reaction time was required for sterically hindered and electron-rich aryl groups (**160b**  $\rightarrow$  **161b**, 120 h, and **160c**  $\rightarrow$  **161c**, 84 h).

Scheme 60. Copper(I)-Catalyzed 1,2-Silylation of Aldehydes Using **L10**·CuOtBu



As already mentioned, detailed studies were conducted to elucidate the mechanism (Scheme 61). The formation of

Scheme 61. Mechanism of Copper(I)-Catalyzed 1,2-Silylation of Aldehydes Using **L10**·CuOtBu



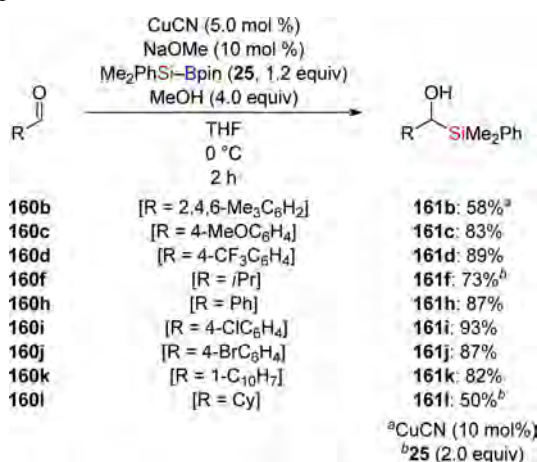
**L10**·Cu–SiMe<sub>2</sub>Ph (**163**) from **L10**·CuOtBu and Me<sub>2</sub>PhSi–Bpin (**25**) was confirmed in an independent stoichiometric experiment. Its presence in the reaction mixture during the catalytic process was likewise secured with the aid of <sup>1</sup>H NMR spectroscopy indicating that **163** is the copper complex with the longest lifetime. Hence, insertion of the aldehyde **160** into the Cu–Si bond is assumed to be rate-determining (**163**  $\rightarrow$  **164**). Subsequent transmetalation of **164** with another molecule of **25** should be fast, giving rise to **166** and Cu–SiMe<sub>2</sub>Ph (**163**) (**164**  $\rightarrow$  **163** + **166**). The same step must also be substantially faster than the competing [1,2]-Brook rearrangement (**164**  $\rightarrow$  **165**), which is observed in stoichiometric experiments where no Me<sub>2</sub>PhSi–Bpin (**25**) is available for the regeneration of **L10**·Cu–SiMe<sub>2</sub>Ph (**163**). Attempted reaction of isolated [1,2]-Brook rearrangement product **165** with Me<sub>2</sub>PhSi–Bpin (**25**) did not produce any boric ester **166**, suggesting that **165** is not involved in the catalysis and that there is no rapid equilibrium between **165** and **164**.<sup>68</sup>

A more reactive catalytic system evolves from a combination of CuCN and NaOMe in THF/MeOH without added ligands (Scheme 62).<sup>68</sup> Fast turnover at significantly lower temperatures enabled the efficient transformation of aromatic and aliphatic aldehydes into  $\alpha$ -silyl alcohols (**160**  $\rightarrow$  **161**). In agreement with previous results (cf. Scheme 60), electron-deficient unhindered aldehydes performed best whereas double the amount of the catalyst was required to obtain reasonable yields for sterically demanding substrate **160b** (**160b**  $\rightarrow$  **161b**, 58% yield). Aliphatic aldehydes **160g** and **160l** gave decent yields only when using excess Me<sub>2</sub>PhSi–Bpin (**25**) (**160g**  $\rightarrow$  **161g** and **160l**  $\rightarrow$  **161l**). Notably, the order of reagent addition is pivotal to consistent results.

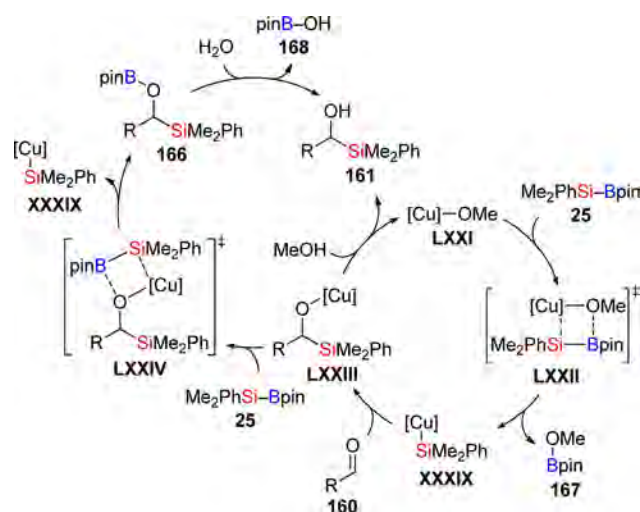
In many aspects the catalytic cycle for the CuCN/NaOMe system resembles the one investigated in detail for **L10**·CuOtBu (cf. Scheme 61). It is initiated by the boron-to-copper transmetalation of the in situ-formed Cu(I)–OMe complex **LXXI** and Me<sub>2</sub>PhSi–Bpin (**25**), producing the nucleophilic Cu(I)–SiMe<sub>2</sub>Ph complex **XXXIX** (**LXXI**  $\rightarrow$  **LXXII**  $\rightarrow$  **XXXIX**, Scheme 63). 1,2-Addition to the aldehyde



Scheme 62. Copper(I)-Catalyzed 1,2-Silylation of Aldehydes using CuCN/NaOMe



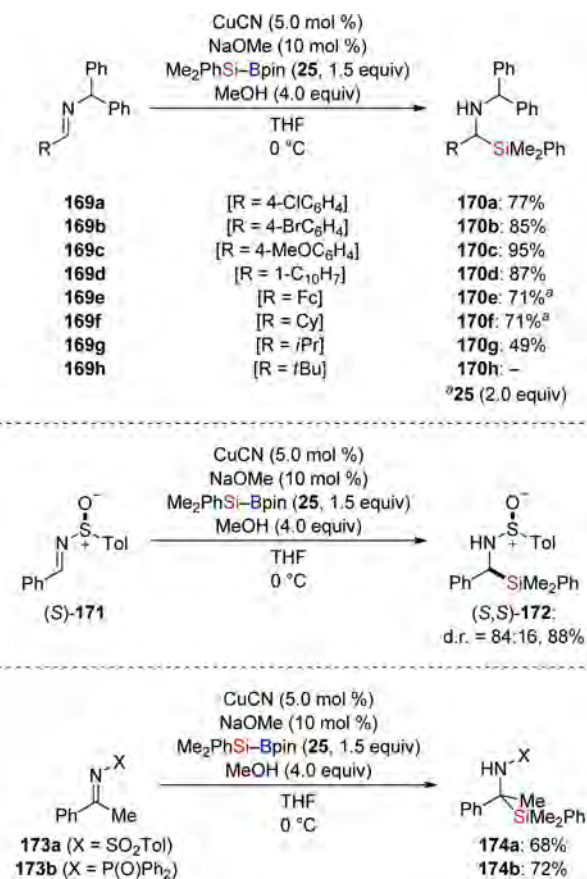
Scheme 63. Mechanism of Copper(I)-Catalyzed 1,2-Silylation of Aldehydes Using CuCN/NaOMe



160 (XXXIX → LXXIII) is followed by protonation of the thus-obtained copper alkoxide LXXIII in the presence of MeOH (LXXIII → LXXI + 161). Without added MeOH, most likely another  $\sigma$ -bond metathesis of intermediate LXXIII with 25 occurs, resulting in the formation of 166 and Cu(I)-SiMe<sub>2</sub>Ph (XXXIX) (LXXIII → LXXIV → XXXIX + 166). Hydrolysis during the aqueous workup affords the  $\alpha$ -silyl alcohol 161 (166 → 161).

**4.3.2. Imines.** Activation of the Si-B bond through copper(I)-catalyzed transmetalation was exploited in our laboratories for the generation of silicon nucleophiles that cleanly add to imine electrophiles to form  $\alpha$ -silylated amines (Scheme 64).<sup>69</sup> A range of substituents at the nitrogen atom, e.g., SO<sub>2</sub>Tol, P(O)Ph<sub>2</sub>, phenyl, or benzhydryl, are tolerated under the reaction conditions, and the substrate scope of aldehyde-derived imines was investigated using the benzhydryl group (Scheme 64, upper). Good yields were obtained for aryl- as well as hindered alkyl-substituted compounds with the latter requiring an increased amount of Me<sub>2</sub>PhSi-Bpin (25) (169a–g → 170a–g). In contrast, no conversion was observed for an imine with a tertiary alkyl group (169h → 170h). Apart from that, a diastereocontrolled addition to the enantiopure sulfinylimine (S)-171 was reported, yielding the chiral  $\alpha$ -

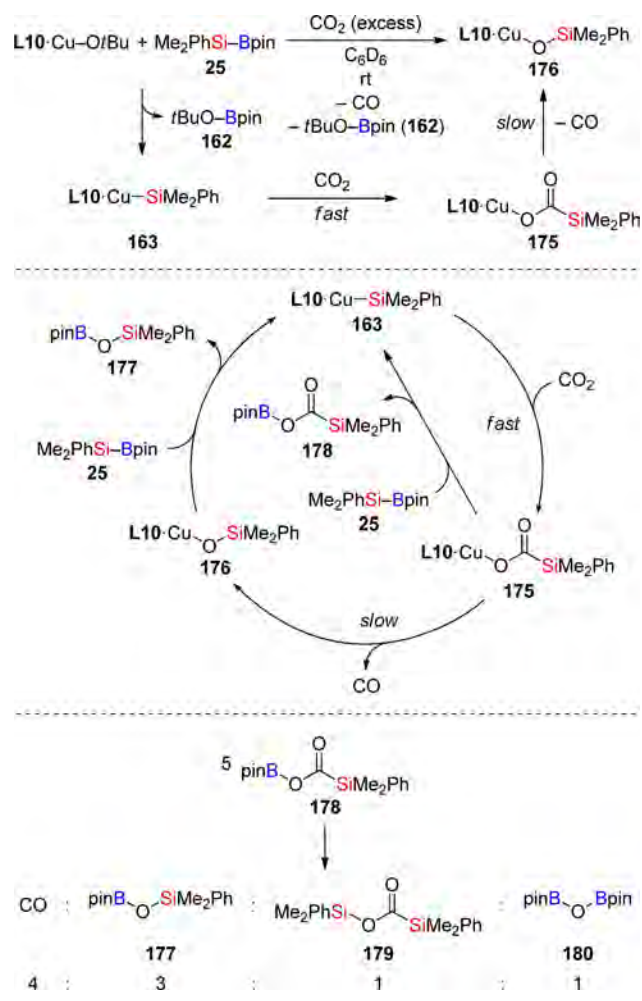
Scheme 64. Copper(I)-Catalyzed 1,2-Silylation of Imines



silylated amine (S,S)-172 in good yield and with decent diastereoselectivity [(S)-171 → (S,S)-172, Scheme 64, center]. Challenging ketimines proved to be suitable substrates for the silylation as well, and this time electron-withdrawing groups at the nitrogen atom were indispensable for a successful transformation (Scheme 64, lower). As to the mechanism, in the presence of an alcohol additive the reaction is assumed to proceed analogously to the 1,2-addition of nucleophilic silicon to aldehydes (cf. Scheme 63, right cycle in section 4.3.1).

**4.3.3. Carbon Dioxide.** The intriguing copper(I)-mediated reduction of carbon dioxide with Me<sub>2</sub>PhSi-Bpin (25) was studied by Kleeberg, Marder, and co-workers (Scheme 65, upper).<sup>70</sup> In an initial experiment, the reaction of stoichiometrically generated L10-Cu-SiMe<sub>2</sub>Ph (163) with excess carbon dioxide was monitored by <sup>1</sup>H and <sup>13</sup>C NMR spectroscopy whereat fast insertion of carbon dioxide into the Cu-Si bond was detected (163 → 175). Over time, slow but clean decomposition of 175 accounted for the formation of copper(I) silanolate 176 with concomitant evolution of carbon monoxide (175 → 176). Complexes 163, 175, and 176 were spectroscopically and crystallographically characterized. Quantum-chemical calculations verified a higher activation barrier for the decomposition versus insertion,<sup>70,71</sup> and the former is assumed to be rate-determining in the overall process. Competing [1,2]-Brook rearrangement, which occurred during the 1,2-addition to aldehydes (cf. Scheme 61 in section 4.3.1),<sup>68</sup> was not seen in this system.

Toward the development of a catalytic version, the authors anticipated that complex L10-CuOSiMe<sub>2</sub>Ph (176) should be capable of participating in a transmetalation with additional

Scheme 65. Copper(I)-Catalyzed Reduction of Carbon Dioxide with Me<sub>2</sub>PhSi-Bpin (25)

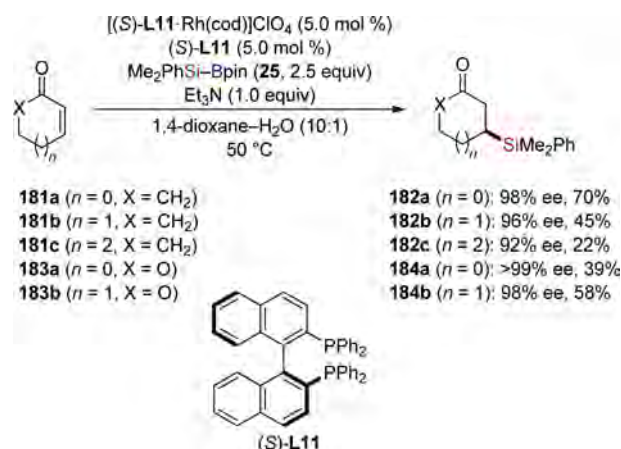
Me<sub>2</sub>PhSi-Bpin (25) to yield pinBOSiMe<sub>2</sub>Ph (177) and regenerate L10-Cu-SiMe<sub>2</sub>Ph (163) (176  $\rightarrow$  163 + 177, Scheme 65, center). However, an unexpected observation was made when using excess Me<sub>2</sub>PhSi-Bpin (25): complete consumption of carbon dioxide resulted in only 70% conversion to carbon monoxide, indicating a more complicated reaction sequence in this process. From the analysis of a crude reaction mixture before completion, compound pinBO(CO)-SiMe<sub>2</sub>Ph (178) was identified as a possible intermediate, suggesting that transmetalation is feasible not only with L10-CuOSiMe<sub>2</sub>Ph (176) but also with L10-CuO(CO)SiMe<sub>2</sub>Ph (175) (175  $\rightarrow$  163 + 178). Compound pinBO(CO)SiMe<sub>2</sub>Ph (178) then decomposes, affording carbon monoxide as well as compounds 177, 179, and 180 (Scheme 65, lower). The fact that not all of the carbon dioxide is converted into carbon monoxide is rationalized by this observation.

#### 4.4. 1,4-Addition to $\alpha,\beta$ -Unsaturated Carbonyl and Carboxyl Compounds<sup>5</sup>

The enantioselective conjugate silyl transfer onto  $\alpha,\beta$ -unsaturated acceptors had remained elusive<sup>72</sup> until we recognized the potential of Me<sub>2</sub>PhSi-Bpin (25) to serve as silicon anion equivalent in rhodium(I)-catalyzed processes.<sup>73</sup> In the presence of a preformed rhodium complex and an additional equivalent of (S)-binap [(S)-L11], cyclic enones and  $\alpha,\beta$ -unsaturated lactones of different ring sizes were

converted into the corresponding  $\beta$ -silylated products with high enantiomeric purities (181a-c  $\rightarrow$  182a-c and 183a-b  $\rightarrow$  184a-b, Scheme 66).<sup>73a,c</sup> The choice of the base additive was

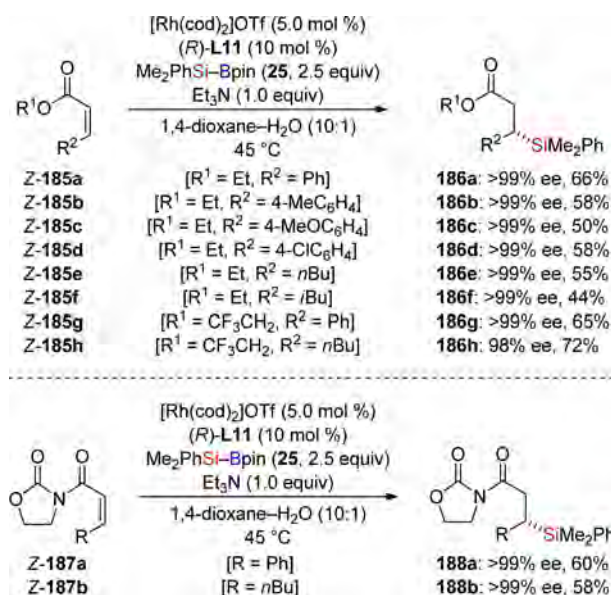
Scheme 66. Rhodium(I)-Catalyzed Conjugate Silylation of Cyclic Acceptors



crucial for full conversion as well as high enantioselection, and Et<sub>3</sub>N emerged as optimal from a systematic survey of organic and inorganic bases.

Later, it was found that preformation of the rhodium(I) complex was not necessary and a straightforward combination of [Rh(cod)<sub>2</sub>]OTf and (R)-L11 enabled the in situ generation of the active catalyst.<sup>73b,c</sup> Thus, reaction of acyclic  $\alpha,\beta$ -unsaturated esters bearing aryl or alkyl substituents at the  $\beta$ -position afforded  $\alpha$ -chiral silanes with impressive enantioselectivities of >99% ee (Z-185a-h  $\rightarrow$  186a-h, Scheme 67, upper). Aside from that, synthetically useful imides performed well with comparable results (Z-187a  $\rightarrow$  188a and Z-187b  $\rightarrow$  188b, Scheme 67, lower). In both cases, the success of the transformation hinges upon the utilization of Z-configured substrates. Concomitant 1,4-reduction of the acceptors

Scheme 67. Rhodium(I)-Catalyzed Conjugate Silylation of Acyclic Acceptors

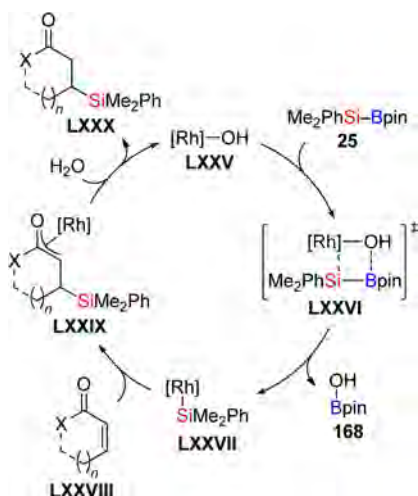




accounts for the moderate yields, and the origin of this side-reaction still requires clarification.

The proposed catalytic cycle is in accordance with the mechanistic picture established by Hayashi et al. for the rhodium(I)-catalyzed 1,4-addition of carbon nucleophiles (Scheme 68).<sup>74</sup> After the initial chemoselective coordination

**Scheme 68. Mechanism of the Rhodium(I)-Catalyzed Conjugate Silylation**

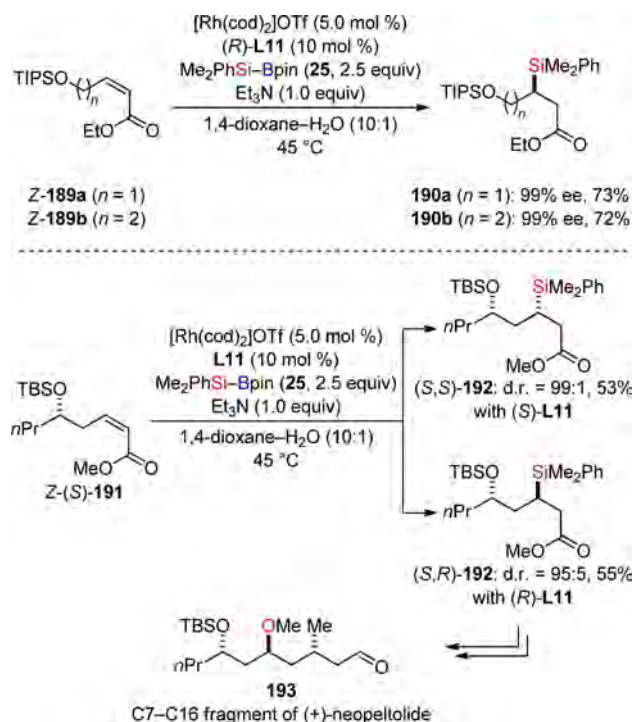


of Rh(I)–OH (LXXV) to Me<sub>2</sub>PhSi–Bpin (25), formal  $\sigma$ -bond metathesis delivers the nucleophilic Rh(I)–SiMe<sub>2</sub>Ph complex LXXVII (LXXV  $\rightarrow$  LXXVI  $\rightarrow$  LXXVII). Subsequent insertion of the  $\alpha,\beta$ -unsaturated acceptor into the Rh(I)–Si bond is followed by hydrolysis of the rhodium enolate LXXIX, affording the product and catalytically active LXXV (LXXVII  $\rightarrow$  LXXIX  $\rightarrow$  LXXX + LXXV).

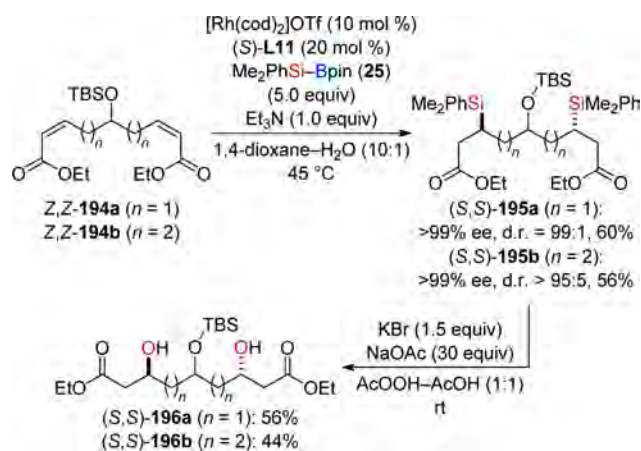
With regard to the implementation of this protocol into natural product synthesis, we extended the substrate scope to functionalized, e.g.,  $\gamma$ - and  $\delta$ -silyloxy-substituted,  $\alpha,\beta$ -unsaturated acceptors Z-189a and Z-189b that participated in the conjugate silylation in good yields and with excellent 99% enantiomeric excess (ee) in both cases (Scheme 69, upper).<sup>75</sup> Catalyst-controlled diastereoselective transformation of the chiral  $\delta$ -silyloxy-substituted  $\alpha,\beta$ -unsaturated ester Z-(S)-191 allowed for the synthesis of either diastereomer (S,S)-192 and (S,R)-192 with diastereomeric ratio (dr) = 99:1 and dr = 95:5, respectively (Z-(S)-191  $\rightarrow$  (S,S)-192 and Z-(S)-191  $\rightarrow$  (S,R)-192, Scheme 69, lower). The anti-isomer was then elaborated into the C7–C16 fragment 193 of (+)-neopeltolide including a Fleming oxidation as key step for the construction of the MeO-substituted stereocenter [(S,R)-192  $\rightarrow$  193, Scheme 69, lower].

We also took advantage of the highly catalyst-controlled stereoselection of the rhodium(I)-catalyzed process to perform a two-directional desymmetrization of prochiral bis( $\alpha,\beta$ -unsaturated) compounds (Scheme 70).<sup>76</sup> By means of a double 1,4-addition of nucleophilic silicon to Z,Z-194a and Z,Z-194b, pseudo C<sub>2</sub>-symmetric disilylated products (S,S)-195a and (S,S)-195b, respectively, were obtained, each virtually as the sole isomer (Z,Z-194a  $\rightarrow$  (S,S)-195a and Z,Z-194b  $\rightarrow$  (S,S)-195b). Subsequent stereospecific oxidative degradation of the C–Si bonds using the Fleming protocol provided access to stereodefined 1,3,5- and 1,4,7-triols (S,S)-196a and (S,S)-196b in only one step [(S,S)-195a  $\rightarrow$  (S,S)-196a and (S,S)-195b  $\rightarrow$  (S,S)-196b].

**Scheme 69. Rhodium(I)-Catalyzed Conjugate Silylation in the Synthesis of the C7–C16 Fragment of (+)-Neopeltolide**

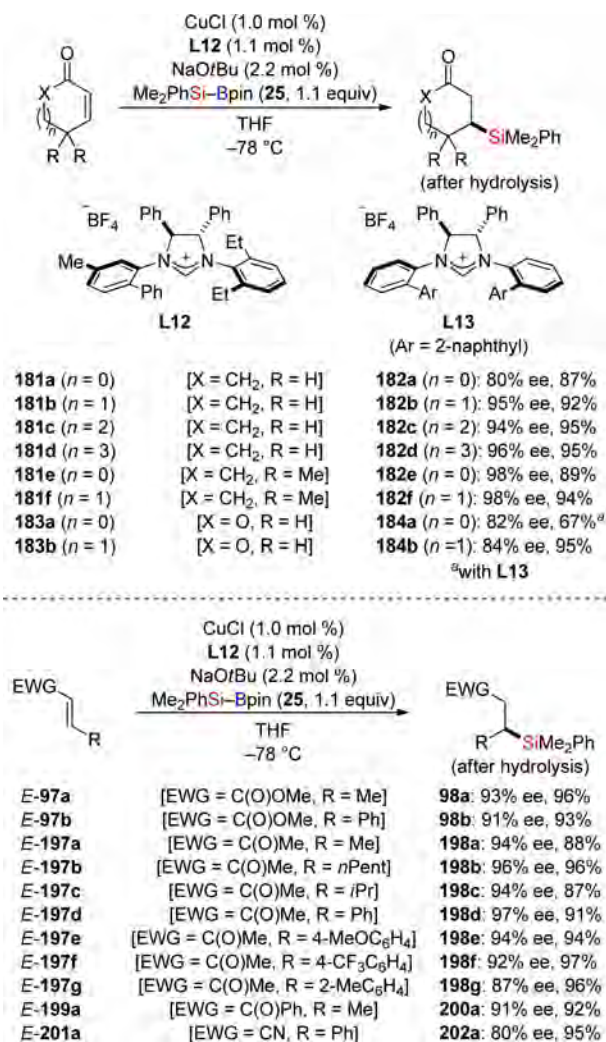


**Scheme 70. Rhodium(I)-Catalyzed Conjugate Silylation in Two-Directional Desymmetrization**



Apart from rhodium(I), Lee and Hoveyda succeeded in developing a generally applicable enantioselective conjugate silyl transfer that relies on the copper(I)-catalyzed activation of Me<sub>2</sub>PhSi–Bpin (25).<sup>77</sup> Using a combination of CuCl, NaOtBu, and the chiral carbene precursor L12 in THF at –78 °C, all representative cyclic enones 181a–d and  $\delta$ -lactone 183b reacted with superb chemical yields and good enantiomeric purities (Scheme 71, upper). Remarkably, even sterically demanding  $\gamma,\gamma$ -dimethyl-substituted acceptors are susceptible to the conjugate silylation (181e  $\rightarrow$  182e and 181f  $\rightarrow$  182f). However, for (SH)-furan-2-one (183a) Hoveyda's optimal precatalyst proved to be ineffective so that Procter and co-workers designed the new ligand L13 that finally allowed for the enantioselective synthesis of the  $\beta$ -silicon-substituted  $\gamma$ -butyrolactone 184a in 82% ee (183a  $\rightarrow$  184a).<sup>78</sup> Moreover, acyclic  $\alpha,\beta$ -unsaturated carbonyls and carboxyls (including

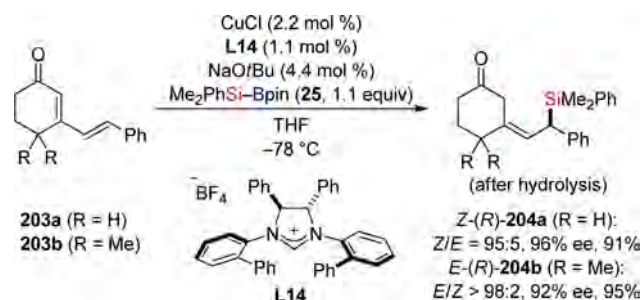
Scheme 71. Copper(I)-Catalyzed Conjugate Silylation



nitriles) substituted with different aryl or alkyl groups at the  $\beta$ -carbon atom afforded the desired products with again high yields and levels of enantioselection (Scheme 71, lower).

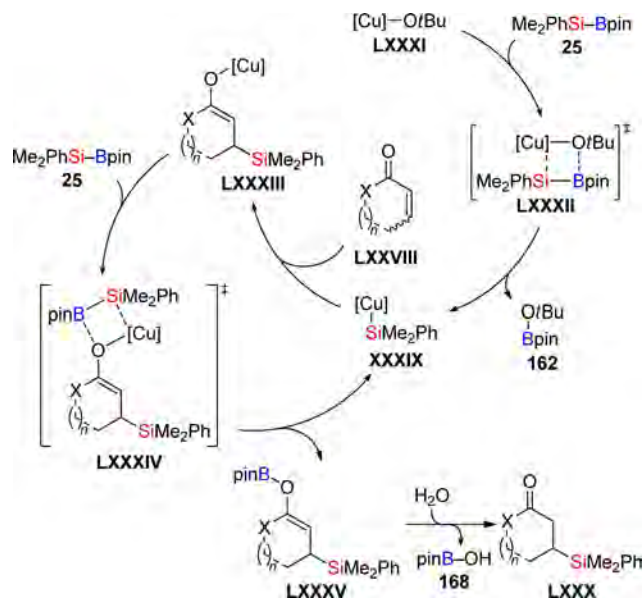
The potential of the catalytic system was further investigated in unconventional 1,6-addition reactions to  $\alpha,\beta,\gamma,\delta$ -dienones **203a** and **203b** (Scheme 72).<sup>77</sup> This time with  $\text{C}_2$ -symmetric **L14** as the appropriate ligand precursor, 1,6-addition products were observed exclusively with high control of the double-bond geometry and enantioselectivity (**203a**  $\rightarrow$  *Z*-(*R*)-**204a** and **203b**  $\rightarrow$  *E*-(*R*)-**204b**).

Scheme 72. Copper(I)-Catalyzed Asymmetric 1,6-Addition of Nucleophilic Silicon



Concerning the mechanism (Scheme 73), a  $\sigma$ -bond metathesis of  $\text{Cu(I)-OtBu}$  (**LXXXI**) with  $\text{Me}_2\text{PhSi-Bpin}$  (**25**) is

Scheme 73. Mechanism of the Copper(I)-Catalyzed Conjugate Silylation



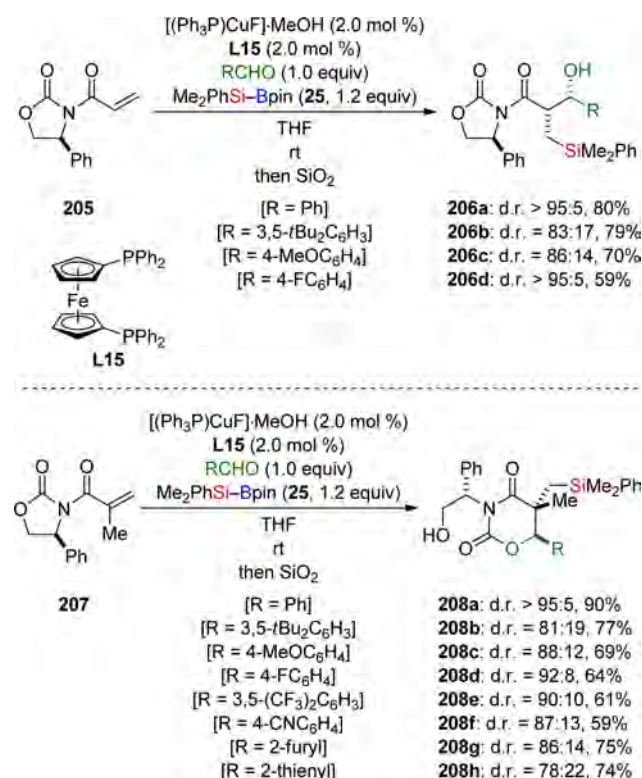
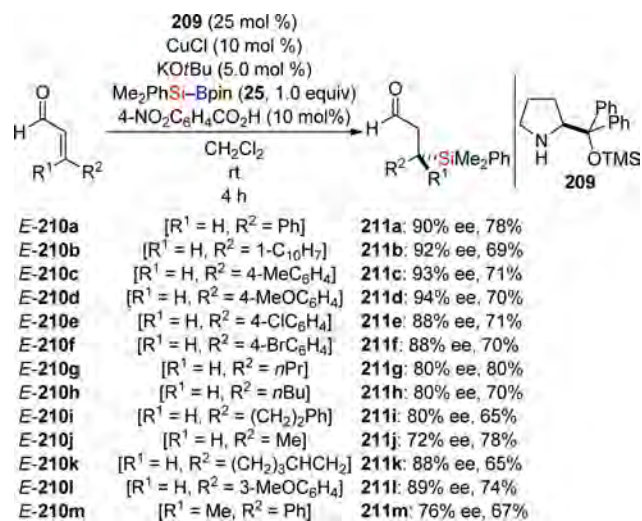
assumed to initiate the catalytic cycle, generating the  $\text{Cu(I)-SiMe}_2\text{Ph}$  nucleophile **XXXIX** (**LXXXI**  $\rightarrow$  **LXXXII**  $\rightarrow$  **XXXIX**). Subsequent 1,4-addition of **XXXIX** onto the  $\alpha,\beta$ -unsaturated acceptor **LXXXVIII** affords the oxygen enolate **LXXXIII** (**XXXIX**  $\rightarrow$  **LXXXIII**), which, under the aprotic conditions, undergoes another  $\sigma$ -bond metathesis to regenerate the catalytically active  $\text{Cu(I)-SiMe}_2\text{Ph}$  (**XXXIX**) and boron enolate **LXXXIV** (**LXXXIII**  $\rightarrow$  **LXXXIV**  $\rightarrow$  **LXXXV**). Final hydrolysis furnishes the  $\beta$ -silylated carbonyl or carboxyl compound (**LXXXV**  $\rightarrow$  **LXXX**).

Shortly after the report by Lee and Hoveyda,<sup>77</sup> Riant and co-workers introduced a diastereoselective domino silylative aldol reaction using  $\text{Me}_2\text{PhSi-Bpin}$  (**25**) as pronucleophile.<sup>79</sup> A copper(I) catalyst generated from  $[(\text{Ph}_3\text{P})\text{CuF}]\cdot\text{MeOH}$  and diphenylphosphinoferrrocene (**dppf**) (**L15**) promoted the conjugate silyl transfer onto the chiral acryloyloxazolidinone **205**, and the resulting enolate was trapped with various aldehydes (Scheme 74, upper). Thus, aldol structures **206a-d** were obtained in good yields and with good diastereoselectivities (**205**  $\rightarrow$  **206a-d**). The employment of methacryloyloxazolidinone **207** led to the formation of rearranged products **208a-h**, which are assumed to arise from an intramolecular ring-opening of the oxazolidinone by the hydroxyl group of the aldol adduct (**207**  $\rightarrow$  **208a-h**, Scheme 74, lower). Further improvement of the diastereoselection was achieved by changing the substituent at the chiral center of the oxazolidinone moiety (not shown).

Last year, Ibrahim, Córdova, and co-workers merged the copper(I)-catalyzed activation of  $\text{Me}_2\text{PhSi-Bpin}$  (**25**) with chiral amine catalysis into a protocol that enables the enantioselective conjugate silylation of challenging  $\alpha,\beta$ -unsaturated aldehydes (Scheme 75).<sup>80</sup> Chemoselective 1,4-addition (versus 1,2-addition) occurred in the presence of proline derivative **209** and  $\text{CuCl/KOtBu}$  to yield the corresponding products in good yields and with high enantiomeric purities (**E-210a-l**  $\rightarrow$  **211a-l**). It is noteworthy



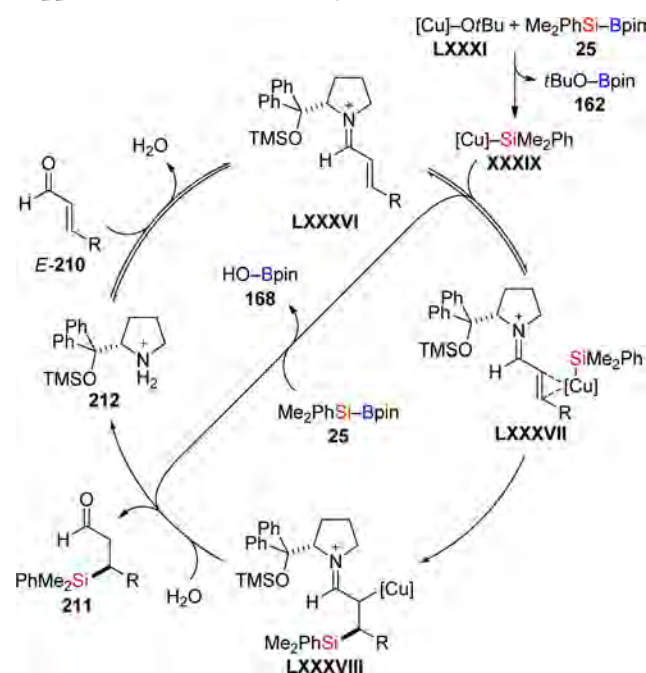
Scheme 74. Copper(I)-Catalyzed Domino Silylative Aldol Reaction

Scheme 75. Combined Copper(I)/Iminium Ion-Catalyzed Conjugate Silylation of  $\alpha,\beta$ -Unsaturated Aldehydes

that even the  $\beta,\beta$ -disubstituted acceptor *E*-210m was converted successfully with 67% yield and 76% ee (*E*-210m  $\rightarrow$  211m).

On the basis of experimental results as well as density functional theory calculations, the authors proposed a catalytic cycle (Scheme 76): initial formation of an iminium ion (*E*-210  $\rightarrow$  LXXXVI) is followed by coordination of the Cu(I)–SiMe<sub>2</sub>Ph nucleophile XXXIX to the sterically less-hindered face of the  $\pi$ -system of the activated acceptor (LXXXVI  $\rightarrow$  LXXXVII). Subsequent transfer of the SiMe<sub>2</sub>Ph group onto the  $\beta$ -carbon in LXXXVII furnishes an alkylcopper intermediate (LXXXVII  $\rightarrow$  LXXXVIII), which upon reaction with water delivers product 211 and regenerates the chiral ammonium ion

Scheme 76. Proposed Catalytic Cycle of the Combined Copper(I)/Iminium Ion Catalysis



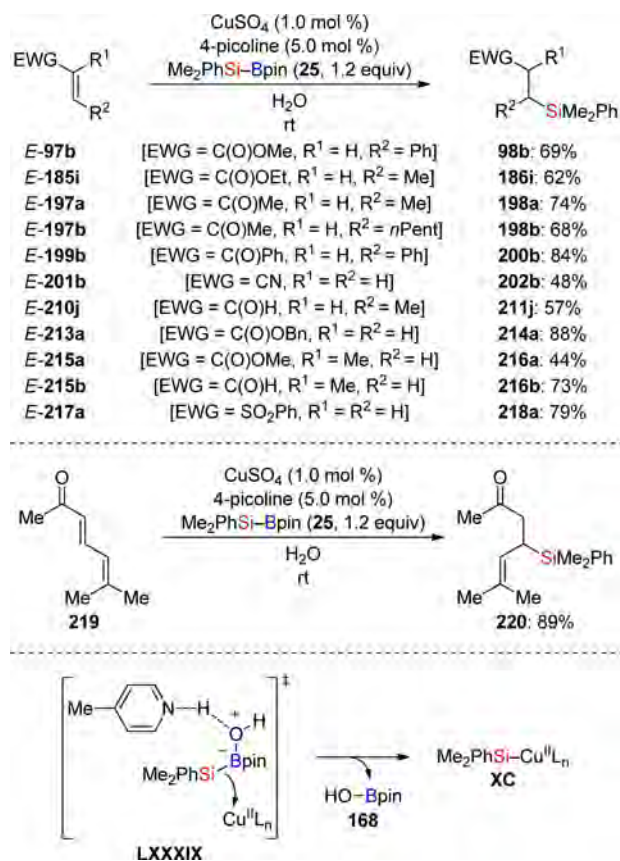
**212** as well as the nucleophilic Cu(I)–SiMe<sub>2</sub>Ph XXXIX (LXXXVIII  $\rightarrow$  XXXIX).

Opposed to copper(I)-mediated transmetalation reactions, Calderone and Santos postulated the participation of a copper(II) complex under aerobic conditions with water as solvent.<sup>81</sup> The active catalyst generated from  $\text{CuSO}_4$  and 4-picoline transferred the SiMe<sub>2</sub>Ph group to a wide range of acceptors including enones, enals,  $\alpha,\beta$ -unsaturated esters, sulfones, and nitriles (Scheme 77, upper). Even  $\alpha$ -substituted substrates *E*-215a and *E*-215b underwent the conjugate silylation with acceptable yields (*E*-215a  $\rightarrow$  216a and *E*-215b  $\rightarrow$  216b). In contrast to Hoveyda's protocol (cf. Scheme 72),<sup>77</sup> conversion of  $\alpha,\beta,\gamma,\delta$ -dienone 219 exclusively produced the 1,4-adduct 220 (219  $\rightarrow$  220, Scheme 77, center). However, this regioselectivity might be explained by the increased steric demand owing to two substituents at the  $\delta$ -position.

With regard to the mechanism, the  $\text{L}_n\text{Cu(II)-SiMe}_2\text{Ph}$  nucleophile XC is assumed to be generated through transition state LXXXIX (Scheme 77, lower). Here, 4-picoline not only serves as ligand for copper(II) but also as Brønsted base for the deprotonation of a nucleophilic water molecule. Thus, an  $\text{sp}^3$ -hybridized borate with a weakened Si–B bond is formed and a transmetalation occurs to form  $\text{L}_n\text{Cu(II)-SiMe}_2\text{Ph}$  (XC). When copper(I) salts were used as precatalysts, reasonable results were achieved as well, yet the authors suspect that in aqueous media copper(I) disproportionates to copper(II) and copper(0) so that the actual catalyst is a copper(II) complex.

Beyond metal-catalyzed protocols, O'Brien and Hoveyda introduced the first metal-free enantioselective conjugate silylation of  $\alpha,\beta$ -unsaturated compounds that relies on the chemoselective activation of the Si–B bond using *N*-heterocyclic carbenes (NHCs).<sup>35</sup> At the outset, the potential of such an activation was investigated by reacting stoichiometric amounts of the NHC generated from 221 with  $\text{Me}_2\text{PhSi-Bpin}$  (**25** + 221/1,8-diazabicyclo[5.4.0]undec-7-ene (DBU)  $\rightarrow$  222, Scheme 78, upper). Nucleophilic attack at the more Lewis acidic boron atom results in the formation of the  $\text{sp}^3$ -hybridized

Scheme 77. Copper(II)-Catalyzed Conjugate Silylation



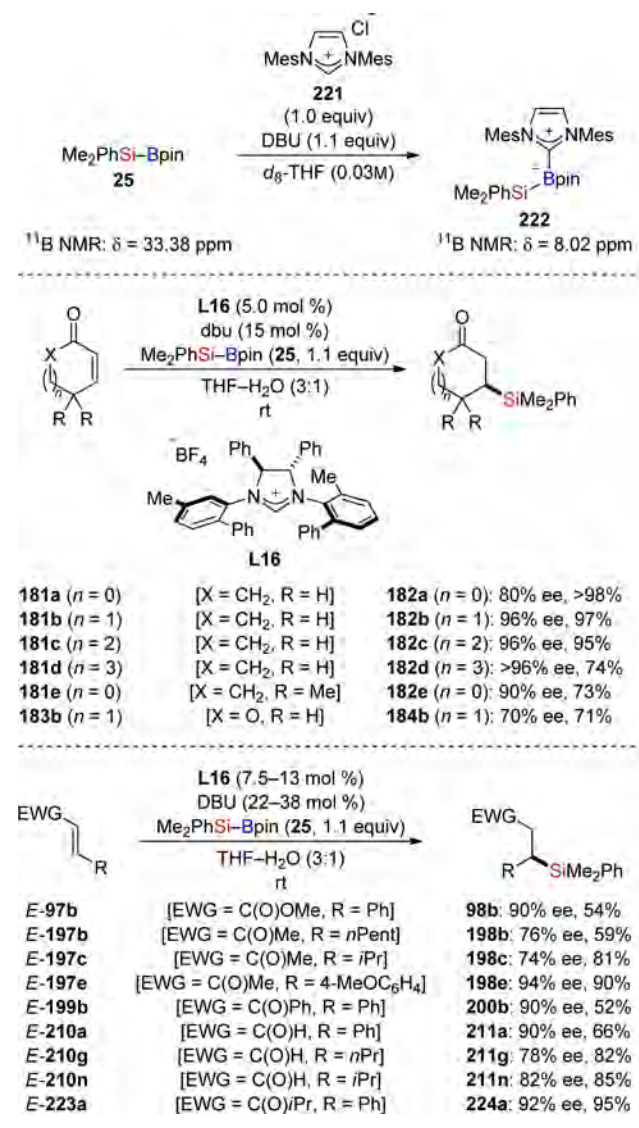
borate 222 that was detected by <sup>11</sup>B NMR (33.38 ppm for 25 and 8.02 ppm for 222). From this complex the SiMe<sub>2</sub>Ph group is assumed to be transferred onto an  $\alpha,\beta$ -unsaturated acceptor.

From a systematic survey, it was found that chiral imidazolium salt L16 as carbene precursor in THF/H<sub>2</sub>O (3:1) is optimal, providing good yields and enantioselectivities for cyclic enones (181a–d → 182a–d, Scheme 78, center). Sterically congested 181e as well as lactone 183b displayed lower reactivities, which is reflected in decreased conversions and yields, respectively (181e → 182e and 183b → 184b). Prolonged reaction times led to partial decomposition of the carbene catalyst under the aqueous reaction conditions, and an unselective conjugate silylation became apparent albeit at a slower rate (versus NHC-catalyzed). On account of this, increased catalyst loadings were employed for the conversion of acyclic acceptors, which were generally less reactive as compared to their cyclic analogues (Scheme 78, lower). Despite moderate yields for some substrates, high enantiomeric purities were obtained throughout. Notably, with this protocol  $\alpha,\beta$ -unsaturated aldehydes chemoselectively undergo 1,4- instead of 1,2-addition reactions (E-210a, E-210g, and E-210n → 211a, 211g, and 211n).

#### 4.5. Allylic and Propargylic Substitution

**4.5.1. Allylic Precursors.** In the context of C–Si bond-forming reactions, the allylic substitution of linear allylic precursors was realized by us exploiting the copper(I)-induced generation of silicon nucleophiles.<sup>82</sup> With optimized reaction conditions, the effect of the leaving group on the regioselectivity was probed (Scheme 79, upper). In analogy to a previous study,<sup>83</sup> similar trends were observed, i.e.,  $\gamma$ -selectivity for halides and phosphates (225a–227a →  $\gamma$ -232a +

Scheme 78. N-Heterocyclic Carbene-Catalyzed Conjugate Silylation

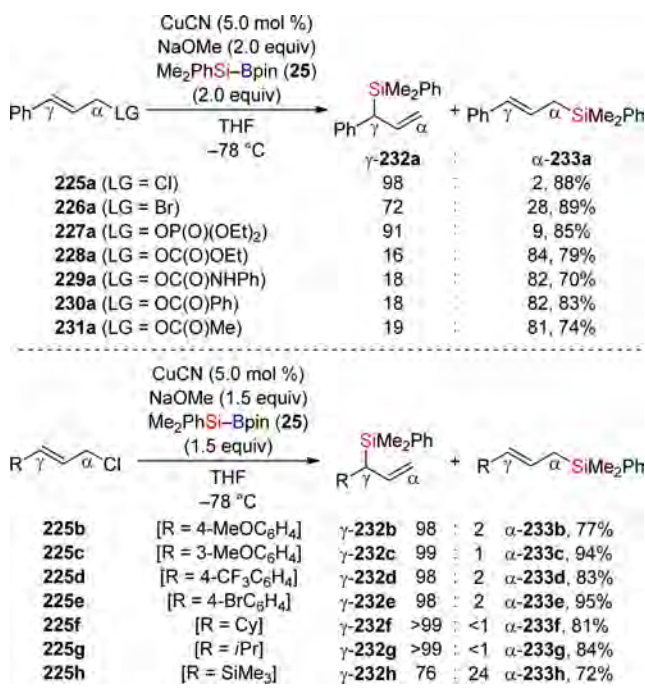


$\alpha$ -233a) and  $\alpha$ -selectivity for carbonates, carbamates, and carboxylates albeit with eroded  $\alpha$ -selectivities for the latter (228a–231a →  $\gamma$ -232a +  $\alpha$ -233a). Subsequently, the substrate scope was examined with chloride as the best-performing leaving group whereat generally good yields and excellent regioselectivities were obtained for both aryl- and alkyl-substituted precursors (225b–g →  $\gamma$ -232b–g Scheme 79, lower). The modest  $\gamma$ -selectivity for the silyl-substituted 225h is explained by a steric rather than an electronic effect because its carbon analogue (R = *t*Bu, not shown) reacted with even worse regioselectivity ( $\gamma/\alpha$  = 62:38).

As with the above shown copper(I)-mediated reactions, the key feature of the catalytic cycle is a  $\sigma$ -bond metathesis of a copper(I) alkoxide and Me<sub>2</sub>PhSi-Bpin (25). However, with the present system only the utilization of small OMe (CuOMe) secures smooth Si–B bond activation while sterically hindered OtBu (CuOtBu) does not catalyze the reaction. Interestingly, added phosphine ligands significantly decreased the reaction rate, providing essentially the same high regioselectivities as under “ligand-free” reaction conditions.

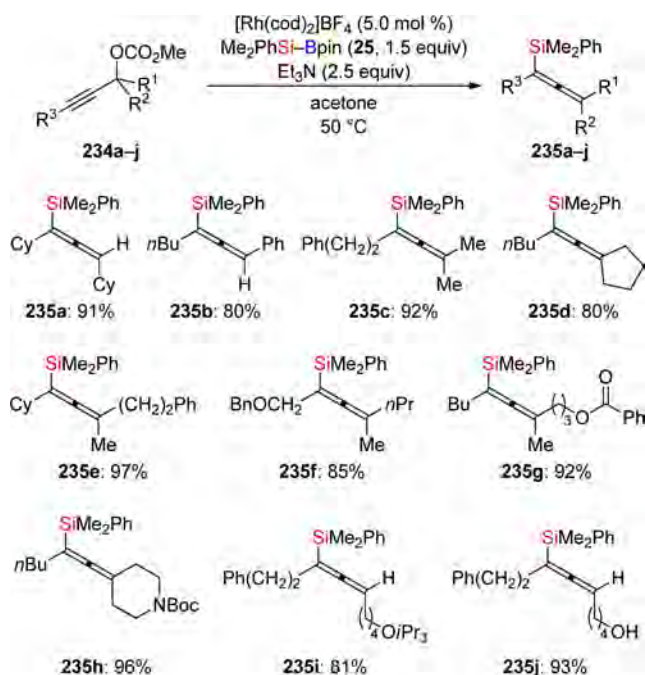


Scheme 79. Copper(I)-Catalyzed Branched Selective Allylic Substitution



**4.5.2. Propargylic Precursors.** Besides allylic substrates, propargylic systems also were evaluated in S<sub>N</sub>2' reactions. In 2009 Sawamura and co-workers modified the rhodium(I)-catalyzed Si-B transmetalation developed in our group<sup>73</sup> and elaborated a practical protocol for the transformation of propargylic carbonates into the corresponding allenyllic silanes (Scheme 80).<sup>84</sup> Various solvents, e.g., THF, toluene, hexane, and 1,4-dioxane were viable; however, the best results were achieved with dimethylformamide (DMF) or acetone. Similarly

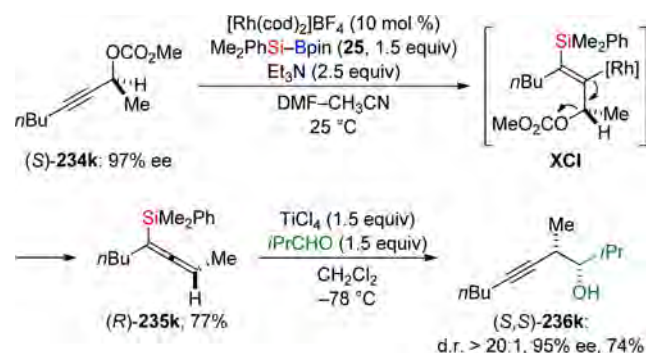
Scheme 80. Rhodium(I)-Catalyzed Regioselective Propargylic Substitution



to the rhodium(I)-catalyzed conjugate silylation,<sup>73</sup> the use of Et<sub>3</sub>N was indispensable for high conversion. No reaction occurred when silylboronic esters other than Me<sub>2</sub>PhSi-Bpin (25) were used, e.g., FMe<sub>2</sub>Si-Bpin (43), (*i*PrO)Me<sub>2</sub>Si-Bpin (50), or (Et<sub>2</sub>N)Me<sub>2</sub>Si-Bpin (45). With the optimal catalytic system, a range of allenyllic silanes with different functional groups was synthesized in good yields (234a-j → 235a-j). Only terminal alkynes (R<sup>3</sup> = H, not shown) were not sufficiently reactive, yielding only small quantities or no product at all.

To gain more insight into the stereochemical course of the substitution, the authors performed a reaction with the optically active propargylic carbonate (*S*)-234k followed by a titanium(IV)-mediated addition of the thus-obtained allenyllic silanes (*R*)-235k to isobutyraldehyde [(*S*)-234k → (*S,S*)-236k, Scheme 81]. Only a negligible erosion of the

Scheme 81. Rhodium(I)-Catalyzed Propargylic Substitution with an Enantioenriched Precursor



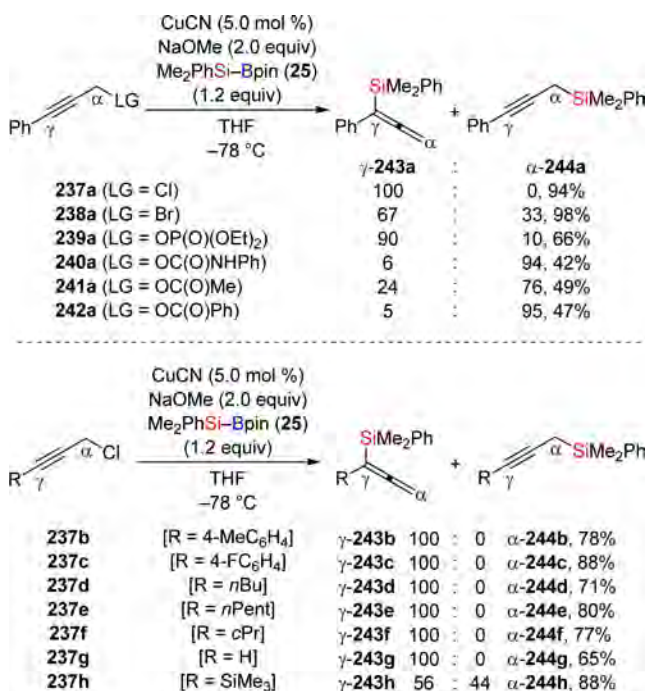
enantiomeric purity occurred in this sequence (97% ee → 95% ee). On the basis of the observed results, the authors suggested a reaction pathway that involves regioselective 1,2-addition of a Rh-SiMe<sub>2</sub>Ph complex across the triple bond of (*S*)-234k, yielding intermediate XCI and subsequent anti- $\beta$ -elimination to give allenyllic silane (*R*)-235k [(*S*)-234k → XCI → (*R*)-235k].

Encouraged by the performance of the copper(I)-based catalytic system in allylic transposition reactions, we decided to test the established conditions in propargylic substitutions.<sup>85</sup> In accordance with recent related results,<sup>86</sup> chloride outcompeted other leaving groups in terms of regioselectivity (237a →  $\gamma$ -243a, Scheme 82, upper). High  $\gamma$ -selectivity was achieved for phosphate (239a →  $\gamma$ -243a +  $\alpha$ -244a,  $\gamma/\alpha$  = 90:10), although bromide performed poorly (238a →  $\gamma$ -243a +  $\alpha$ -244a,  $\gamma/\alpha$  = 67:33). The remaining common oxygen leaving groups including carbonate gave lower chemical yields while favoring the  $\alpha$ -substitution, and this is in contrast to Sawamura's results<sup>84</sup> (240a-242a →  $\gamma$ -243a +  $\alpha$ -244a).

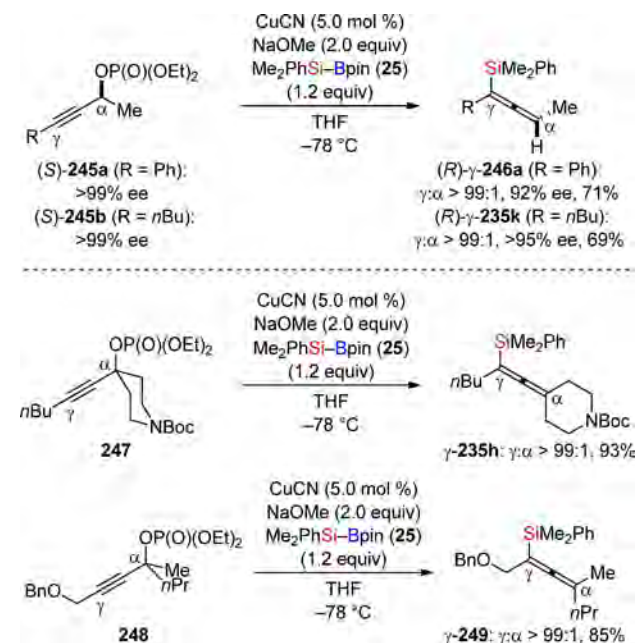
Concerning the substrate scope, all aryl- and alkyl-substituted propargylic chlorides were cleanly converted into allenyllic silanes (237b-g →  $\gamma$ -243b-g, Scheme 82, lower). As opposed to Sawamura's investigations, a terminal alkyne, i.e., the parent propargylic chloride 237g, was suitable for the transformation (237g →  $\gamma$ -243g). A terminal SiMe<sub>3</sub> group, in turn, was detrimental to the  $\gamma/\alpha$ -ratio (237h →  $\gamma$ -243h +  $\alpha$ -244h,  $\gamma/\alpha$  = 56:44).

Next, enantiospecific displacements were investigated (Scheme 83, upper). Because  $\alpha$ -chiral enantiomerically enriched propargylic chlorides are not available,  $\alpha$ -chiral

Scheme 82. Copper(I)-Catalyzed Regioselective Propargylic Substitution: Survey of Leaving Groups and Substrate Scope



Scheme 83. Copper(I)-Catalyzed Propargylic Substitution of α-Chiral and Tertiary Propargylic Phosphates



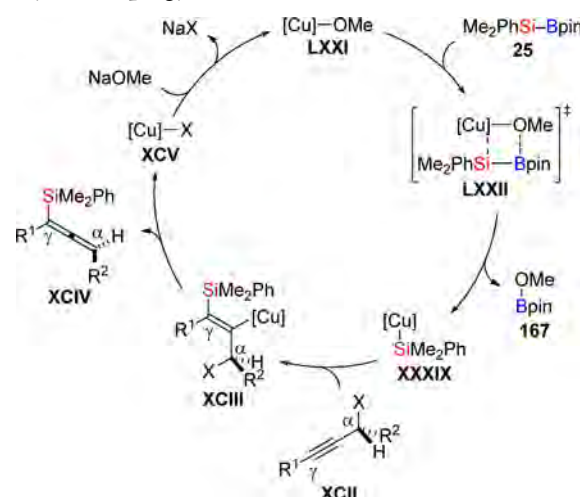
phosphates were chosen owing to their easy accessibility and the promising γ/α-ratios. Under the standard protocol, both phenyl- and *n*-butyl-substituted (S)-245a and (S)-245b, respectively, were converted into the corresponding enantioenriched allenes with high levels of central-to-axial chirality transfer and excellent regiocontrol [(S)-245a → (R)-γ-246a and (S)-245b → (R)-γ-235k].

Apart from that, our protocol is applicable to tertiary propargylic phosphates. Representative substrates underwent the reaction affording the fully substituted allenes in high yields

and with superb γ-selectivities (247 → γ-235h and 248 → γ-249, Scheme 83, lower).

A conceivable catalytic cycle is depicted in Scheme 84. After the generation of nucleophilic Cu-SiMe<sub>2</sub>Ph (XXXIX) (LXXI

Scheme 84. Proposed Mechanism of the Copper(I)-Catalyzed Propargylic Substitution

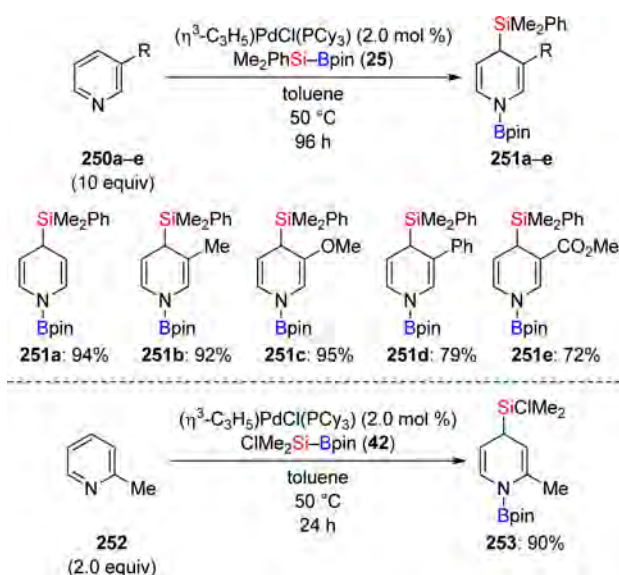


→ LXXII → XXXIX), its syn-selective 1,2-addition across the carbon-carbon triple bond of XCII is followed by an anti-selective β-elimination (XXXIX → XCIII → XCIV + XCV). This seems reasonable because the stereochemical course (cf. Scheme 83, upper) is identical to that determined by the Sawamura group in the rhodium(I)-catalyzed variant (cf. Scheme 81).<sup>84</sup> Finally, salt metathesis of [Cu]-X complex CXV and NaOMe closes the catalytic cycle regenerating LXXI (XCV → LXXI).

#### 4.6. Dearomatization of Pyridines and Pyrazine

A new reaction, namely, a pyridine dearomatization, was recently disclosed by Oshima, Ohmura, and Sugimoto (Scheme 85).<sup>87</sup> This palladium(0)-catalyzed process worked well with

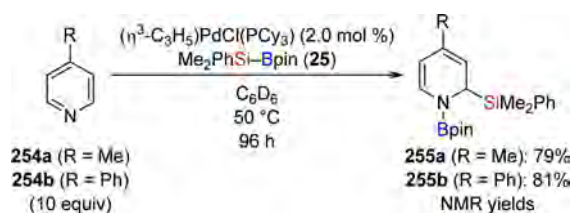
Scheme 85. Silaboration of Substituted Pyridines: 1,4-Addition





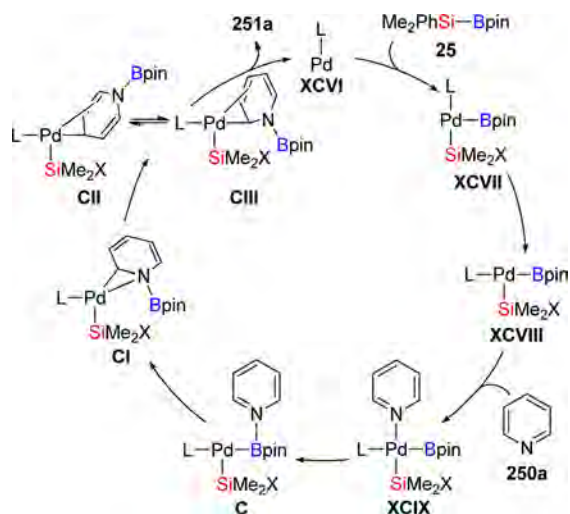
$\text{Me}_2\text{PhSi-Bpin}$  (**25**) for pyridine (**250a**) and 3-substituted pyridines (**250b–e**). The 1,4-addition yielded dihydropyridines **251a–e** in excellent yields that were converted into the corresponding silylated pyridines by the reaction with benzaldehyde (not shown). To obtain any conversion with 2-picoline (**252**), the reagent had to be replaced by the more reactive  $\text{ClMe}_2\text{Si-Bpin}$  (**42**), again yielding the 1,4-addition product in high yield (**252**  $\rightarrow$  **253**, Scheme 85, lower). However, the presence of a methyl or phenyl substituent in the 4-position steered the silyl group toward the 2-position to afford 1,2-addition (**254a**  $\rightarrow$  **255a** and **254b**  $\rightarrow$  **255b**, Scheme 86).<sup>87</sup>

**Scheme 86. Silaboration of 4-Substituted Pyridines: 1,2-Addition**



The surprisingly facile dearomatization prompted Ariafard, Yates, and co-workers to investigate the mechanism in detail by quantum-chemical calculations (Scheme 87).<sup>88</sup> After oxidative

**Scheme 87. Mechanistic Rationale for the Silaboration of Pyridines**

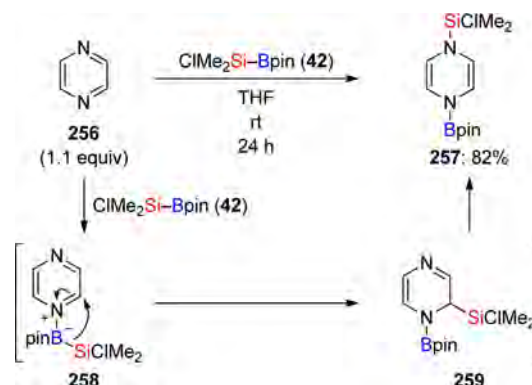


addition of the Si–B bond to the monoligated palladium–phosphine complex **XCVI** followed by initial coordination of pyridine (**XCVII**  $\rightarrow$  **XCVIII**  $\rightarrow$  **XCIX**), the latter migrates from palladium to boron in a highly endergonic step (**XCIX**  $\rightarrow$  **C**). The subsequent dearomatizing insertion of the pyridine into the Pd–B bond (**C**  $\rightarrow$  **CI**) is accompanied by the transformation of the dative into a very strong covalent B–N bond that makes this step feasible. The trans-complex **CI** must isomerize to the two reductive elimination precursors **CII** and **CIII** that were found to be in equilibrium. As the reductive elimination is the rate-determining step, electronic and steric effects in the precursors **CII** and **CIII** govern the regioselectivity. If the pyridine is not substituted in the 4-position, kinetic as well as thermodynamic effects favor **CII**,

leading to the 1,4-addition (**CII**  $\rightarrow$  **251a**). If the pyridine bears a substituent in the 4-position, **CIII** is favored due to steric repulsion, leading to the 1,2-addition (**CIII**  $\rightarrow$  **255**, cf. Scheme 86).

A single example of a transition metal-free transformation of pyrazine (**256**) into silaborated 1,4-dihydropyrazine was recently reported by Oshima, Ohmura, and Suginoe (**256**  $\rightarrow$  **257**, Scheme 88).<sup>36</sup> The authors propose a mechanism in

**Scheme 88. Transition Metal-Free Silaboration of Pyrazine**



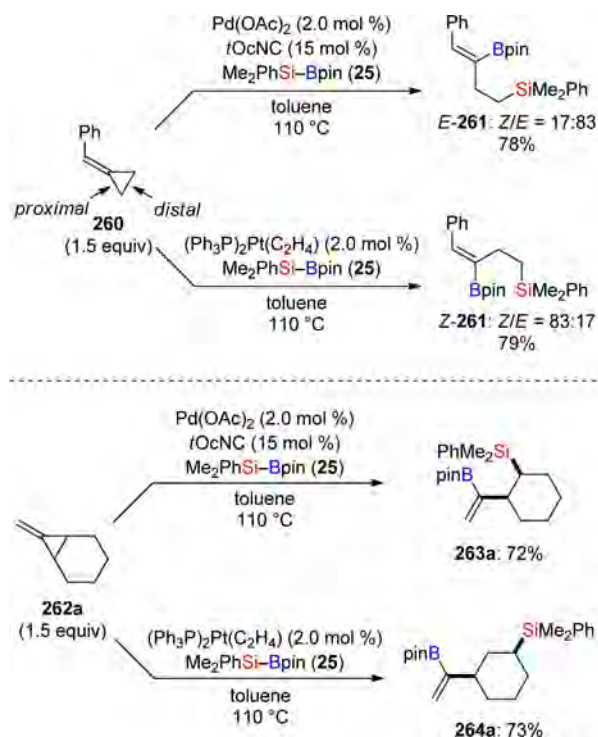
which one of the nitrogen atoms of **256** coordinates to the boron atom of  $\text{ClMe}_2\text{Si-Bpin}$  (**42**), thereby activating the Si–B bond to induce migration of the silyl group to the  $\alpha$ -carbon atom of **258** (**258**  $\rightarrow$  **259**). The intermediate **259** (1,2-addition) is believed to undergo a rearrangement to **257** (1,4-addition) accompanied by the formation of a new Si–N bond. Dearomatization is again facilitated by the formation of a strong covalent B–N bond in **257**.

## 5. FUNCTIONALIZATION OF STRAINED-RING COMPOUNDS

### 5.1. Methyleneecyclopropanes

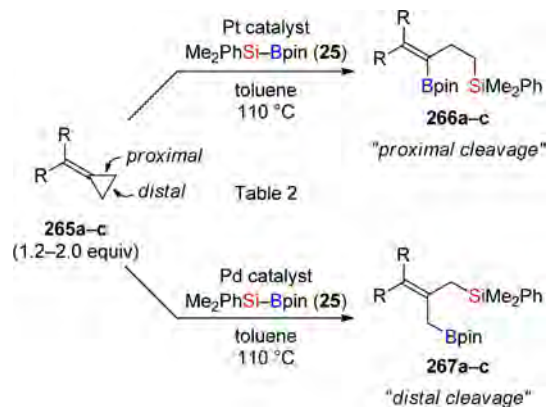
Methyleneecyclopropanes (MCPs) are a class of highly reactive compounds displaying diverse reactivity due to substantial ring strain. Potential reactions include 1,2-addition across the C–C double bond, C–C bond cleavage of the distal, or one of the proximal C–C bonds. Suginoe, Matsuda, and Ito systematically investigated the reactions of MCPs with  $\text{Me}_2\text{PhSi-Bpin}$  (**25**) under transition metal catalysis. Early examples had already indicated a significant dependence of the product distribution on the transition metal catalyst, either palladium or platinum (Scheme 89).<sup>89</sup> The reaction of phenyl-substituted MCP **260** with  $\text{Me}_2\text{PhSi-Bpin}$  (**25**) in the presence of a palladium catalyst yielded predominantly *E*-**261** with *E* alkene geometry whereas a platinum catalyst produced mainly *Z*-**261** (Scheme 89, upper). Diastereodivergence is due to the discrimination between either of the proximal C–C bonds. Another interesting result was obtained in the reaction of annulated MCP **262a** (Scheme 89, lower). Employment of a palladium–isocyanide catalyst resulted in proximal C–C bond cleavage, yielding the expected constitutional isomer **263a**. When  $(\text{Ph}_3\text{P})_2\text{Pt}(\text{C}_2\text{H}_4)$  was used as catalyst, however, the silicon atom was connected to carbon atom one position away from the alkene despite proximal C–C bond cleavage (**262a**  $\rightarrow$  **264a**). The authors explained the unexpected outcome by  $\beta$ -hydride elimination from a homoallylic platinum intermediate followed by readdition in opposite orientation (cf. Scheme 31 in section 4.1.2).

Scheme 89. Diastereodivergence through Regioselective Proximal C–C Bond Cleavage



A remarkable observation was made when the same group changed the palladium–isonitrile catalyst to palladium–phosphine or –phosphite catalysts (Scheme 90).<sup>89</sup> Although

Scheme 90. Selective Distal or Proximal C–C Bond Cleavage



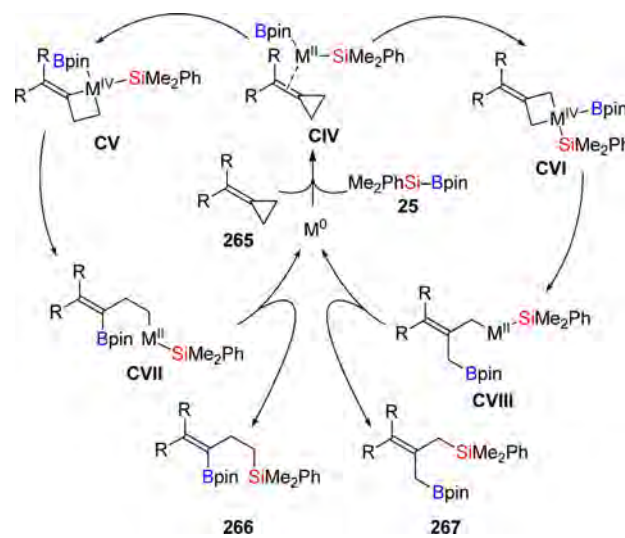
the platinum catalyst still induced proximal bond cleavage in 265a–c (265a–c → 266a–c), the palladium(0)-catalyzed reactions produced 267a–c exclusively (265a–c → 267a–c), and these are derived from distal C–C bond cleavage (Scheme 90 and Table 2). These examples represent a remarkable transition metal effect on the selectivity, making all the isomers depicted in Table 2 accessible in good yields.

The proposed mechanism of these transformations proceeds via an initial oxidative addition of Me<sub>2</sub>PhSi–Bpin (25) to the transition metal (Scheme 91, middle).<sup>89</sup> Subsequently, the proximal (counterclockwise) or the distal (clockwise) C–C bond of the coordinated MCP is cleaved in another oxidative addition, resulting in the metallacyclobutanes CV and CVI with

Table 2. Selective Distal or Proximal C–C Bond Cleavage

entry	substrate	catalyst	product	yield[%]
1		(Ph <sub>3</sub> P) <sub>2</sub> Pt(C <sub>2</sub> H <sub>4</sub> ) (2.0 mol %)		75
2		Pd(dba) <sub>2</sub> /(EtO) <sub>3</sub> P (2.0/4.0 mol %)		73
3		Pt(dba) <sub>2</sub> /MePh <sub>2</sub> P (5.0/10 mol %)		71
4		Pd(dba) <sub>2</sub> /(EtO) <sub>3</sub> P (5.0/10 mol %)		72
5		Pt(dba) <sub>2</sub> /MePh <sub>2</sub> P (5.0/10 mol %)		62
6		Pd(dba) <sub>2</sub> /(EtO) <sub>3</sub> P (5.0/10 mol %)		70

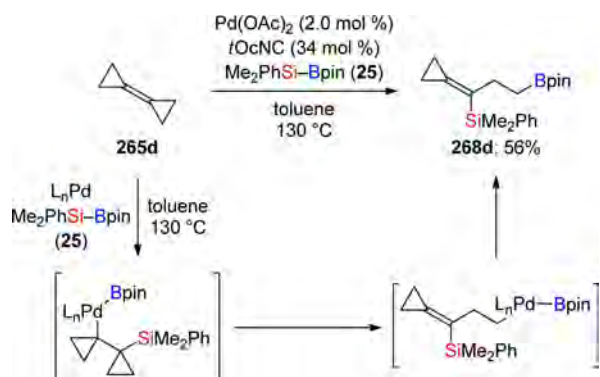
Scheme 91. Proposed Mechanisms for the Selective C–C Bond Cleavage of Methylenecyclopropanes



the metal in the oxidation state +IV. The catalytic cycles close by two reductive elimination steps, forming a vinylic C–B bond and then a homoallylic C–Si bond in the proximal case (CV → CVII → 266) and an allylic C–B and then a C–Si bond for the distal case (CVI → CVIII → 267), respectively.

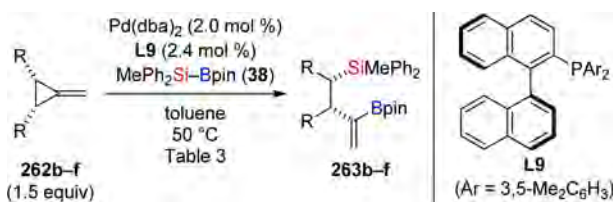
The reaction of Me<sub>2</sub>PhSi–Bpin (25) with bicyclopropylidene (265d) was described by Pohlmann and de Meijere a decade ago.<sup>90</sup> This palladium(0)-catalyzed process also involved proximal C–C bond cleavage (265d → 268d, Scheme 92). As opposed to known difunctionalization of MCPs, the authors assigned the C–Het connectivities differently. According to comparison of <sup>13</sup>C NMR data, the C–Si bond is vinylic and the C–B bond is homoallylic. The suggested mechanism involves a silapalladation of the double bond followed by a cyclo-



Scheme 92. Addition of Me<sub>2</sub>PhSi-Bpin (25) to Bicyclopolyidene (265d)

propylmethyl-to-homoallyl rearrangement. The C-B bond is formed by the final reductive elimination yielding **268d**. This distinct mechanism requires further clarification.

A particularly nice advancement of the palladium(0)-catalyzed silaboration of MCPs was reported by Sugimoto and co-workers five years ago. *meso*-MCPs were efficiently desymmetrized employing a chiral palladium catalyst (Scheme 93 and Table 3).<sup>91</sup> A screening of chiral phosphine ligands

Scheme 93. Desymmetrizing Proximal C-C Bond Cleavage of *meso*-MethylenecyclopropanesTable 3. Desymmetrizing Proximal C-C Bond Cleavage of *meso*-Methylenecyclopropanes

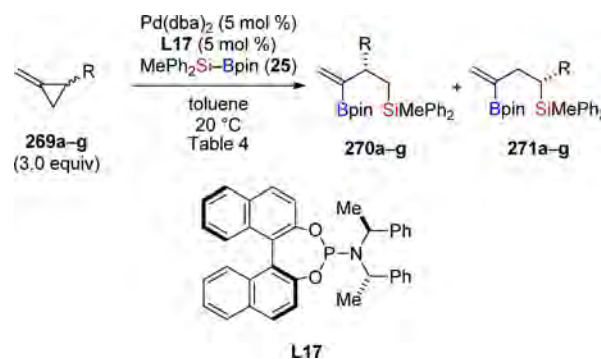
entry	substrate	product	yield [%]	ee [%]
1			72	90
2			95	91
3			85	90
4			72	81
5			50	89

revealed that the axially chiral monophosphine ligand **L9** induced high enantioselectivities and also the use of MePh<sub>2</sub>Si-Bpin (**38**) instead of Me<sub>2</sub>PhSi-Bpin (**25**) had a positive influence on the reaction rate as well as the selectivity. With this catalytic system the ring-opened products were obtained in moderate to excellent yields and with very good enantiomeric

excesses (**262b-f** → **263b-f**). The same group just reported an improved catalytic system for this reaction using polymer-based chiral phosphine ligands.<sup>92</sup> These ligands in combination with Pd(dba)<sub>2</sub> were superior to the former monomeric phosphines both in terms of catalytic activity and enantioselectivity, affording the analogous products with improved enantiomeric excesses (≤96% ee, not shown).

The laboratory of Sugimoto introduced another asymmetric silaboration reaction with MCPs, that is, the kinetic resolution of 1-alkyl-2-methylenecyclopropanes (**269a-g** → **270a-g** and **271a-g**, Scheme 94).<sup>93</sup> Racemic mixtures of these substituted

Scheme 94. Kinetic Resolution of Racemic Methylenecyclopropanes



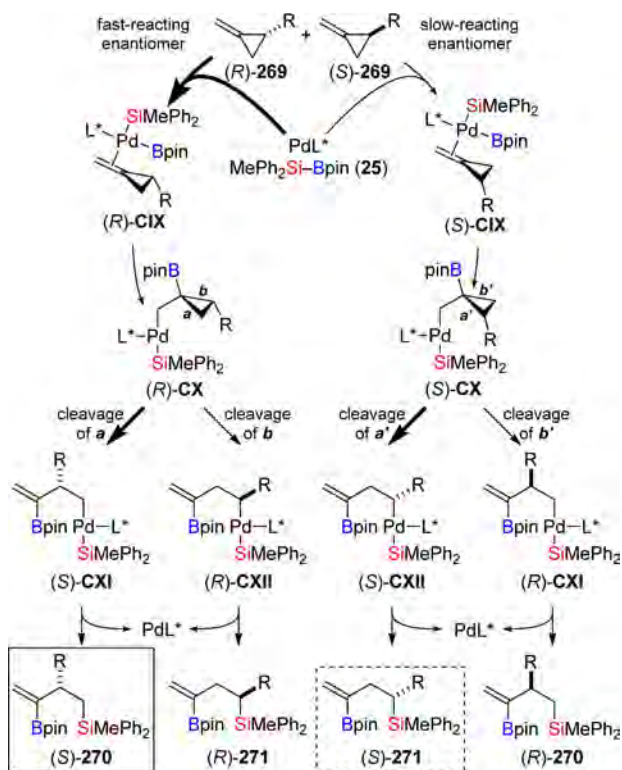
MCPs were resolved with the aid of a palladium-phosphoramidite catalyst yielding the two different constitutional isomers **270a-g** and **271a-g** in enantiomerically enriched form (Table 4).

Table 4. Kinetic Resolution of Racemic Methylenecyclopropanes

entry	R	yield [%] (270+271)	270/271 ratio	ee of 270 [%]
1	C <sub>6</sub> H <sub>13</sub> ( <b>269a</b> )	90	78:22	91 ( <b>270a</b> )
2	(CH <sub>2</sub> ) <sub>2</sub> Ph ( <b>269b</b> )	97	80:20	90 ( <b>270b</b> )
3	CH <sub>2</sub> OSiMe <sub>2</sub> ( <i>t</i> Bu) ( <b>269c</b> )	85	86:14	92 ( <b>270c</b> )
4	(CH <sub>2</sub> ) <sub>3</sub> OSiMe <sub>2</sub> ( <i>t</i> Bu) ( <b>269d</b> )	97	77:23	90 ( <b>270d</b> )
5	(CH <sub>2</sub> ) <sub>2</sub> OAc ( <b>269e</b> )	71	80:20	90 ( <b>270e</b> )
6	(CH <sub>2</sub> ) <sub>3</sub> Cl ( <b>269f</b> )	69	77:23	87 ( <b>270f</b> )
7	(CH <sub>2</sub> ) <sub>2</sub> N(phthaloyl) ( <b>269g</b> )	84	81:19	85 ( <b>270g</b> )

The occurrence of the two constitutional isomers in both enantiomeric forms indicates that this reaction might not be a simple kinetic resolution pathway in which one enantiomer reacts faster in a certain reaction step than the other.<sup>93</sup> It rather resembles a situation where a parallel kinetic resolution is operative in which diastereomeric intermediates [(*R*)-CX and (*S*)-CX, Scheme 95] resulting from the reaction of either enantiomer with the B-Pd-Si complex are transformed into different constitutional isomers rather than enantiomers. The initial discrimination of the enantiomers was found not to be very selective (3:2–4:1), but in combination with the subsequent regioselective C-C bond cleavage in favor of the *a* and *a'* bond in (*R*)-CX and (*S*)-CX, respectively, high enantioselectivities were obtained for both products. This represents a scholarly example of synergism in two consecutive

Scheme 95. Plausible Reaction Pathways for the Kinetic Resolution of Racemic Methylene cyclopropanes



asymmetric transformations leading to high selectivities although the individual steps are not particularly selective themselves.

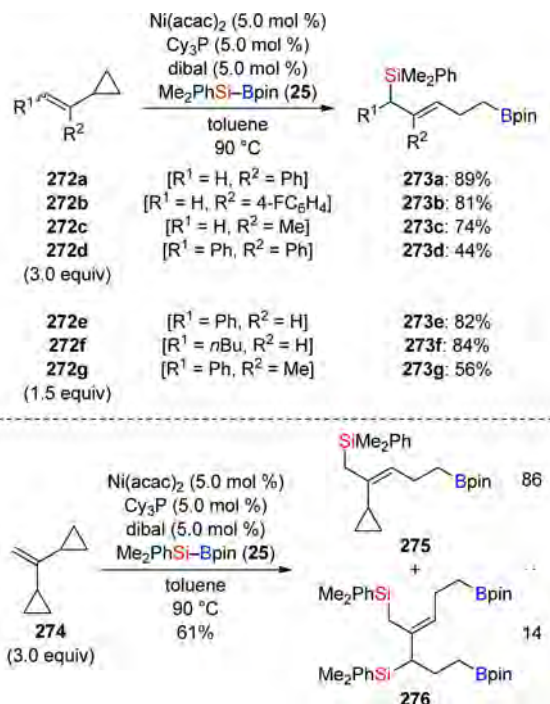
## 5.2. Vinylcyclopropanes and Vinylcyclobutanes

Double bonds attached to small strained rings do not undergo simple transition metal-catalyzed 1,2-addition of Si-B bonds. Investigations by Suginome, Ito, and co-workers showed that addition reactions involve opening of the strained ring.<sup>94</sup> Several vinylcyclopropanes were silaborated in the presence of a nickel(0) catalyst diastereoselectively affording allylic silanes with a homoallylic boryl group (272a-g  $\rightarrow$  273a-g, Scheme 96, upper). This method was even applicable to trisubstituted alkenes (272d and 272g), albeit in decreased yields. The application of 1,1-dicyclopropylethene resulted in the formation of a mixture of mono- 275 and disilaborated 276, containing two allylic silyl groups (Scheme 96, lower). It must be noted here that Oshima and co-workers had reported a single example of an uncatalyzed silylation of a vinylcyclopropane using the aforementioned borate  $\text{Me}_2\text{PhSi-BEt}_3\text{Li}$  (81) (not shown).<sup>95</sup>

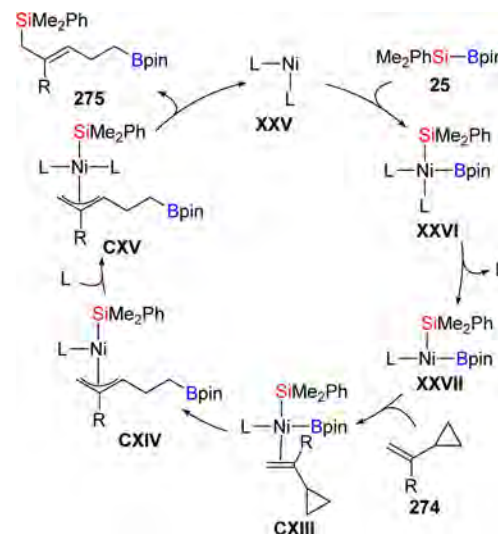
A possible reaction mechanism is depicted in Scheme 97.<sup>94</sup> Its key feature is the migratory C-C bond cleavage ( $\text{CXIII} \rightarrow \text{CXIV}$ ), which results in the formation of a new C-B bond in the allylnickel complex CXIV. Reductive elimination delivers the silyl group to the terminal position ( $\text{CXIV} \rightarrow \text{CXV} \rightarrow \text{XXV} + 275$ ). It is noteworthy that, in all cases (including  $\text{R} = \text{Me}$  and  $\text{Ph}$ ), a single double-bond isomer was observed. A drawback of the catalytic system is an undesired isomerization of the vinylcyclopropane to cyclopentene, which makes higher substrate loadings necessary to obtain satisfying yields with regard to  $\text{Me}_2\text{PhSi-Bpin}$  (25).<sup>94</sup>

This methodology was further extended to vinylcyclobutanes that showed a similar reactivity.<sup>94</sup> The products resulting from the same mechanism with a homologated borylalkyl chain were

Scheme 96. Silaboration of Vinylcyclopropanes with C-C Bond Cleavage



Scheme 97. Mechanistic Rationale for the Silaboration of Vinylcyclopropanes



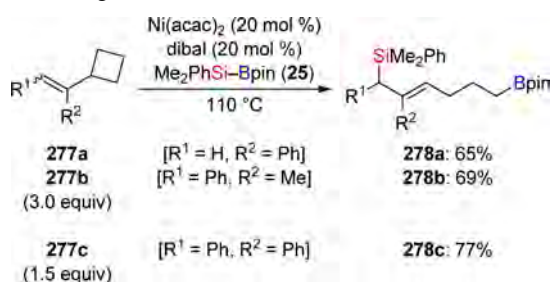
isolated in good yields (277a-c  $\rightarrow$  278a-c, Scheme 98). Also in this case, an undesired side-reaction was detected, a nickel(0)-catalyzed double-bond migration of the vinylcyclobutane to the corresponding methylenecyclobutane (not shown).

## 5.3. Biphenylene

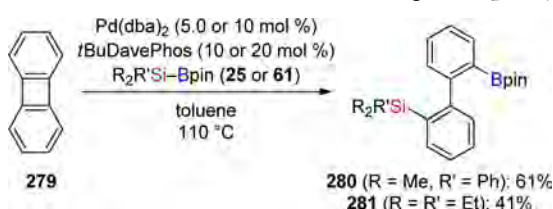
In a series of transformations with biphenylene, Matsuda and Kirikae demonstrated their efficient palladium(0)-catalyzed ring-opening with  $\text{Me}_2\text{PhSi-Bpin}$  (25) as well as  $\text{Et}_3\text{Si-Bpin}$  (61), leading to difunctionalized biaryls (279  $\rightarrow$  280 or 281, Scheme 99).<sup>96</sup> The authors proposed a mechanism in which the palladium-phosphine catalyst is involved in two consecutive oxidative additions of the Si-B bond and then the C-C



Scheme 98. Silaboration of Vinylcyclobutanes with C–C Bond Cleavage

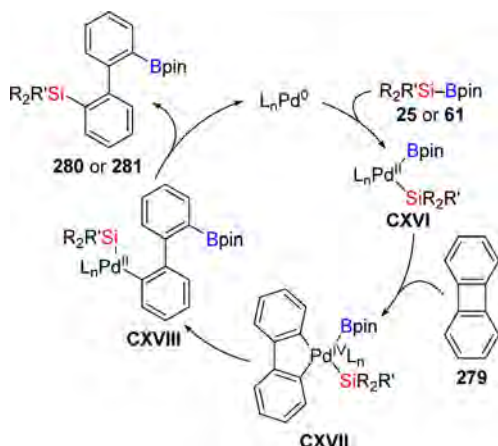


Scheme 99. Silaborative C–C Bond Cleavage of Biphenylene



bond of biphenylene (palladium(0) → CXVI → CXVII, Scheme 100). The palladacycle CXVII collapses by two reductive elimination steps, thereby forming the new C–Si and C–B bonds (CXVII → CXVIII → palladium(0) + 280 or 281).

Scheme 100. Proposed Mechanism for the Silaboration of Biphenylene

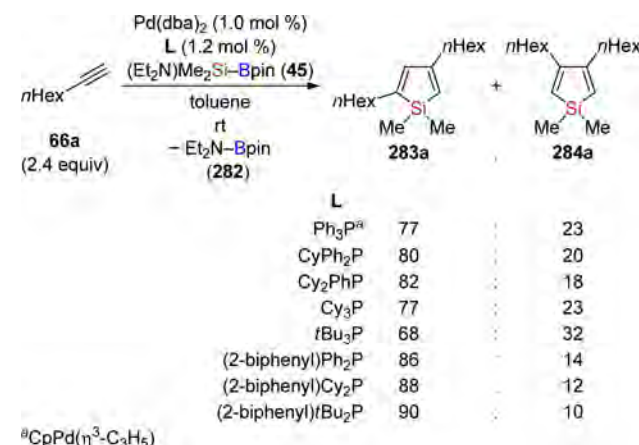


## 6. (2 + 2 + 1)- AND (4 + 1)-CYCLOADDITIONS OF MULTIPLE-BOND SYSTEMS

Oxidative addition of the Si–B bond to a transition metal generates complexes coordinated by both a silyl and a boryl group. This intermediate can react with multiple bonds in several modes by transferring both groups onto the multiple-bond system in the vast majority of cases. A remarkably different reactivity was discovered by the Suginome group when employing amino-substituted silylboronic esters 40, 44, 45, and 47 with the general formula (R'<sub>2</sub>N)R<sub>2</sub>Si–Bpin instead of Me<sub>2</sub>PhSi–Bpin (25) in palladium(0)-catalyzed reactions with terminal alkynes.<sup>31</sup> Siloles were formed in high yields rather than adducts from “simple” addition of the Si–B bond across the C–C triple bond. The authors explained this observation by

the formation of a palladium–silylene complex resulting from β-elimination of R'<sub>2</sub>N–Bpin (282 for R' = Et) after oxidative addition (cf. Scheme 10, lower, in section 3). The silylene is subsequently transferred to two molecules of the alkyne in a formal (2 + 2 + 1)-cycloaddition reaction, yielding 2,4- and 3,4-siloles in various ratios (66a → 283a and 284a, Scheme 101).

Scheme 101. (2 + 2 + 1)-Cycloaddition of Oct-1-yne: Ligand Screening

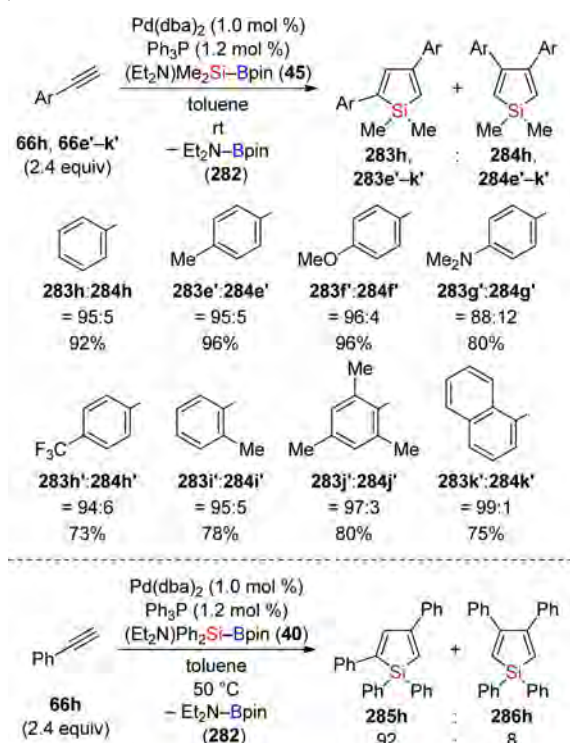


The reaction was general for all amino-substituted silylboronic esters (R'<sub>2</sub>N)R<sub>2</sub>Si–Bpin (R = Me and Ph and NR'<sub>2</sub> = NEt<sub>2</sub>, NMe<sub>2</sub>, and pyrrolidino) tested. An extensive screening of phosphine ligands in the reaction with oct-1-yne (66a) using (Et<sub>2</sub>N)Me<sub>2</sub>Si–Bpin (45) allowed for an increased regioisomeric ratio in favor of the 2,4-silole (rs ≤ 90:10) with sterically demanding and electron-rich phosphines (L). For dec-1-yne, the selectivity was even better (rs = 96:4, not shown).

Similar conditions were applied to aryl-substituted alkynes, yielding 2,4-diarylsiloles as the main products in high yields with generally good to excellent regioselectivities (66h and 66e'–k' → 283h and 284e'–k', Scheme 102, upper). A Pd(dba)<sub>2</sub>/Ph<sub>3</sub>P catalyst system facilitated the cycloaddition of electron-rich, electron-poor, and likewise sterically hindered substrates at room temperature. Another feature of this reaction is the possibility to alternatively introduce the Ph<sub>2</sub>Si instead of the Me<sub>2</sub>Si unit as both silylene precursors 40 and 45 are available (Scheme 102, lower).

Shortly thereafter, this novel concept of generating the palladium–silylene reagent from amino-substituted Si–B precursors was applied to (4 + 1)-cycloaddition with 1,3-dienes to give silacyclopent-3-enes (Scheme 103).<sup>97</sup> Careful catalyst tuning revealed that MePh<sub>2</sub>P is the optimal ligand in combination with Pd(dba)<sub>2</sub> for this transformation. Moreover, an excess of the ligand over palladium was crucial for good conversion. As yields of the silacyclopent-3-ene and the aminoborane byproduct differ significantly under various reaction conditions, the authors suggest that silylene formation and its transfer to the 1,3-diene occur sequentially. Under these optimized conditions, several mono-, di- and trisubstituted buta-1,3-dienes were subjected to the reaction with (Et<sub>2</sub>N)Me<sub>2</sub>Si–Bpin (45) (Scheme 103, upper). Aryl- and alkyl-substituted as well as functionalized 1,3-dienes underwent the reaction in excellent yields. The silacyclopent-3-ene products could be oxidized with 2,3-dichloro-5,6-dicyano-1,4-benzoquinone (DDQ) (or chloranil) to the corresponding siloles, as

Scheme 102. (2 + 2 + 1)-Cycloaddition of Aryl-Substituted Alkynes



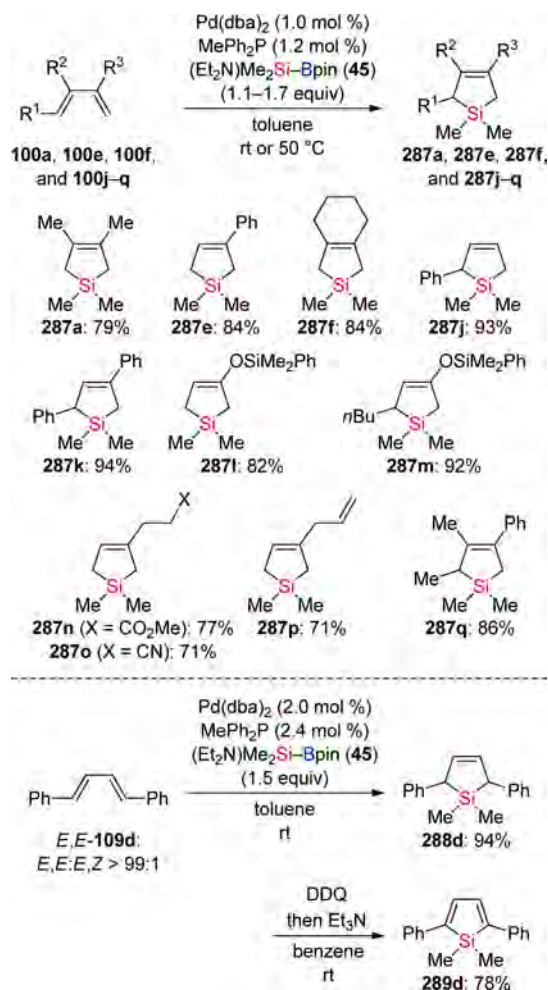
shown in one example (109d → 288d → 289d, Scheme 103, lower).

The stereochemical course of the reaction was studied by the employment of two isomers of dodeca-5,7-diene (Scheme 104).<sup>97</sup> The *E,E*-isomer (*E,E*-109c) led to *cis*-288c exclusively whereas the *E,Z*-isomer (*E,Z*-109c) yielded *trans*-288c, which is in agreement with a stereospecific reaction expected for a concerted (4 + 1)-cycloaddition. The introduction of diphenylsilylene was nicely showcased in the reaction with buta-1,3-diene (100d) (not shown) and cyclohexa-1,3-diene (103a) (Scheme 105).<sup>97</sup> The latter reacted with (Et<sub>2</sub>N)Ph<sub>2</sub>Si-Bpin (40) to give 7-silanorbornene (290a) in 88% yield.

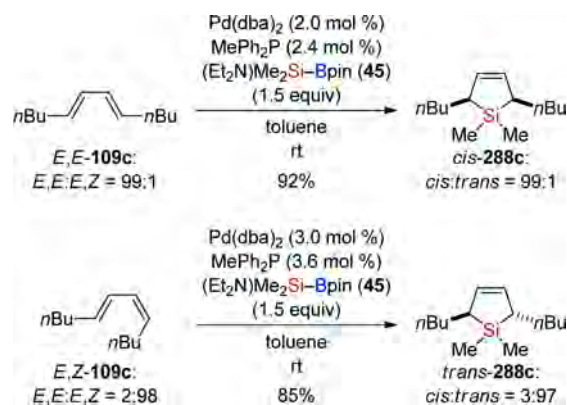
Just recently, Masuda, Ohmura, and Sugimoto transferred this newly developed concept to the (4 + 1)-cycloaddition of 2-vinylindoles (Scheme 106).<sup>98</sup> The reaction proceeded as expected for  $\alpha$ -styryl-substituted indole 291 and led to the formation of tricyclic product 292. As 292 was not stable on silica gel, it was subsequently oxidized to indole-annulated silole 293, which was isolated in a decent yield. This reaction followed the general mechanism observed for 1,3-dienes before. However, when the  $\alpha$ -styryl substituent at the indole was exchanged by a  $\beta$ -styryl substituent, disilylated 295 was obtained as a single diastereomer in excellent yield (294 → 295, Scheme 107).<sup>98</sup> Formation of the silacyclopentene unit substituted with a dimethylhydrosilyl group was general for all indoles bearing a linear alkenyl substituent in the 2-position (not shown). In contrast, no reaction was observed for 3-alkenyl-substituted indole 296 (Scheme 107).<sup>98</sup>

To elucidate the mechanism of this unexpected reaction, deuterated analogues of 294 were prepared and subjected to the established protocol (Scheme 108, upper).<sup>98</sup> It turned out that a deuterium atom attached to the  $\beta$ -carbon atom of the styrene substituent remained unaffected during the reaction (297 → 298). Conversely, a deuterium atom installed at the 3-

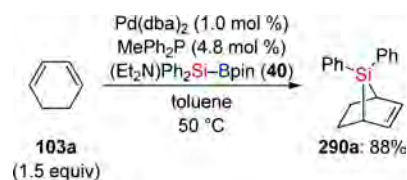
Scheme 103. (4 + 1)-Cycloaddition of 1,3-Dienes



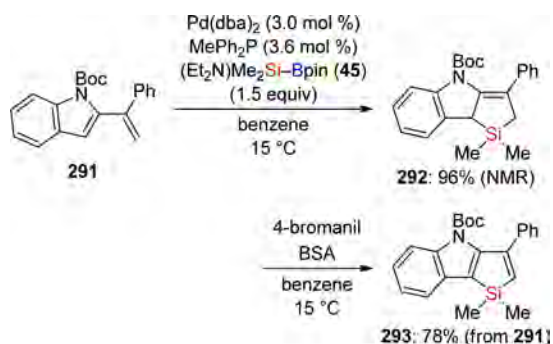
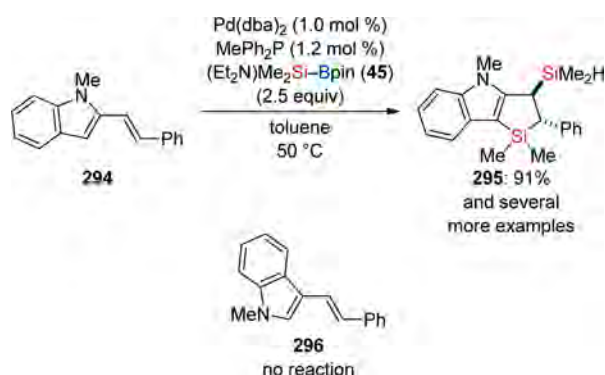
Scheme 104. Probing the Mechanism: Stereospecific (4 + 1)-Cycloaddition



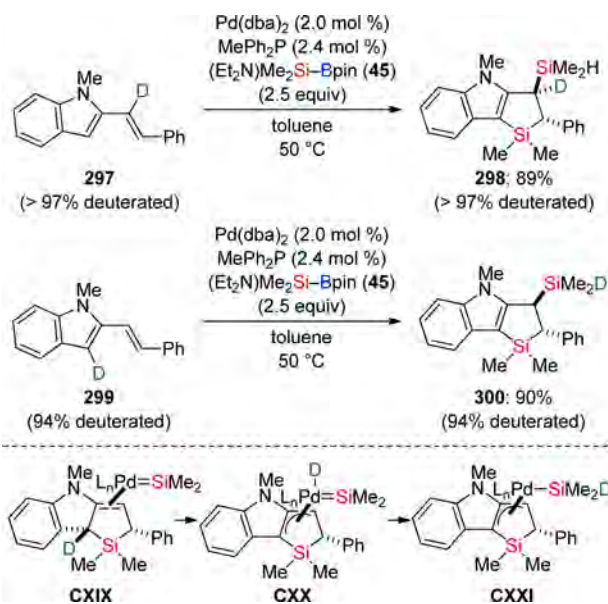
Scheme 105. Silylene Addition to Cyclohexa-1,3-diene





Scheme 106. (4 + 1)-Cycloaddition of  $\alpha$ -Styryl-Substituted IndoleScheme 107. Double Silylation of  $\beta$ -Styryl-Substituted Indoles

Scheme 108. Elucidation of the Double Silylation Mechanism by Deuterium Labeling



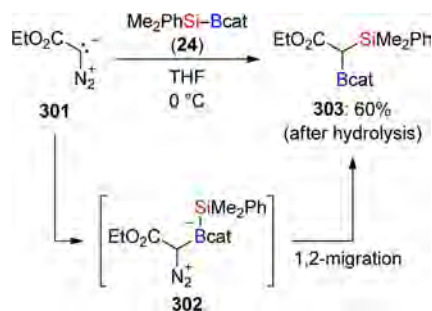
position of the indole was found to be attached to the exocyclic silicon atom of the target compound (299  $\rightarrow$  300). These results prompted the authors to suggest a mechanism in which, after the initial (4 + 1)-cycloaddition, another equivalent of the palladium–silylene complex reacts in an oxidative addition with the silacyclopentene intermediate CXIX, resulting in the allylpalladium–silylene intermediate CXX (CXIX  $\rightarrow$  CXX, Scheme 108, lower). A subsequent conversion of the

deuterido(silylene)palladium species CXX into a deuteriosilyl-palladium intermediate CXXI (CXX  $\rightarrow$  CXXI) is followed by the terminal reductive elimination forming the disilylated product 300 and regenerating the catalyst.

## 7. FUNCTIONALIZATION OF CARBENOIDS AND RELATED COMPOUNDS

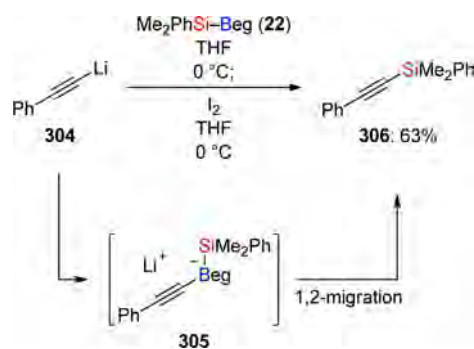
Si–B interelement compounds are reactive toward charged and neutral nucleophiles. The boron atom is the electrophilic site, and nucleophilic attack of a carbon nucleophile at the boron atom releases the silicon atom as a nucleofuge. That reaction is stepwise and proceeds through an ate complex, followed by 1,2-migration of the silicon atom to the boron-substituted carbon atom. If the carbon atom is substituted with an appropriate leaving group, both electrophilic boron and nucleophilic silicon will remain in the molecule, corresponding to a geminal functionalization. That is ideally realized in main group metal carbenoids, and the Shimizu–Hiyama group reported several beautiful transformations on that basis.<sup>33,34,99–101</sup> The idea, however, traces back to a seminal paper by Buynak and Geng where transition metal-free reactions of  $\text{Me}_2\text{PhSi-Bcat}$  (24) and  $\text{Me}_2\text{PhSi-Beg}$  (22) with nucleophiles were investigated.<sup>14</sup> One resonance structure of a diazo compound resembles in a way the carbenoid situation, that is, a carbanion with a leaving group attached to it; its reaction with 24 yielded a geminally functionalized carbon atom in the  $\alpha$ -position of a carboxyl group (301  $\rightarrow$  302  $\rightarrow$  303, Scheme 109). The same authors

Scheme 109. Geminal Functionalization of a Diazo Compound



also disclosed reactions of 22 with metalated alkenes (not shown) and alkynes (304  $\rightarrow$  305  $\rightarrow$  306, Scheme 110); the intermediate ate complex is “decomposed” by the addition of iodine with concomitant formation of the C–Si bond.

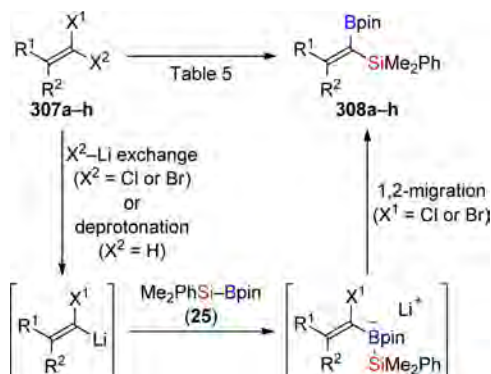
Scheme 110. Zweifel-Type Procedure Using Si–B Interelement Compound



## 7.1. Carbenoids

The laboratory of Shimizu and Hiyama began the systematic investigation of carbenoid insertion into Si–B bonds with the geminal functionalization of alkylidene-type carbenoids (**307a–h**  $\rightarrow$  **308a–h**, Scheme 111).<sup>33</sup> The carbenoids were generated

**Scheme 111. Geminal Functionalization of Alkylidene-Type Carbenoids**



by either halogen–metal exchange or deprotonation at low temperature. Addition of  $\text{Me}_2\text{PhSi-Bpin}$  (**25**) at that temperature followed by gradual warming to room temperature then afforded 1,1-difunctionalized alkenes; it was shown that the 1,2-migration already occurs above  $-50^\circ\text{C}$ . The procedure is applicable to a broad spectrum of carbenoid precursors (Table 5), and even *E*-1,4-dichlorobut-2-ene yielded, after an additional elimination step, targeted buta-1,3-diene as a single diastereomer (**307f**  $\rightarrow$  **E-308f**, Table 5, entry 6). No erosion of the enantiomeric purity was seen in the reaction of a chiral allylic alcohol (**307c**  $\rightarrow$  **Z-308c**, Table 5, entry 3). The double-bond geometry of **Z-308c** corroborates a mechanism that involves “inversion” at the carbenoid carbon atom in the 1,2-migration step as the directed bromide–lithium exchange at **307c** is stereoselective.

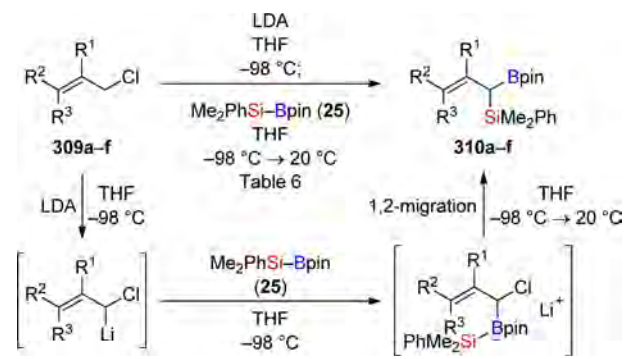
Application of the above methodology to allylic chlorides was indeed successful (**309a–f**  $\rightarrow$  **310a–f**, Scheme 112).<sup>34</sup> Conventional deprotonation with lithium diisopropylamide (LDA) at low temperature formed the intermediate carbenoid. Ate complex formation with  $\text{Me}_2\text{PhSi-Bpin}$  (**25**) was followed by 1,2-migration (1,1-difunctionalization), and no competing 1,4-migration was observed (1,3-difunctionalization). The protocol is general (Table 6), and the double-bond geometry of the allylic substrate is retained in the 1,1-difunctionalized building block (*E*-**309c**  $\rightarrow$  *E*-**310c** and *Z*-**309d**  $\rightarrow$  *Z*-**310d**, Table 6, entries 3 and 4). An interesting variation of the allylic difunctionalization was reported by Murakami (**311**  $\rightarrow$  **312**, Scheme 113).<sup>102</sup> The strained cyclic allylic bromide reacted in reasonable yield and is the only example of an  $\alpha$ -substituted allylic halide participating in this reaction.

A particularly nice example was accomplished in an intriguing one-pot sequence (**313**  $\rightarrow$  **315**  $\rightarrow$  **314**, Scheme 114).<sup>99</sup> The  $\text{CF}_3$ -substituted carbinol **313** was diastereoselectively transformed into the epoxide-derived carbenoid **315**; the usual carbenoid insertion into  $\text{Me}_2\text{PhSi-Bpin}$  (**25**) then generated an intermediate with a geminally functionalized carbon atom. The alkoxide group in the  $\beta$ -position of the silicon atom allowed for a Peterson syn-elimination, furnishing a tetrasubstituted alkene with excellent diastereocontrol. The alkene configuration is set at an early stage in the epoxide-forming step

**Table 5. Insertion of Alkylidene Carbenoids into the Si–B Bond**

entry	substrate	metalation	product	yield [%]
1		$n\text{BuLi}$ , THF– $\text{Et}_2\text{O}$ (2:1), $-110^\circ\text{C}$		84
2		$n\text{BuLi}$ , THF– $\text{Et}_2\text{O}$ (2:1), $-110^\circ\text{C}$		84
3		$n\text{BuLi}$ , $\text{Et}_2\text{O}$ , $-110^\circ\text{C}$		45
4		$n\text{BuLi}$ , THF– $\text{Et}_2\text{O}$ (2:1), $-110^\circ\text{C}$		60
5		$\text{LiTMP}$ , THF– $\text{Et}_2\text{O}$ (2:1), $-110^\circ\text{C}$		81
6		$\text{LiTMP}$ , THF, $-90^\circ\text{C}$		75
7		$n\text{BuLi}$ , THF, $-90^\circ\text{C}$		89
8		$\text{LiTMP}$ , THF, $-90^\circ\text{C}$		49

**Scheme 112. Geminal Functionalization of Allylic Carbenoids**



and has been rationalized by a lithium–fluorine chelation model.

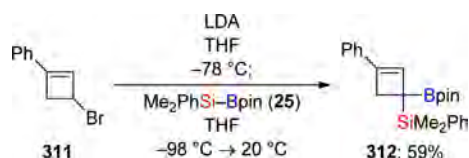
The ease of the generation of  $\alpha$ -oxygen-substituted carbanions through deprotonation of weak C–H acids makes them attractive carbenoid-type intermediates. Aggarwal et al. recently disclosed an enantioselective geminal functionalization on the basis of Hoppe’s asymmetric deprotonation<sup>103</sup> (**316a**



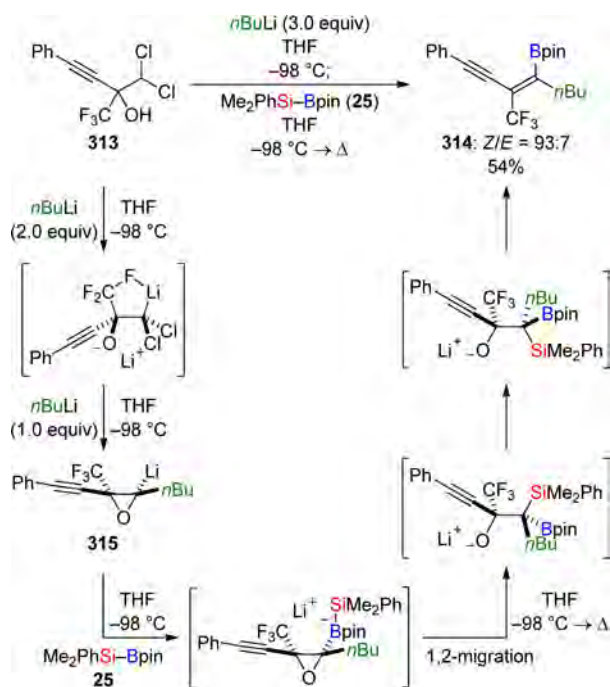
Table 6. Insertion of Allylic Carbenoids into the Si–B Bond

entry	substrate	E/Z ratio	product	E/Z ratio	yield [%]
1		—		—	82
2		85:15		83:17	86
3		> 99:1		> 99:1	75
4		< 1:99		< 1:99	79
5		—		—	72
6		—		—	73

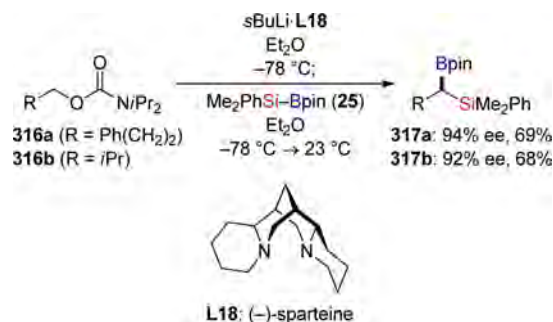
Scheme 113. Difunctionalization of a Strained Allylic Bromide



Scheme 114. Generation of Epoxide-Derived Carbenoids and Subsequent Insertion into an Si–B Bond



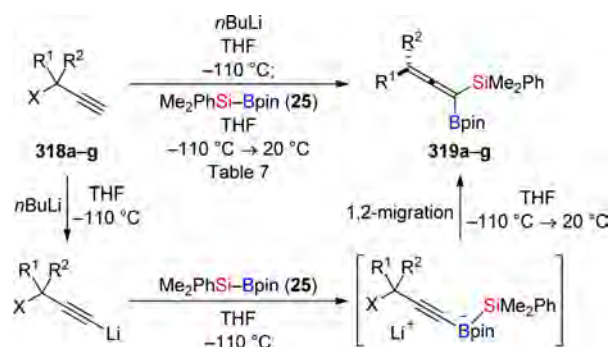
and **316b** → **317a** and **317b**, Scheme 115).<sup>104</sup> (–)-Sparteine-mediated  $\alpha$ -deprotonation of a carbamate generates an enantiomerically enriched, configurationally stable lithium–carbanion pair; its carbenoid character is then reflected in the

Scheme 115. Insertion of the Si–B Bond into an Enantiomerically Enriched  $\alpha$ -Oxygen-Substituted Lithium–Carbanion Pair with Carbenoid Character

electrophilic substitution with **Me<sub>2</sub>PhSi–Bpin (25)** and subsequent racemization-free 1,2-migration.

Shimizu et al. were later able to extend the geminal functionalization to terminal propargylic precursors with chloride and oxygen leaving groups (**318a–g** → **319a–g**, Scheme 116).<sup>101</sup> Metalation of the alkyne terminus forms an

Scheme 116. Geminal Functionalization of “Vinylogous” Alkylidene Carbenoids



intermediate that corresponds to a “vinylogous” alkylidene-type carbenoid, and 1,2-migration of the silicon atom results in the propargylic displacement of the leaving group. By this, a fair number of terminal alkynes with a propargylic leaving group and with at least one additional substituent at the propargylic carbon atom are transformed into 1,1-difunctionalized allenes (Table 7). Reactions mixtures were usually warmed to room temperature but, for the mesylate, full conversion and higher isolated yield (75% versus 51%) were seen even at  $-78\text{ }^{\circ}\text{C}$  with added **Me<sub>3</sub>SiCl (318g** → **319g**, Table 7, entry 7). **Me<sub>3</sub>SiCl** was proposed to improve the leaving group capability by complexation of the mesyl group. The modified protocol was applied to an enantioselective substitution, but there was partial racemization [(*S*)-**320** → (*R*)-**321**, Scheme 117].<sup>101</sup>

Shimizu et al. also reported a carbenoid insertion approach to trimetallmethanes, that is, methanes with three (different) main group substituents (**322** → **323**, Scheme 118).<sup>100</sup> A fourth main group substituent was introduced by deprotonation and electrophilic substitution with an appropriate electrophile (**323** → **324**, Scheme 118). By this, a tetrametallmethane was made available in a short synthesis.

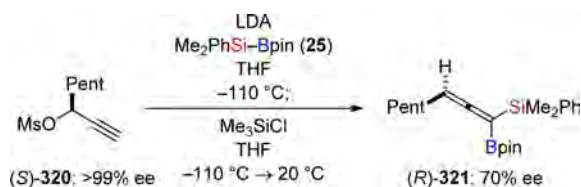
## 7.2. Isonitriles

Prior to the work of Shimizu, Hiyama, and co-workers<sup>33,34,99–101</sup> but half a decade after the pioneering investigation of Buynak and Geng,<sup>14</sup> Ito and co-workers

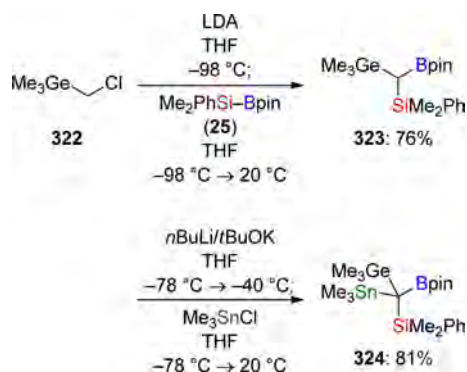
Table 7. Insertion of “Vinylogous” Alkylidene Carbenoids into the Si–B Bond

entry	substrate	product	yield [%]
1			70
2			77
3			53
4			41
5			50
6			83
7			51

Scheme 117. Enantioselective Geminal Functionalization of a Chiral Propargylic Mesylate



Scheme 118. Preparation of a Tri- and a Tetrametallmethane



reported the transition metal-free insertion of isocyanides into the Si–B bond of several Si–B compounds (325a–f  $\rightarrow$  326a–f after borane protection, Scheme 119).<sup>105</sup> A large number of isocyanides reacted with  $\text{Me}_2\text{PhSi-B}(\text{N}i\text{Pr}_2)_2$  (95) at elevated or even room temperature; the (boryl)(silyl)iminomethanes are isolated as their borane complexes (Table 8). The reaction also works with other Si–B compounds, e.g.,  $\text{Me}_2\text{PhSi-Bpin}$  (25) (325a  $\rightarrow$  327a, Scheme 120).

Suginome, Fukuda, and Ito observed an interesting skeletal rearrangement when (boryl)(silyl)iminomethane 328a was treated in refluxing toluene (Scheme 121, upper).<sup>106</sup> Under

Scheme 119. Insertion of Isonitriles into the Si–B Bond

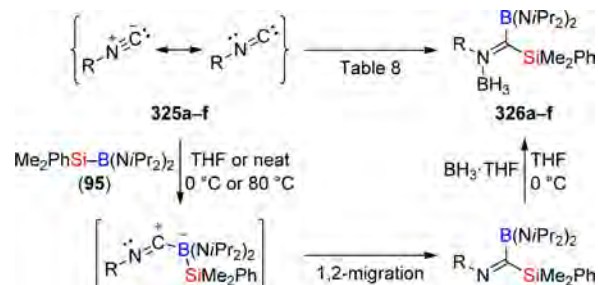
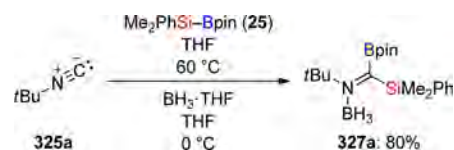


Table 8. Insertion of Isonitriles into the Si–B Bond

entry	substrate	solvent	<i>T</i> [°C]	product	yield [%]
1		neat	20		89
2		THF	80		76
3		THF	80		73
4		THF	80		75
5		THF	80		82
6		THF	20		60

Scheme 120. Variation of the Si–B Compound in the Isonitrile Insertion

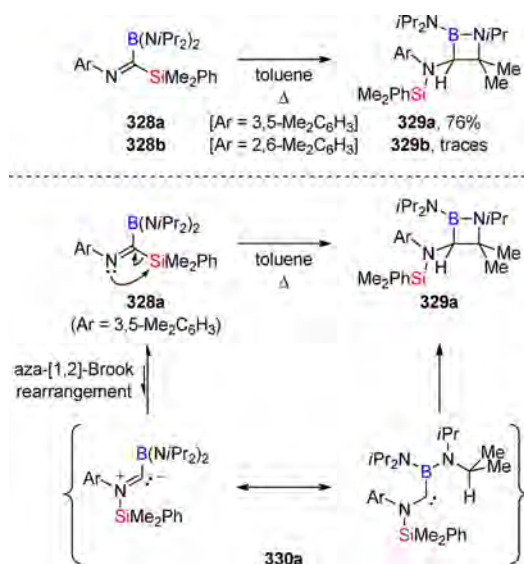


these conditions, 1,2-azaboretidine 329a was formed with an appreciable yield of 76% (328a  $\rightarrow$  329a). In contrast, sterically more congested 328b only afforded traces of the corresponding 1,2-azaboretidine 329b (328b  $\rightarrow$  329b). A possible pathway for the rearrangement is shown in Scheme 121 (lower). Reversible aza-[1,2]-Brook rearrangement generates the (amino)(boryl)-carbene species 330a (328a  $\rightarrow$  330a), which subsequently inserts into the C–H bond of the isopropylamino group, forming the azaboretidine ring (330a  $\rightarrow$  329a).

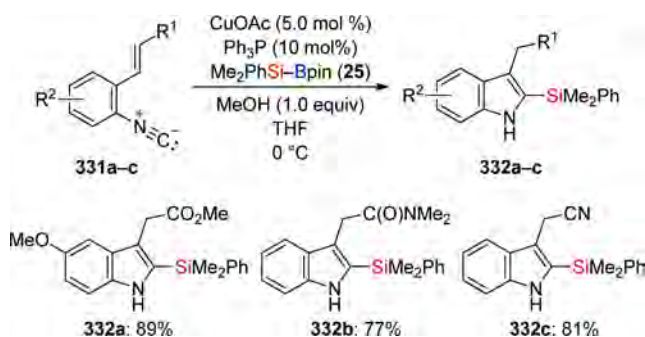
Chatani and co-workers recently developed a copper(I)-catalyzed indole synthesis involving an isocyanide (331a–c  $\rightarrow$  332a–c, Scheme 122).<sup>107</sup> The catalytic cycle (Scheme 123) of this domino reaction is proposed to begin with an intermolecular silyl transfer from the catalytically generated monosilyl copper(I) reagent XXXIX onto the isocyanide group



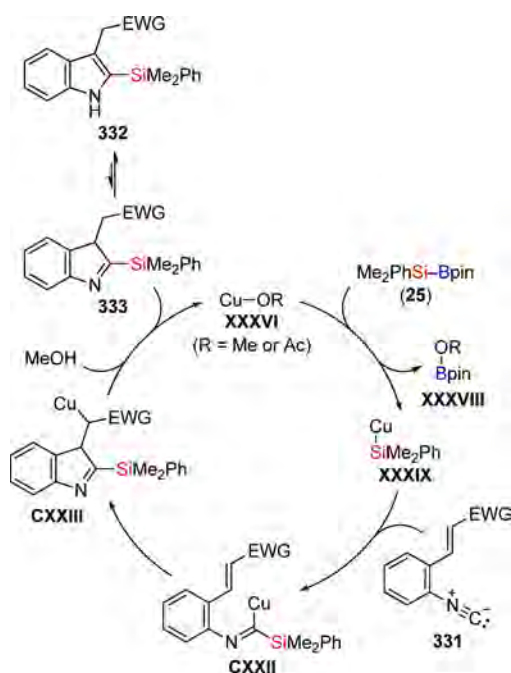
Scheme 121. Formation of 1,2-Azaboretinedines from (Boryl)(silyl)iminomethanes



Scheme 122. Copper(I)-Catalyzed Indole Synthesis through Isonitrile Insertion–Conjugate Addition



Scheme 123. Proposed Mechanism of the Copper(I)-Catalyzed Domino Isonitrile Insertion–Conjugate Addition



(331 + XXXIX → CXXII). Subsequent intramolecular 1,4-addition of the thus-formed imido copper(I) intermediate CXXII yields the indole ring (CXXII → CXXIII). Hydrolysis of copper(I) enolate CXXIII with MeOH liberates the indole tautomer 333 (indolenine) and regenerates the copper(I) methoxide catalyst (CXXIII → 333 → 332 + XXXVI).

## 8. SUMMARY

After a slow start half a century ago, Si–B chemistry rapidly grew into an independent area of synthetic main group chemistry over the past decade(s). The selective incorporation of both a silicon and a boron atom into an unsaturated molecule in a single synthetic operation is valuable as both newly formed functional groups are extraordinarily versatile linchpins for subsequent (mainly) C–C bond formation. Creative application of the transition metal-catalyzed Si–B bond activation to various classes of unsaturated compounds combined with subtle effects of the ligand or other additives provided unique regio- and diastereodivergent as well as regio- and stereoselective accesses to difunctional building blocks. These are usually difficult to make by more established methods. The portfolio extends not just to oxidative addition/reduction elimination mechanisms but also to transition metal-alkoxide-catalyzed heterolytic activation of the Si–B interelement linkage through transmetalation. By this, a transition metal–silicon reagent forms that transfers the silicon atom to unsaturated molecule as a nucleophile while the boron atom is sacrificed in the transmetalation step. With copper as the transition metal, the net monofunctionalization resembles the chemistry of silicon-based cuprates catalytic in copper, and similar reactivity and selectivity are seen for several acceptors.<sup>108</sup> As to asymmetric transformations, Si–B chemistry is superior to existing methods.

These developments and recent progress in transition metal-free catalyses bode well for the future of this exciting field, and it is not a stretch to predict that organocatalyzed and more enantioselective variants will evolve over the next couple of years.

## AUTHOR INFORMATION

### Corresponding Author

\*E-mail: martin.oestreich@tu-berlin.de.

### Notes

The authors declare no competing financial interest.

### Biographies



Martin Oestreich (born in 1971 in Pforzheim/Germany) is currently Professor of Organic Chemistry at the Technische Universität Berlin. He received his diploma degree with Paul Knochel (Marburg, 1996) and his doctoral degree with Dieter Hoppe (Münster, 1999). After a two-year postdoctoral stint with Larry E. Overman (Irvine, 1999–2001), he completed his habilitation with Reinhard Brückner (Freiburg, 2001–2005) and was appointed as Professor of Organic Chemistry at the Westfälische Wilhelms-Universität Münster (2006–2011). He also held visiting positions at Cardiff University in Wales (2005) and at The Australian National University in Canberra (2010).



Eduard Hartmann (born 1982 in Uspenka/Kazakhstan) studied chemistry at the Westfälische Wilhelms-Universität Münster (2004–2008) and spent a three-month research stay with Victor Snieckus at Queen's University in Kingston (2007). He earned his diploma degree with Martin Oestreich (2008) and completed his doctoral degree in the same group in Münster and then at the Technische Universität Berlin (2009–2012). His graduate research was supported by a predoctoral fellowship from the Fonds der Chemischen Industrie (2009–2011). He just embarked on postdoctoral training with Scott E. Denmark at the University of Illinois at Urbana–Champaign.



Marius Mewald (born 1984 in Münster/Germany) studied chemistry at the Westfälische Wilhelms-Universität Münster (2004–2009) and spent a three-month research internship at Hoffmann-La Roche in Basel (2008). He obtained his diploma degree with Martin Oestreich (2009) and is currently pursuing graduate research in the same group, now at the Technische Universität Berlin. He plans to do postdoctoral work with Mohammad Movassaghi at the Massachusetts Institute of Technology next year.

## ACKNOWLEDGMENTS

We thank the Deutsche Forschungsgemeinschaft (Oe 249/3-1 and Oe 249/3-2), the Fonds der Chemischen Industrie (predoctoral fellowship to E.H.), and the NRW Graduate

School of Chemistry (predoctoral fellowship to D.J.V.) for generous support throughout the last six years. Dr. Gertrud Auer (Freiburg), Dr. Christian Walter (Freiburg/Münster), Dr. Devendra J. Vyas (Münster), and Dr. Eduard Hartmann (Münster/Berlin) deserve particular mention for their enthusiasm and commitment. M.O. is indebted to the Einstein Foundation (Berlin) for an endowed professorship.

## REFERENCES

- (1) Tamao, K.; Yamaguchi, S. *J. Organomet. Chem.* **2000**, *611*, 3.
- (2) For general reviews, see: (a) Suginome, M.; Matsuda, T.; Ohmura, T.; Seki, A.; Murakami, M. In *Comprehensive Organometallic Chemistry III*; Mingos, D. M. P., Crabtree, R. H., Ojima, I., Eds.; Elsevier: Oxford, U.K., 2007; Vol. 10, pp 725–787 (general review of interelement addition across C–C multiple bonds). (b) Burks, H. E.; Morken, J. P. *Chem. Commun.* **2007**, 4717 (transition metal-catalyzed enantioselective addition of B–B, Si–Si, and Si–B bonds across unsaturated C–C bonds). (c) Beletskaya, I.; Moberg, C. *Chem. Rev.* **2006**, *106*, 2320 (transition metal-catalyzed addition of interelement bonds across unsaturated C–C bonds). (d) Suginome, M.; Ito, Y. *Chem. Rev.* **2000**, *100*, 3221 (transition metal-catalyzed addition of silicon-based interelement bonds across unsaturated C–C bonds). (e) Beletskaya, I.; Moberg, C. *Chem. Rev.* **1999**, *99*, 3435 (transition metal-catalyzed addition of interelement bonds across C–C triple bonds). (f) Han, L.-B.; Tanaka, M. *Chem. Commun.* **1999**, 395 (transition metal-catalyzed addition of interelement bonds across unsaturated C–C bonds involving oxidative addition/reductive elimination). (g) Ito, Y. *J. Organomet. Chem.* **1999**, *576*, 300 (transition metal-catalyzed addition of Si–Si and Si–B bonds across unsaturated C–C bonds).
- (3) For reviews focusing on Si–Si bond activation, see: (a) Suginome, M.; Ito, Y. *J. Organomet. Chem.* **2003**, *685*, 218 (intramolecular). (b) Pannell, K. H.; Sharma, H. K. *Chem. Rev.* **1995**, *95*, 1351 (general). (c) Horn, K. A. *Chem. Rev.* **1995**, *95*, 1371 (general).
- (4) For reviews focusing on Si–B bond activation, see: (a) Hartmann, E.; Oestreich, M. *Chim. Oggi* **2011**, *29*, 34 (transition metal-catalyzed addition of interelement bonds across unsaturated C–C bonds involving transmetalation). (b) Ohmura, T.; Suginome, M. *Bull. Chem. Soc. Jpn.* **2009**, *82*, 29 (transition metal-catalyzed addition of interelement bonds across unsaturated C–C bonds involving oxidative addition/reductive elimination). (c) Suginome, M.; Ito, Y. *J. Organomet. Chem.* **2003**, *680*, 43 (review with focus on boryl-substituted allylic silanes as target molecules).
- (5) Hartmann, E.; Vyas, D. J.; Oestreich, M. *Chem. Commun.* **2011**, 47, 7917 (conjugate addition involving Si–B and B–B bond activation).
- (6) Transition metal-catalyzed B–B bond activation involving oxidative addition/reductive elimination or transmetalation recently attracted considerable attention. For reviews covering all facets of the field, see: (a) Takaya, J.; Iwasawa, N. *ACS Catal.* **2012**, *2*, 1993. (b) Calow, A. D. J.; Whiting, A. *Org. Biomol. Chem.* **2012**, *10*, 5485. (c) Cid, J.; Gulyás, H.; Carbó, J. J.; Fernández, E. *Chem. Soc. Rev.* **2012**, *41*, 3558. (d) Schiffner, J. A.; Muther, K.; Oestreich, M. *Angew. Chem., Int. Ed.* **2010**, *49*, 1194. (e) Mantilli, L.; Mazet, C. *ChemCatChem* **2010**, *2*, 501. (f) Bonet, A.; Sole, C.; Gulyás, H.; Fernández, E. *Curr. Org. Chem.* **2010**, *14*, 2531. (g) Dang, L.; Lin, Z.; Marder, T. B. *Chem. Commun.* **2009**, 3987. (h) Lillo, V.; Bonet, A.; Fernández, E. *Dalton Trans.* **2009**, 2899. (i) Ishiyama, T.; Miyauro, N. *Chem. Rec.* **2004**, *3*, 271. (j) Ishiyama, T.; Miyauro, N. *J. Organomet. Chem.* **2000**, *611*, 392. (k) Marder, T. B.; Norman, N. C. *Top. Catal.* **1998**, *5*, 63.
- (7) Seyferth, D.; Kögler, H. P. *J. Inorg. Nucl. Chem.* **1960**, *15*, 99.
- (8) Cowley, A. H.; Sisler, H. H.; Ryschkewitsch, G. E. *J. Am. Chem. Soc.* **1960**, *82*, 501.
- (9) (a) Seyferth et al. also accomplished the preparation of the silicon-substituted borate  $\text{Li}[\text{Ph}_3\text{Si}-\text{BPh}_3]$  without heteroatoms at the boron atom: Seyferth, D.; Raab, G.; Grim, S. O. *J. Org. Chem.* **1961**, *26*, 3034. Later, Nöth and co-workers reported the synthesis of



- several related borates mainly derived from methoxy-substituted boranes: (b) Biffar, W.; Nöth, H. *Angew. Chem., Int. Ed. Engl.* **1980**, *19*, 58. (c) Biffar, W.; Nöth, H. *Chem. Ber.* **1982**, *115*, 934. (d) Lippert, W.; Nöth, H.; Ponikvar, W.; Seifert, T. *Eur. J. Inorg. Chem.* **1999**, 817.
- (10) (a) Nöth, H.; Höllner, G. *Angew. Chem., Int. Ed. Engl.* **1962**, *1*, 551. (b) Nöth, H.; Höllner, G. *Chem. Ber.* **1966**, *99*, 2197.
- (11) For the preparation of, e.g.,  $\text{H}_3\text{Si}-\text{B}(\text{NMe}_2)_2$ , see: Amberger, E.; Römer, R. Z. *Allg. Anorg. Chem.* **1966**, 345, 1.
- (12) (a) Bonnefon, E.; Birot, M.; Dunogues, J.; Pillot, J.-P.; Courseille, C.; Taulelle, F. *Main Group Met. Chem.* **1996**, *19*, 761. (b) Araujo Da Silva, J. C.; Birot, M.; Pillot, J.-P.; Pétraud, M. J. *Organomet. Chem.* **2002**, *646*, 179.
- (13) Biffar, W.; Nöth, H.; Schwerthöffer, R. *Liebigs Ann. Chem.* **1981**, 2067.
- (14) Buynak, J. D.; Geng, B. *Organometallics* **1995**, *14*, 3112.
- (15) Chavant, P. Y.; Vaultier, M. J. *Organomet. Chem.* **1993**, *455*, 37.
- (16) (a) Suginome, M.; Nakamura, H.; Ito, Y. *Chem. Commun.* **1996**, 2777. (b) Suginome, M.; Matsuda, T.; Nakamura, H.; Ito, Y. *Tetrahedron* **1999**, *55*, 8787.
- (17) Onozawa, S.-y.; Hatanaka, Y.; Tanaka, M. *Chem. Commun.* **1997**, 1229.
- (18) Habereeder, T.; Nöth, H. *Appl. Organomet. Chem.* **2003**, *17*, 525.
- (19) Suginome, M.; Ohmura, T.; Miyake, Y.; Mitani, S.; Ito, Y.; Murakami, M. *J. Am. Chem. Soc.* **2003**, *125*, 11174.
- (20) Tucker, C. E.; Davidson, J.; Knochel, P. J. *Org. Chem.* **1992**, *57*, 3482.
- (21) Hoffmann, R. W.; Metternich, R.; Lanz, J. W. *Liebigs Ann. Chem.* **1987**, 881.
- (22) Suginome, M.; Matsuda, T.; Ito, Y. *Organometallics* **2000**, *19*, 4647.
- (23) Ohmura, T.; Masuda, K.; Furukawa, H.; Suginome, M. *Organometallics* **2007**, *26*, 1291.
- (24) Tamao, K.; Kawachi, A.; Ito, Y. *J. Am. Chem. Soc.* **1992**, *114*, 3989.
- (25) For earlier work on alkoxy substitution at the silicon atom, see: Pfeiffer, J.; Maringgele, W.; Meller, A. Z. *Allg. Anorg. Chem.* **1984**, *511*, 185.
- (26) Suginome, M.; Noguchi, H.; Hasui, T.; Murakami, M. *Bull. Chem. Soc. Jpn.* **2005**, *78*, 323.
- (27) Boebel, T. A.; Hartwig, J. F. *Organometallics* **2008**, *27*, 6013.
- (28) For a tantalum-mediated Si–B bond formation, see: Jiang, Q.; Carroll, P. J.; Berry, D. H. *Organometallics* **1993**, *12*, 177.
- (29) For Si–B bond formation involving silylenes, see: (a) Metzler, N.; Denk, M. *Chem. Commun.* **1996**, 2657. (b) Holtmann, U.; Jutzi, P.; Kühler, T.; Neumann, B.; Stamm, H.-G. *Organometallics* **1999**, *18*, 5531. (c) Takeda, N.; Kajiwara, T.; Tokitoh, N. *Chem. Lett.* **2001**, *30*, 1076. (d) Kajiwara, T.; Takeda, N.; Sasamori, T.; Tokitoh, N. *Chem. Commun.* **2004**, 2218. (e) Kajiwara, T.; Takeda, N.; Sasamori, T.; Tokitoh, N. *Organometallics* **2004**, *23*, 4723. (f) Kajiwara, T.; Takeda, N.; Sasamori, T.; Tokitoh, N. *Organometallics* **2008**, *27*, 880.
- (30) For Si–B bond formation from metalated disilenes, see: Inoue, S.; Ichinohe, M.; Sekiguchi, A. *Chem. Lett.* **2008**, *37*, 1044.
- (31) Ohmura, T.; Masuda, K.; Suginome, M. *J. Am. Chem. Soc.* **2008**, *130*, 1526.
- (32) Kawachi, A.; Minamimoto, T.; Tamao, K. *Chem. Lett.* **2001**, *30*, 1216.
- (33) (a) Hata, T.; Kitagawa, H.; Masai, H.; Kurahashi, T.; Shimizu, M.; Hiyama, T. *Angew. Chem., Int. Ed.* **2001**, *40*, 790. (b) Kurahashi, T.; Hata, T.; Masai, H.; Kitagawa, H.; Shimizu, M.; Hiyama, T. *Tetrahedron* **2002**, *58*, 6381.
- (34) Shimizu, M.; Kitagawa, H.; Kurahashi, T.; Hiyama, T. *Angew. Chem., Int. Ed.* **2001**, *40*, 4283.
- (35) O'Brien, J. M.; Hoveyda, A. H. *J. Am. Chem. Soc.* **2011**, *133*, 7712.
- (36) Oshima, K.; Ohmura, T.; Suginome, M. *Chem. Commun.* **2012**, *48*, 8571.
- (37) Matsumoto, A.; Ito, Y. *J. Org. Chem.* **2000**, *65*, 5707.
- (38) Ohmura, T.; Oshima, K.; Suginome, M. *Chem. Commun.* **2008**, 1416.
- (39) Ohmura, T.; Oshima, K.; Taniguchi, H.; Suginome, M. *J. Am. Chem. Soc.* **2010**, *132*, 12194.
- (40) Ohmura, T.; Oshima, K.; Suginome, M. *Angew. Chem., Int. Ed.* **2011**, *50*, 12501.
- (41) Sagawa, T.; Asano, Y.; Ozawa, F. *Organometallics* **2002**, *21*, 5879.
- (42) Sakaki, S.; Biswas, B.; Musashi, Y.; Sugimoto, M. *J. Organomet. Chem.* **2000**, *611*, 288.
- (43) Suginome, M.; Matsuda, T.; Ito, Y. *Organometallics* **1998**, *17*, 5233.
- (44) Nozaki, K.; Wakamatsu, K.; Nonaka, T.; Tückmantel, W.; Oshima, K.; Utimoto, K. *Tetrahedron Lett.* **1986**, *27*, 2007.
- (45) Wang, P.; Yeo, X.-L.; Loh, T.-P. *J. Am. Chem. Soc.* **2011**, *133*, 1254.
- (46) Liepins, V.; Karlström, A. S. E.; Bäckvall, J.-E. *J. Org. Chem.* **2002**, *67*, 2136.
- (47) Suginome, M.; Nakamura, H.; Ito, Y. *Angew. Chem., Int. Ed. Engl.* **1997**, *36*, 2516.
- (48) Ohmura, T.; Furukawa, H.; Suginome, M. *J. Am. Chem. Soc.* **2006**, *128*, 13366.
- (49) Ohmura, T.; Takasaki, Y.; Furukawa, H.; Suginome, M. *Angew. Chem., Int. Ed.* **2009**, *48*, 2372.
- (50) Ito, H.; Horita, Y.; Yamamoto, E. *Chem. Commun.* **2012**, *48*, 8006.
- (51) Suginome, M.; Matsuda, T.; Yoshimoto, T.; Ito, Y. *Org. Lett.* **1999**, *1*, 1567.
- (52) Durieux, G.; Gerdin, M.; Moberg, C.; Jutand, A. *Eur. J. Inorg. Chem.* **2008**, 4236.
- (53) Gerdin, M.; Moberg, C. *Adv. Synth. Catal.* **2005**, *347*, 749.
- (54) Suginome, M.; Nakamura, H.; Matsuda, T.; Ito, Y. *J. Am. Chem. Soc.* **1998**, *120*, 4248.
- (55) Saito, N.; Kobayashi, A.; Sato, Y. *Angew. Chem., Int. Ed.* **2012**, *51*, 1228.
- (56) Shimizu, M.; Kurahashi, T.; Hiyama, T. *Synlett* **2001**, 1006.
- (57) Gerdin, M.; Moberg, C. *Org. Lett.* **2006**, *8*, 2929.
- (58) Lüken, C.; Moberg, C. *Org. Lett.* **2008**, *10*, 2505.
- (59) Gerdin, M.; Nadakudity, S. K.; Worch, C.; Moberg, C. *Adv. Synth. Catal.* **2010**, *352*, 2559.
- (60) Onozawa, S.; Hatanaka, Y.; Tanaka, M. *Chem. Commun.* **1999**, 1863.
- (61) Suginome, M.; Ohmori, Y.; Ito, Y. *Synlett* **1999**, 1567.
- (62) Suginome, M.; Ohmori, Y.; Ito, Y. *J. Am. Chem. Soc.* **2001**, *123*, 4601.
- (63) Suginome, M.; Ohmori, Y.; Ito, Y. *J. Organomet. Chem.* **2000**, *611*, 403.
- (64) Abe, Y.; Kuramoto, K.; Ehara, M.; Nakatsuji, H.; Suginome, M.; Murakami, M.; Ito, Y. *Organometallics* **2008**, *27*, 1736.
- (65) Chang, K.-J.; Rayaburapu, D. K.; Yang, F.-Y.; Cheng, C.-H. *J. Am. Chem. Soc.* **2005**, *127*, 126.
- (66) Ohmura, T.; Suginome, M. *Org. Lett.* **2006**, *8*, 2503.
- (67) Ohmura, T.; Taniguchi, H.; Suginome, M. *J. Am. Chem. Soc.* **2006**, *128*, 13682.
- (68) Kleeberg, C.; Feldmann, E.; Hartmann, E.; Vyas, D. J.; Oestreich, M. *Chem.—Eur. J.* **2011**, *17*, 13538.
- (69) Vyas, D. J.; Fröhlich, R.; Oestreich, M. *Org. Lett.* **2011**, *13*, 2094.
- (70) Kleeberg, C.; Cheung, M. S.; Lin, Z.; Marder, T. B. *J. Am. Chem. Soc.* **2011**, *133*, 19060.
- (71) Ariafard, A.; Brookes, N. J.; Stranger, R.; Yates, B. F. *Organometallics* **2011**, *30*, 1340.
- (72) (a) Hayashi, T.; Matsumoto, Y.; Ito, Y. *J. Am. Chem. Soc.* **1988**, *110*, 5579. (b) Matsumoto, Y.; Hayashi, T.; Ito, Y. *Tetrahedron* **1994**, *50*, 335.
- (73) (a) Walter, C.; Auer, G.; Oestreich, M. *Angew. Chem., Int. Ed.* **2006**, *45*, 5675. (b) Walter, C.; Oestreich, M. *Angew. Chem., Int. Ed.* **2008**, *47*, 3818. (c) Walter, C.; Fröhlich, R.; Oestreich, M. *Tetrahedron* **2009**, *65*, 5513.
- (74) Hayashi, T.; Takahashi, M.; Takaya, Y.; Ogasawara, M. *J. Am. Chem. Soc.* **2002**, *124*, 5052.

- (75) Hartmann, E.; Oestreich, M. *Angew. Chem., Int. Ed.* **2010**, *49*, 6195.
- (76) Hartmann, E.; Oestreich, M. *Org. Lett.* **2012**, *14*, 2406.
- (77) Lee, K.-s.; Hoveyda, A. H. *J. Am. Chem. Soc.* **2010**, *132*, 2898.
- (78) Harb, H. Y.; Collins, K. D.; Garcia Altur, J. V.; Bowker, S.; Campbell, L.; Procter, D. J. *Org. Lett.* **2010**, *12*, 5446.
- (79) Welle, A.; Petriguet, J.; Tinant, B.; Wouters, J.; Riant, O. *Chem.—Eur. J.* **2010**, *16*, 10980.
- (80) Ibrahim, I.; Santoro, S.; Himo, F.; Córdova, A. *Adv. Synth. Catal.* **2011**, *353*, 245.
- (81) Calderone, J. A.; Santos, W. L. *Org. Lett.* **2012**, *14*, 2090.
- (82) Vyas, D. J.; Oestreich, M. *Angew. Chem., Int. Ed.* **2010**, *49*, 8513.
- (83) Vyas, D. J.; Oestreich, M. *Chem. Commun.* **2010**, *46*, 568.
- (84) Ohmiya, H.; Ito, H.; Sawamura, M. *Org. Lett.* **2009**, *11*, 5618.
- (85) Vyas, D. J.; Hazra, C. K.; Oestreich, M. *Org. Lett.* **2011**, *13*, 4462.
- (86) Hazra, C. K.; Oestreich, M. *Org. Lett.* **2012**, *14*, 4010.
- (87) Oshima, K.; Ohmura, T.; Sugimoto, M. *J. Am. Chem. Soc.* **2011**, *133*, 7324.
- (88) Ariafard, A.; Tabatabaie, E. S.; Monfared, A. T.; Assar, S. H. A.; Hyland, C. J. T.; Yates, B. F. *Organometallics* **2012**, *31*, 1680.
- (89) Sugimoto, M.; Matsuda, T.; Ito, Y. *J. Am. Chem. Soc.* **2000**, *122*, 11015.
- (90) Pohlmann, T.; de Meijere, A. *Org. Lett.* **2000**, *2*, 3877.
- (91) Ohmura, T.; Taniguchi, H.; Kondo, Y.; Sugimoto, M. *J. Am. Chem. Soc.* **2007**, *129*, 3518.
- (92) Akai, Y.; Yamamoto, T.; Nagata, Y.; Ohmura, T.; Sugimoto, M. *J. Am. Chem. Soc.* **2012**, *134*, 11092.
- (93) Ohmura, T.; Taniguchi, H.; Sugimoto, M. *Org. Lett.* **2009**, *11*, 2880.
- (94) Sugimoto, M.; Matsuda, T.; Yoshimoto, T.; Ito, Y. *Organometallics* **2002**, *21*, 1537.
- (95) Fugami, K.; Oshima, K.; Utimoto, K.; Nozaki, H. *Bull. Chem. Soc. Jpn.* **1987**, *60*, 2509.
- (96) Matsuda, T.; Kirikae, H. *Organometallics* **2011**, *30*, 3923.
- (97) Ohmura, T.; Masuda, K.; Takase, I.; Sugimoto, M. *J. Am. Chem. Soc.* **2009**, *131*, 16624.
- (98) Masuda, K.; Ohmura, T.; Sugimoto, M. *Organometallics* **2011**, *30*, 1322.
- (99) Shimizu, M.; Fujimoto, T.; Minezaki, H.; Hata, T.; Hiyama, T. *J. Am. Chem. Soc.* **2001**, *123*, 6947.
- (100) Shimizu, M.; Kurahashi, T.; Kitagawa, H.; Shimono, K.; Hiyama, T. *J. Organomet. Chem.* **2003**, *686*, 286.
- (101) Shimizu, M.; Kurahashi, T.; Kitagawa, H.; Hiyama, T. *Org. Lett.* **2003**, *5*, 225.
- (102) Murakami, M.; Usui, I.; Hasegawa, M.; Matsuda, T. *J. Am. Chem. Soc.* **2005**, *127*, 1366.
- (103) Hoppe, D.; Hense, T. *Angew. Chem., Int. Ed.* **1997**, *36*, 2283.
- (104) Aggarwal, V. K.; Binanzer, M.; de Ceglie, M. C.; Gallanti, M.; Glasspoole, B. W.; Kendrick, S. J. F.; Sonawane, R. P.; Vázquez-Romero, A.; Webster, M. P. *Org. Lett.* **2011**, *13*, 1490.
- (105) Sugimoto, M.; Fukuda, T.; Nakamura, H.; Ito, Y. *Organometallics* **2000**, *19*, 719.
- (106) Sugimoto, M.; Fukuda, T.; Ito, Y. *J. Organomet. Chem.* **2002**, *643–644*, 508.
- (107) Tobisu, M.; Fujihara, H.; Koh, K.; Chatani, N. *J. Org. Chem.* **2010**, *75*, 4841.
- (108) (a) For a review, see: Weickgenannt, A.; Oestreich, M. *Chem.—Eur. J.* **2010**, *16*, 402. (b) Oestreich, M.; Weiner, B. *Synlett* **2004**, 2139 (conjugate addition). (c) Auer, G.; Weiner, B.; Oestreich, M. *Synthesis* **2006**, 2113 (conjugate addition). (d) Oestreich, M.; Auer, G. *Adv. Synth. Catal.* **2005**, *347*, 637 (allylic substitution). (e) Schmidtmann, E. S.; Oestreich, M. *Chem. Commun.* **2006**, 3643 (allylic substitution). (f) Reference 83 (allylic substitution). (g) Reference 86 (propargylic substitution). (h) Auer, G.; Oestreich, M. *Chem. Commun.* **2006**, 311 (addition across triple bonds).